MOUNTAIN-PLAINS CONSORTIUM

MPC 15-284 | R. Gerdes, B. Biswas and K. Heaslip

Position Verification Systems for an Automated Highway System

A University Transportation Center sponsored by the U.S. Department of Transportation serving the Mountain-Plains Region. Consortium members:

Colorado State University
North Dakota State University
South Dakota State University
University of Colorado Denver
University of Denver
University of Utah
Utah State University
University of Wyoming

POSITION VERIFICATION SYSTEMS FOR AN AUTOMATED HIGHWAY SYSTEM

Bidisha Biswas
Ryan Gerdes, Ph.D.
Kevin Heaslip, Ph.D., P.E.

Utah Transportation Center
Utah State University
233 Engineering
4110 Old Main Hill
Logan, Utah 84322-4110

This report has been published as a thesis
for the degree of Master of Science in Electrical Engineering, Utah State University.

March 2015

ACKNOWLEDGEMENTS

This report would not have been possible had it not been for the immense support from the following group of people. Foremeost, I feel tremendously blessed to have Dr. Ryan Gerdes as my advisor and mentor. He has throughout been the most supportive and encouraging person to work with. I would like to thank him for believing in me and taking me as his student. For each and every time I made a mistake or asked a silly question he showed immense patience, and as a result I learned a lot more than I had come here for, and for that I thank him again. The guidance I received from Dr. Rajnikant Sharma has been invaluable. Without his constant vigilance and direction, this thesis would have been incomplete. I would also like to thank Dr. Don Cripps and Dr. Tam Chantem for their constant encouragement and understanding. My parents and my little brother have been my biggest strength as always. Nothing would have been possible if not for their constant reassuring presence in all situations, and my grandparents, whose blessings have been my constant companion, and so forever will be.

Special thanks go to Sara and Soudeh for listening to me and helping me each and every time I needed help. I believe I am extremely fortunate to have had the opportunity to know you and am glad I have such good friends in both of you. I thank my lab-mates, Saptarshi and Ruchir, for so many fun and fond memories that we made together.

The acknowledgement will be incomplete if I do not mention all my friends here in the United States and India. Ravi, Subhadeep, Anushka, Deepti, Pooja, Debashree, and all of you who were there for me, I thank you all with all my heart for never letting me miss my family. Forgive me for not mentioning all the other names, but I am thankful to each of you for making my life worthwhile with your presence in it.

DISCLAIMER

ABSTRACT

Automated vehicles promote road safety, fuel efficiency, and reduced travel time by decreasing traffic congestion and driver workload. In a vehicle platoon (grouping vehicles to increase road capacity by managing distance between vehicles using electrical and mechanical coupling) of such automated vehicles, as in automated highway systems (AHS), tracking of inter-vehicular spacing is one of the significant factors under consideration. Because of close spacing, computer-controlled platoons with inter-vehicular communication—the concept of adaptive cruise control (ACC)—become open to cybersecurity attacks.

Cyber physical (CP) and cyber attacks on smart grid electrical systems have been a significant focus of researchers. However, CP attacks on autonomous vehicle platoons have not been examined. This research surveys a number of models of longitudinal vehicle motion and analysis of a special class of CP attacks called false data injection (FDI) on vehicle platoons. In this kind of attack, the configuration of any CP system is exploited to introduce arbitrary errors to gain control over the system. Here, an *n*-vehicle platoon is considered and a linearized vehicle model is used as a test-bed to study vehicle dynamics and control, after false information is fed into the system.

TABLE OF CONTENTS

LIST OF TABLES

LIST OF FIGURES

EXECUTIVE SUMMARY

The development of automated vehicles has come more into the focus of researchers due to progress in areas of potential benefit, such as increasing road safety and fuel efficiency and reducing time road travel by decreasing traffic congestion and, thus, minimizing workload on the driver. For a platoon (which is a method of grouping vehicles that helps increase the capacity of roads by managing the distance between vehicles by using electrical and mechanical coupling) of such vehicles, the inter-vehicular distance is one of the most important facets to be taken into consideration. As in automated highway systems (AHS) (AHS is a technology implementing vehicle platooning), the vehicles' close spacing is controlled by computers, using inter-vehicular communication, which is the concept of adaptive cruise control (ACC). Cyber-physical systems (CPS) are systems that comprise computational elements to communicate among and control physical entities. A platoon of autonomous vehicles is one such system. Owing to such computer control, the system becomes susceptible to various kinds of cyber-physical attacks.
This research entails the survey of a number of vehicle models used in different works pertaining to longitudinal vehicle motion and analysis of a special class of cyber-physical attacks called False Data Injection (FDI) attacks on vehicle platoons moving with longitudinal motion. In this kind of attack, an attacker can exploit the configuration of any cyber-physical system to introduce arbitrary errors into certain state variables so as to gain control over the system. So here, an *n*-vehicle platoon is considered and a linearized vehicle model is used as a test-bed to study vehicle dynamics and control after false information is fed into the system.

1. INTRODUCTION

1.1 Background

Intelligent transportation systems (ITS) are systems that utilize information from the surroundings to improve conveyance by incorporating advanced technologies such as wireless communication, sensing, etc. [1]. ITS can be said to include the concepts of automated highway systems (AHS), which uses vehicle-to-road communication, and intelligent vehicle highway systems (IVHS), which uses vehicle-to-vehicle communication [2].

Cooperative autonomous vehicles, specifically, have been of great interest since the 1960s, as they help maintain a stable vehicle platoon by using inter-vehicular sensing capabilities, hence ameliorating traffic congestion and reducing workload on the driver [1]. An autonomous vehicle is basically a driverless car that travels between destinations without any human operator. It is capable of gathering sensory information from its surroundings so as to keep track of the positions of the objects, while an automated vehicle is one that will need the intervention of a driver, although it will have sensory devices to gather surrounding information.

Research endeavors in the field of automobiles have resulted in the development of advanced driver-assistance systems (ADAS). One of the main purposes of these is to automate major driving tasks, hence reducing driver's workload [3]. These systems make use of the information that is gathered by on-board sensors, which scan the vehicle's environment. Significant progress can be made when vehicles not only sense information but also communicate intelligently with other vehicles and roadside infrastructure. This constitutes the field of cooperative driving, in which the vehicles on the road communicate with each other, resulting in better collective behavior. This is the concept of adaptive cruise control (ACC), which was introduced some years ago. ACC systems try to achieve and maintain specified time headways, using environmental sensors—radar, lidar, and even vision-based systems—that measure the distance and relative velocity between the ACC-equipped vehicle and the preceding vehicle. The vehicle's acceleration and deceleration is automatically adjusted, based on the input from these sensors. This leaves the driver with the control of steering only.

Consequently, work has been done on vehicle-following applications, especially tracking vehicle-to-vehicle spacing errors, as can be seen in automated highway systems (AHS) [4]. The AHS concept combines onboard vehicular intelligence with intelligent technologies on infrastructure and communication to connect them [5]. It can create a virtually collision-free environment in which driving will be predictable and reliable [6].

String stability is an important notion related to AHS; it involves gradual attenuation of errors propagating through the stream of vehicles over time [4]. For any interconnected system, string stability implies the boundedness of the states of the system, given that the initial states are uniformly bounded [7]. Following widespread adoption of cruise control on vehicles, adaptive cruise control has come under focus to tackle relative speed and maintaining distance between current and preceding vehicles. Work has been done on designing controllers for the improvement of longitudinal motion by maintaining a constant time headway, utilizing data from the sensors attached to the vehicles [8]. Tai and Tomizuka [9] have worked on longitudinal velocity tracking with emphasis on ways to determine the desired traction or brake torque for desired velocity tracking. Majdoub et al. [10] have worked on designing a controller that is able to tightly regulate chassis and wheel velocities, in both acceleration and deceleration driving modes and despite changing and uncertain driving conditions.

But in all these cases, it is possible that someone with harmful intent might try to compromise different parts of an ITS (such as the sensor data being transmitted) to introduce erroneous measurements. Thus, in this work, a class of cyber-physical attacks called false data injection attacks have been introduced. In these, an attacker can exploit the sensor and sensor data of the vehicles to successfully introduce arbitrary errors into certain state variables so as to gain control over the platoon and introduce unwanted modifications. Three different attack scenarios have been considered: first, the attacker tampers with the sensor information being transmitted to the victimized vehicle, second it manipulates the information such that the victim's acceleration is affected, and in the third scenario, the attacker sends the correct information but with a delay.

In general, FDI (False Data Injection) attacks (or deception attacks) are an important class of cyberattacks against the sensing, measuring, and monitoring system of smart grids or smart cars or any CPS (cyber-physical system). These attacks compromise the readings of sensors to mislead the whole system's operation. For example, in power grids, these attacks aim to compromise the readings of multiple power-grid sensors and phasor measurement units in order to mislead operation and control centers, i.e., the attacker knows the configuration of the target system.

1.2 Related Work

As communication devices are being installed in modern high-speed vehicles and in other mobile and wireless network settings, issues of security and privacy must be taken seriously. Zarki et al. [11] have tried to explore some security-related challenges in an AHS environment. They sketched a vehicular communication infrastructure DAHNI (driver ad hoc networking infrastructure) and discussed certain networking related security issues. Several methodologies have been studied to try to detect and prevent FDI attacks into wireless sensor networks (WSN) and vehicular ad hoc networks (VANET) [12–15]. Zhu et al. [12] have presented a scheme in which the base station can verify the authenticity of a report given that the number of compromised sensor nodes in a WSN does not exceed a threshold. They focus on detecting and filtering false data packets either from the base station or while the packets are en route to the base station. This policy can be particularly useful for large-scale sensor networks where a sensor report needs to be relayed over several hops before it reaches the base station. Here, all the nodes that are involved in relaying the report to the base station authenticate the report in an interleaved, hop-by-hop fashion. They assume that the adversary can eavesdrop on all traffic, inject packets, and replay older packets, and that the adversary can take full control of compromised nodes.

Studer et al. [13] focus on the security requirements of VANETs. They deal with three specific attacks where vehicles falsely claim to be in the area of relevance (AOR): an attacker in opposing traffic that claims to be driving the same direction as the vehicle, an attacker on the side of the road that claims to be a legitimate vehicle, and an attacker that claims to be in front of the receiver.

In their work, Cao et al. [14] investigated techniques to protect the driver against FDI attacks. They used the concept of proof of relevance (PoR), which is achieved by the authentic consensus comprising the vehicles collecting information from other witnesses in the detecting area. After the information is collected, the vehicles disperse the same along their routes to notify other drivers so as to achieve a verifiable consensus. The vehicles then may verify all the signatures in the event report before accepting and responding; thus PoR keeps the network immune to false data. A very secure and efficient signature collection protocol is necessary to attain authentic consensus.

Mo et al. [15] studied the effects of FDI attacks on state estimation carried over sensor networks a discrete-time linear time invariant Gaussian system. A Kalman filter has been used to perform state estimation, and they assume that the system has a failure detector. The aim of the attacker is to

compromise a subset of sensors and send inaccurate readings to the state estimator. In this scenario, the attacker needs to design the false data so as to not trigger the alarm. The main aim of the paper is to set all the estimation biases the attacker can inject in the system without being detected.

Also, the same has been studied in power grids in the electricity market. Sinopoli et al. [16] have studied FDI attacks as a potential class of cyber-attack against state estimation in deregulated electricity markets. They show that with knowledge of the system configuration, such attacks circumvent the measured data in supervisory control and data acquisition (SCADA) systems, leading to financial misconduct. Mo and Sinopoli [17, 18] in their work have studied false data attacks in a cyber-physical system that comprises a linear control system with a Kalman filter, a linear-quadratic-Gaussian (LQG) controller, and a failure detector. Integrity attacks (integrity, in terms of data and network security, is the assurance that information can only be accessed or modified by those authorized to do so; thus, any outsider trying to modify any information that may hamper the authenticity is an integrity attack) on a CPS is considered, which is modeled as a discrete linear time-invariant system equipped with a Kalman filter, LQG controller, and a failure detector [18]. They assumed that an attacker wishes to disturb the system by injecting external control inputs and fake sensor measurements. In order to perform the attack without being detected, the attacker also needs to carefully design its actions to fool the failure detector. In this work, they considered a scenario in which a vehicle is moving along the x-axis and, at a certain time, either the velocity sensor or the position sensor is compromised. And as a result, they found that the attacker cannot destabilize the system by simply compromising the velocity sensor and it can only arbitrarily manipulate the position of the vehicle.

In the work by Liu et al. [19], a novel FDI attack was designed which bypasses all the existing detection schemes and was therefore capable of arbitrarily manipulating power system states, posing dangerous threats to the control of power system. Their main idea comprises two realistic attack goals:

- *random* FDI attacks, in which the attacker aims to find any attack vector as long as it can result in a wrong estimation of state variables
- *targeted* FDI attacks, in which the attacker aims to find an attack vector that can inject a specific error into certain state variables

Their study showed that in one case the attacker needed to compromise 30%-70% of the sensing devices to get a reasonable probability to construct an attacker vector, while in the second case, when an attacker targeted the weakest link of a power system, much fewer of the sensing devices needed to be compromised.

In the work done by Yu [20], two representative FDI attacks are presented that target the state estimation and the energy transmission in smart grids.

- FDI attacks against state estimation
  - How the adversary can choose specific sensing devices to compromise to cause the most significant deviation of the system state estimation is considered.
  - A least-effort attack model is developed that will efficiently identify the optimal set of parameters to launch FDI attacks a fixed number of state variables.
- FDI attacks against energy transmission
  - Various types of representative attacks are considered in which the adversary may manipulate the quantity of energy supply and response.
  - The attack will cause imbalanced supply and demand, increase the cost of energy distribution, disrupt energy distribution, and manipulate the price of energy.

The simulations presented validated the effectiveness of the attacks and, hence, ways to prevent and detect such attacks were suggested, and upon detection, the work presents developing schemes to localize and isolate the compromised devices.

Aijaz et al. [21] have studied attacks on the hardware, software, and sensor inputs of an inter-vehicle communication system and designed attack trees on routing-based applications VANETs. They have used the system model of the Network on Wheels (NoW) communication system and tried to find potential weaknesses during the specification phase of the NoW communication system. Golle et al. [22] introduced a scheme to detect malicious data in inter-vehicle communication (IVC). Dotzer [23] discussed privacy issues of vehicle communications. Gerlach [24] presented a holistic approach to VANET security. Leinmueller et al. [25] analyzed the impact of falsified position information on geographic routing.

In spite of the varied levels of work done with FDI, they have mostly been limited to smart grids and VANET; meanwhile, little work has been done to understand the false-data attack in context of automated-vehicle platoons, where a platoon is a group of vehicles moving on the road, sharing information of mutual interest with each other.

1.3 Outline of Research

With the advent of time and technology, it is not just becoming easier to gain control over everything around us, making life easier, but at the same time, it is also becoming easier for people with malicious intent to gain mastery over the same systems and turn them against us. If and when an attacker gains access to the sensor information being transmitted to the vehicles preceding and following it and falsifies that information, it might lead to varying types of changes in the velocities of the vehicles and the inter-vehicle spacings. So the autonomous vehicles that aim to reduce load on the driver and minimize accidents might be manipulated in such a manner that they will lead to even more disastrous accidents. Thus, research on FDI with respect to vehicle platoons is an important and necessary study.
There is thus a need to devise different kinds of false data attacks and examine the extent of such data that can damage a vehicle platoon that is otherwise moving in a stable manner. Specifically, the ability to compromise sensor information to achieve the same is an important aspect. If and how an attacker can affect the platoon by introducing false data into the system is thus the nucleus of the research.
The research entails:

- The survey of a number of vehicle models used in different works pertaining to longitudinal vehicle motion
- A vehicle model developed using MATLAB that can be used as a platform to analyze false data injection attacks
  The analysis of individual vehicle movements and operations under different controlling parameters such as position, velocity, and acceleration; implementing a proportional-derivative (PD) controller using the bidirectional-constant spacing platooning strategy

The main proposition is to design an active attacker who is an insider, and who can be either malicious or rational. The false data to be injected into the system must be designed and analyzed as the type and extent needed to generate instability and string instability. False data injection into a system can be of different types. Security breaches can be of the following types: (i) bogus traffic information, (ii) disruption of network operation, (iii) falsifying identity, position, or speed, and (iv) uncovering the identities of other vehicles [26]. On the other hand, the attacker can be (i) an insider or outsider, (ii) malicious or rational, or (iii) active or passive [27]. When an attacker introduces false data into the sensor information, it can take complete control of the platoon or induce instability in it.
Thus, Section 1 presents the idea of autonomous vehicles, their advantages, and different concepts pertaining to the same.

Section 2 comprises a survey of nine different vehicle models that were used in multiple studies related to longitudinal vehicle motion.
Section 3 discusses the vehicle model used and the corresponding string models in both absolute dynamics and error dynamics.

An *n*-vehicle platoon is considered and a linearized vehicle model is used as a test-bed to study vehicle dynamics and control after false information is fed into the system in Section 4.

Section 5 tests the nonlinear model of the vehicle under the different scenarios.
In Section 6, the effects of using PID control is seen. Also, how the presence of oscillations affect the system is observed.

Finally, Section 7 concludes the analysis and addresses future work.

2. STUDY OF VEHICLE MODELS

2.1 Overview

Research in areas of vehicle control or safety has led to the creation of many car products such as anti-lock brake systems, active suspension systems, and the development of automated ground transport, vehicle-follower controller, etc., that have tremendously affected vehicle safety on roadways. And for all these studies, having a good vehicle model to work on has been the most important part of it all. A good vehicle model is one that can be used to predict the dynamics that a real car has. Such a model would be able to simulate a real car in many ways if not all. Multiple vehicle models for the purpose of study of better vehicle control or vehicle platoon control are available, involving longitudinal motion, lateral motion, or both.

In the research to be undertaken for better longitudinal vehicle control under a false data attack, different vehicle models were studied to determine the model best suited for the aforementioned purpose. Longitudinal vehicle models are nonlinear in nature, so most researchers tend to use lateral motion of vehicles for analysis. But in the last few decades, study of longitudinal vehicle motion control has been increasing. In most cases, linearizing methods are used, and the experimentation and observations are considered only with respect to the linear range. Thus, when it comes to the analysis of false data attack on vehicle platoons, it is of utmost importance that the vehicle model chosen be as close to a real vehicle as possible, so that the resulting safety measures can be implemented on a real vehicle, thus improving road safety.

The next section provides a brief mention of the papers that have been studied. Following that are the individual vehicle models with descriptions and their respective uses. All the assumptions that have been considered in each of the models have also been discussed. A table briefly summarizing each of the papers follows immediately. And finally, a discussion as to which model is considered here.

2.2 Papers Reviewed

Brennan and Alleyne [28] and Will and Zak [29] used the bicycle model to design their simulator for vehicle dynamics and control and for designing the control for an automated vehicle, respectively. Tai and Tomizuka [9] used a model that is useful for brake and traction control. Sheikholeslam and Desoer [30] studied longitudinal control of vehicle platoons when there is no communication with the lead vehicle. Addressing the problem of automation of heavy-duty vehicles, Yanakiev and Kanellakopoulos [31] designed a longitudinal truck model. Mammar et al. [8] designed an integrated controller for a string of three vehicles that follows the leader using on-board sensors. The developed model utilizes unidirectional control. No et al. [32] used the Lyapunov theory to design a control for longitudinal motion. Hedrick et al. [33] have linearized a nonlinear model and then designed a longitudinal controller to study the string stability effects on the same. Majdoub et al. [10] designed a nonlinear but simple and accurate vehicle model for the purpose of longitudinal motion study.

2.3 Vehicle Models

2.3.1 Model 1

The Illinois Roadway Simulator (IRS) is a novel, mechatronic, scaled test-bed used to study vehicle dynamics and controls. The focus of the research presented in this paper has been to develop a scaled version of a vehicle and a roadway for safe and economic testing of IRS controller strategies.

The bicycle model was taken as an initial estimate for the dynamics of the scaled IRS vehicle. This model assumes a constant longitudinal velocity of the vehicle and consists of two dynamic degrees of freedom: lateral velocity and yaw rate.

The state space model for the vehicle as used by Brennan and Alleyne [28] is given as follows:

$$\begin{bmatrix} \dot{Y} \\ \ddot{Y} \\ \dot{\psi} \\ \ddot{\psi} \end{bmatrix} = \begin{bmatrix} 0 & 1 & 0 & 0 \\ 0 & \frac{A_1}{v} & -A_1 & \frac{A_2}{v} \\ 0 & 0 & 0 & 1 \\ 0 & \frac{A_3}{v} & -A_3 & \frac{A_4}{v} \end{bmatrix} \begin{bmatrix} Y \\ \ddot{Y} \\ \psi \\ \dot{\psi} \end{bmatrix} + \begin{bmatrix} 0 & 0 \\ B_1 & B_2 \\ 0 & 0 \\ B_3 & B_4 \end{bmatrix} \begin{bmatrix} \delta_f \\ \delta_r \end{bmatrix}, \tag{2.1}$$

where

$A_1 = \frac{C_{\alpha f}+C_{\alpha r}}{m}$,
$A_2 = \frac{C_{\alpha r}L_2-C_{\alpha f}L_1}{m}$,
$A_3 = \frac{C_{\alpha r}L_2-C_{\alpha f}L_1}{I_z}$,
$A_4 = \frac{(C_{\alpha r}L_2^2+C_{\alpha r}L_1^2)}{I_z}$,
$B_1 = \frac{C_{\alpha f}}{m}$,
$B_2 = \frac{C_{\alpha r}}{m}$,
$B_3 = \frac{L_1 C_{\alpha f}}{I_z}$,
$B_4 = \frac{L_2 C_{\alpha r}}{I_z}$,

and the variables are defined as:

m = mass of the vehicle,
I_z = vehicle inertia about vertical axis at center of gravity,
V = vehicle forward velocity,
$C_{\alpha f}, C_{\alpha r}$ = front, rear cornering stiffness,
$L = L_1 + L_2$, which are the link length of the sensor linkages,
δ_f, δ_r = front and rear steering angle (input to the system),
ψ = yaw angle
Y = lateral position relative to some reference,
$\dot{Y}$ = lateral velocity,
$\ddot{Y}$ = lateral acceleration,
$\dot{\psi}$ = angular velocity, and
$\ddot{\psi}$ = angular acceleration.

From Equation 2.1, the transfer function from the input steering angle to the yaw rate is given as follows:

$$\frac{\dot{\psi(s)}}{\delta(s)} = \frac{C_{\alpha f}V^2 m L_1 s + C_{\alpha f}C_{\alpha r}LV}{a_1 s^2 + a_2 s + a_3}. \tag{2.2}$$

And the transfer function from the rear input steering angle to the yaw rate is given as follows:

$$\frac{\dot{\psi}(s)}{\dot{\delta}(s)} = \frac{-C_{\alpha f}V^2 mL_2 s - C_{\alpha f}C_{\alpha r}LV}{a_1 s^2 + a_2 s + a_3}. \tag{2.3}$$

where

$a_1 = I_z mV^2$
$a_2 = V\left(I_z\left(C_{\alpha f} + C_{\alpha r}\right) + \left(C_{\alpha f}L_1^2 + C_{\alpha r}L_2^2\right)\right)$, and
$a_3 = C_{\alpha f}C_{\alpha r}L^2 - mV^2\left(C_{\alpha f}L_1 - C_{\alpha r}L_2\right)$.

Most of the values in the equations (such as vehicle speed, mass, etc.) were experimentally measured and substituted into the transfer function to obtain a reasonable approximation of the vehicle's transfer function. Similar measurements were made for three different such IRS vehicles. The authors then experimentally verified their model by examining the accuracy of the parameters defined. They compared the frequency response of the entire vehicle from front steer input to yaw rate at a forward velocity of 3.0 m/s, with the transfer functions obtained by substituting the identified parameters for the other two vehicles, and it was seen that the experimental values closely follow the reference model, as seen in Figure 2.1.

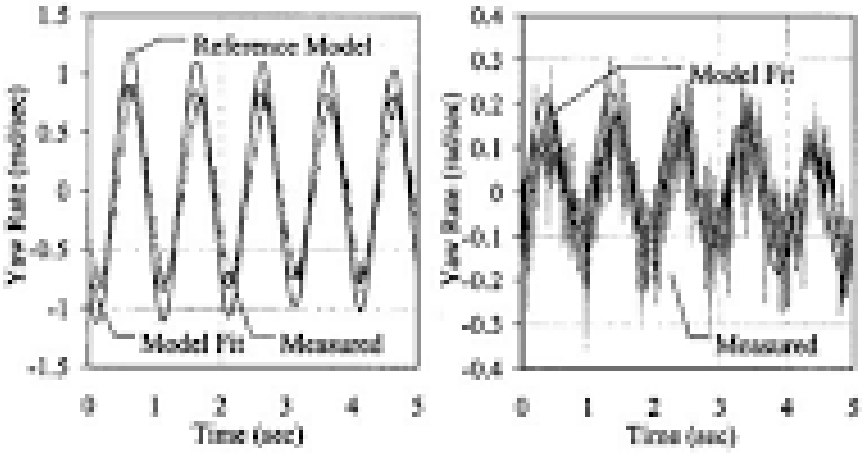

Figure 2.1 Reference model versus experimental yaw rate for front (left) and rear (right) steering.

Apart from evaluation of yaw control schemes, some models were developed for scaled vehicles using this model, which were found to be dynamically similar to actual vehicles, only within a specific range of linear dynamics.

2.3.2 Model 2

The bicycle model has been used here with the vehicle model having four degrees of freedom. The vehicle free-body diagram is given in Figure 2.2. The control inputs to the system are steering angles δ_f (front tires), δ_f (rear tires), and δ_b (brake pedal displacement). Some assumptions were made here before building the vehicle model:

- The vehicle mass can be lumped into three masses.
- The four tires remain in contact with the ground at all times.
- Aerodynamic lift forces, drag forces, and tire-rolling resistance are negligible.
- The deflections in the pitch and roll planes are small.

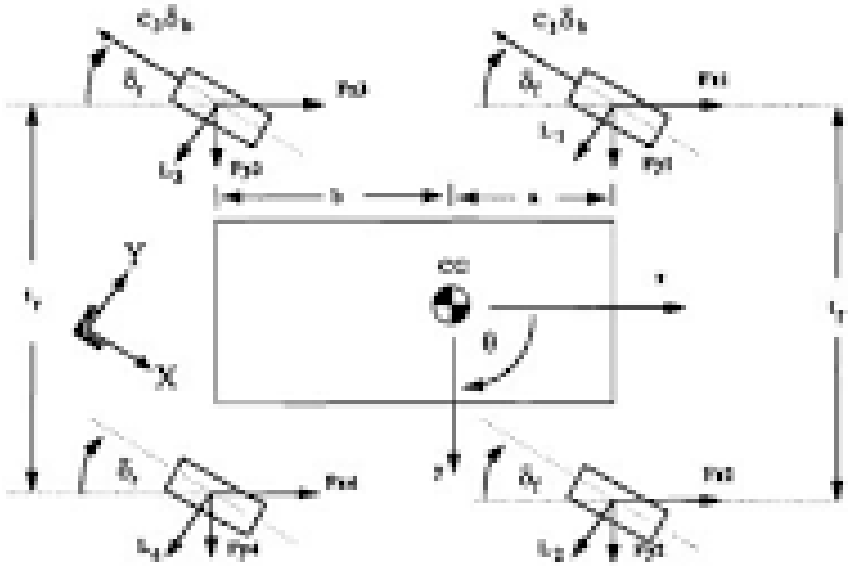

Figure 2.2 Vehicle free body diagram

The state space form is designed to be as follows:

$$\begin{bmatrix} \ddot{x} \\ \ddot{y} \\ \ddot{\theta} \\ \ddot{\phi} \end{bmatrix} = \begin{bmatrix} \dot{y}\dot{\theta} \\ \dot{x}\dot{\theta} + \frac{(-(m_s h_s)^2 g\phi + m_s h_s \beta_{roll}\dot{\phi} + m_s h_s \kappa_{roll}\phi}{m_{tot} I_{roll}} \\ 0 \\ \frac{(m_s h_s g\phi + \beta_{roll}\dot{\phi} + \kappa_{roll}\phi) m_{tot}}{m_{tot} I_{roll} - (m_s h_s)^2} \end{bmatrix} + \begin{bmatrix} \frac{F_x}{m_{tot}} \\ \frac{I_{roll} F_y}{m_{tot} I_{roll} - (m_s h_s)^2} \\ \frac{\tau}{I_z} \\ \frac{-m_s h_s F_y}{m_{tot} I_{roll} - (m_s h_s)^2} \end{bmatrix}, \quad (2.4)$$

where

$\dot{\phi}$ = roll velocity,
$\dot{\theta}$ = yaw velocity,
m_{tot} = total mass,
m_s = sprung mass of the car,
h_s = distance between the center of the sprung mass and the center of the roll axis,
β_{roll} = roll-damping constant,
κ_{roll} = roll-stiffness constant,
I_{roll} = moment of inertia of the vehicle about its roll axis,
F_x = force acting on the vehicle on the x-direction,
F_y = force acting on the vehicle in the y-direction,
I_z = moment of inertia of the vehicle about its z axis,
τ = torque, and
g = acceleration due to gravity.

Now, this model is a nonlinear model. So, to linearize the system and to form a simplified model, a number of assumptions have been considered.

- The longitudinal velocity is a constant.
- No braking is applied, so the brake pedal displacement is a zero.

- Rear-tire steering angle is zero.
- Longitudinal slip is zero.
- The front-wheel steering angle is the only control input.

These assumptions simplify the model into the bicycle model, which is used to design the controller while the original nonlinear model (called the truth model) is used to perform numerical analysis of the closed-loop system. The simplified model has:

$\dot{y}$ = lateral velocity,
θ = yaw angle,
$\dot{\theta}$ = yaw rate or velocity, and
Y = lateral position (considering angular coordinates as well as it is considered that the vehicle will be moving in all directions),

as the state variables. The model is thus now given as:

$$\begin{bmatrix} \ddot{y} \\ \dot{\theta} \\ \ddot{\theta} \\ \dot{Y} \end{bmatrix} = \begin{bmatrix} -2\frac{C_f+C_r}{m_{tot}} & 0 & -U-2\frac{aC_f-bC_r}{I_zU} & 0 \\ 0 & 0 & 1 & 0 \\ -2\frac{aC_f-bC_r}{I_zU} & 0 & -2\frac{a^2C_f-b^2C_r}{I_zU} & 0 \\ -1 & -U & 0 & 0 \end{bmatrix} \begin{bmatrix} \dot{y} \\ \theta \\ \dot{\theta} \\ Y \end{bmatrix} + \begin{bmatrix} 2\frac{C_f}{m_{tot}} \\ 0 \\ 2\frac{aC_f}{I_z} \\ 0 \end{bmatrix} u_1, \tag{2.5}$$

where

U = constant vehicle speed;
C_f and C_r are cornering stiffness for the front and rear wheels, respectively; and
$u_1 = \delta_f$, the front wheel steering angle (the only control input), which are all constant terms (including a and b); and hence make the model a linear model.

The model makes a good approximation of following the desired path as can be seen in Figure 2.3.

As can be seen, a large number of assumptions were made in consideration of designing the model. Also, the system has been linearized completely as the longitudinal motion was taken to be a constant. This model was then used to predict the particular dynamics for steering and braking maneuvers. It has also been used for robust control of yaw-damping of cars.

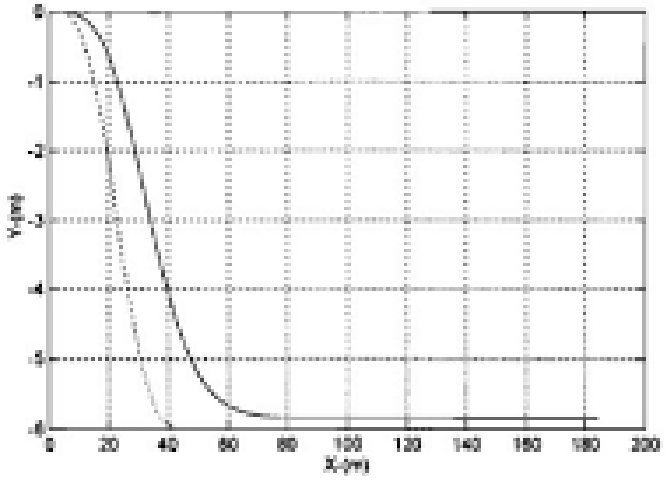

Figure 2.3 Plot showing the design model response and the ideal path

Thus, both the models given by Brennan and Alleyne [28] and Will and Zak [29] use the well-known bicycle model, which considers constant longitudinal motion and has two degrees of freedom: lateral velocity and yaw rate. Thus, it is not a suitable choice for study of longitudinal control.

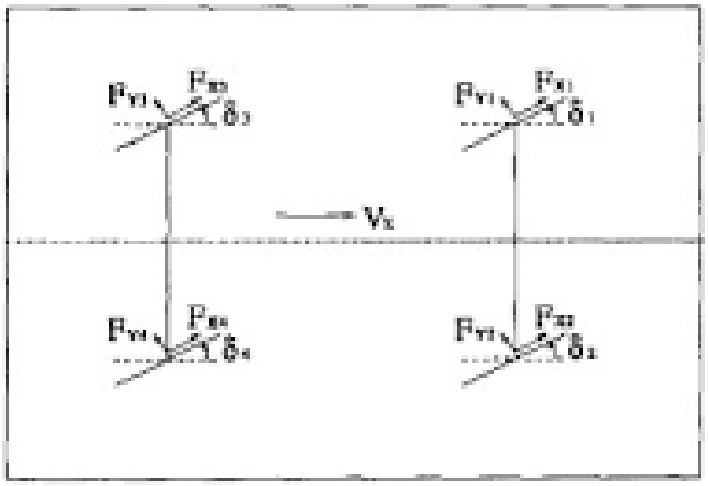

Figure 2.4 Schematic diagram of vehicle

2.3.3 Model 3

Tai and Tomizuka [9] used a longitudinal vehicle model for addressing the longitudinal velocity–tracking problem with emphasis on how to determine the desired traction or brake torque for desired velocity tracking, based on a vehicle with four independent steering wheels. The figure above shows a schematic diagram of a vehicle with four independent steering wheels (Figure 2.4). The vehicle dynamics in the longitudinal direction is considered to be as follows:

$$M\left(\dot{V}_x - \dot{V}_y\dot{\epsilon}\right) = \sum_{i=1}^{4}\left(F_{xi}Cos\delta_i + F_{yi}Sin\delta_i\right) - M_gSin\phi - F_v, \tag{2.6}$$

where

M = total vehicle weight,
F_{xi} = longitudinal tire force in the tire plane,

F_{yi} = side tire force in the tire plane,
δ_i = wheel steering angle,
ϕ = road elevation angle, and
F_v = air drag force.

In vehicle traction and brake control, longitudinal tire force is of highest concern, which is defined to be positive for traction and negative for brake. So, gradually, the model boils down to a wheel-dynamics model. The longitudinal slip (λ) is positive when the vehicle is in traction mode and negative when the vehicle is in brake mode. For some specific range of λ, the force-slip ratio can be given by a linear relationship:

$$F_x = F_z C_5 \lambda \tag{2.7}$$

where

F_z = vertical load on the tire, and
C_5 = a constant that characterizes road and tire conditions.

Tire forces are generated by the relative motion between ground and rolling wheel, which is subject to traction or brake torque. The corresponding equation of motion is given as follows:

$$J_{\omega i}\omega_i = T_{ei} - T_{bi} - F_{xi}R - F_{\omega i} \tag{2.8}$$

where

T_{ed} = engine torque,
T_{bi} = brake torque,
$F_{\omega i}$ = wheel distance,
$J_{\omega i}$ = moment of inertia, and
ω = angular velocity.

Now, some assumptions were made to get the model in terms of longitudinal motion only:

- The coupling between lateral and longitudinal motion is ignored ($\dot{\epsilon}$ = 0),
- The longitudinal slip is very small so that it operates in the linear region only,
- Lateral motion is very small,
- Both engine- and brake-control systems exhibit first-order dynamics.

Taking into consideration the above assumptions, the equation now becomes:

$$M\dot{V}_x = \sum_{i=1}^{4}(F_{xi}). \tag{2.9}$$

With some more assumptions, a linearized wheel dynamics can be obtained which can be used for studying passenger cars and heavy vehicles, with different traction configurations such as front-wheel drive, rear-wheel drive, or four-wheel drive.

This vehicle model does not completely ignore the road–tire interactions, and as a result, all the forces and disturbances of such interactions are present in the vehicle dynamics, making the system comparatively more complex than other linearized models. But it can be used for both traction- and brake-control modes. Also, it is linear only within a range.

2.3.4 Model 4

Sheikholeslam and Desoer [30] have evaluated the performance of longitudinal control laws with no communication of lead-vehicle information in a vehicle platoon.

The longitudinal vehicle dynamics of the *i*th vehicle are modeled as:

$$\dot{F}_i = -\frac{F_i}{\tau_i(\dot{x}_i)} + \frac{u_i}{\tau_i(\dot{x}_i)}, \tag{2.10}$$

$$m_i\ddot{x}_i = F_i - k_{di}x_i^2 - Kmi, \tag{2.11}$$

where

x_i = position of the *i*th vehicle,
F_i = driving force produced by the *i*th vehicle's engine,
m_i = mass of the *i*th vehicle,
$\tau_i(.)$ = engine time lag for the *i*th vehicle,
u_i = throttle command input to the *i*th vehicle's engine,
k_{di} = aerodynamic coefficient for the *i*th vehicle, and
d_{mi} = mechanical drag for the *i*th vehicle.

To linearize and normalize the input-output behavior of each vehicle, exact linearization methods have been applied; both sides of Equation (2.11) is differentiated w.r.t. time and the expression for $\dot{F}_i$ is substituted in terms of $\dot{x}_i$ and $\ddot{x}_i$ from (2.10), to obtain:

$$\dddot{x}_i = b_i(\dot{x}_i, \ddot{x}_i) + a_i(\dot{x}_i u_i), \tag{2.12}$$

where

$$b_i(\dot{x}_i, \ddot{x}_i) = -\frac{1}{\tau_i(\dot{x}_i)}\left[\ddot{x}_i + \frac{K_{di}}{m_i}\dot{x}_i 2 + \frac{d_{mi}}{m_i}\right] - \frac{2K_{di}}{m_i}x_i\dot{\ddot{x}}_i,$$

$$a_i(\dot{x}_i) = \frac{1}{m_i\tau_i(\dot{x}_i)}.$$

Here again, linearization techniques have been applied as per research needs, but the presence of jerk (rate of change of acceleration) in the vehicle dynamics makes it more complex than usual. The degradation of tracking performance when the communication between the leader and the followers is lost is investigated here.

2.3.5 Model 5

Yanakiev and Kanellakopoulos [31] presented the results of adaptive longitudinal control design for heavy vehicles. They developed a turbo-charged diesel engine model suitable for vehicle control and then combined it with automatic transmission, drivetrain, and brake models to obtain a longitudinal heavy-duty vehicle model. They basically developed an adaptive controller for longitudinal control of a heavy-duty vehicle (HDV) using direct adaptation of proportional integral quadratic (PIQ) controller gains.

The angular velocity of the driving wheels (ω_ω) is given by:

$$J_\omega \dot{\omega}_\omega = \frac{M_T}{R_{total}} - F_t h_\omega - M_b, \tag{2.13}$$

where

J_ω = lumped inertia of the wheels,
M_T = turbine torque,
$F_t h_w$ = tractive tire torque,
F_t = tractive tire force,
h_ω = static ground-to-axle height of the driving wheels, and
M_b = braking torque.

The brake actuating system is represented by a first-order linear system with a time constant τ_b where the braking torque M_b is obtained from:

$$\dot{M}_b = \frac{(M_{bc} - M_b)}{\tau_b}, \tag{2.14}$$

where

M_{bc} = commanded braking torque.

This is an approximation of complicated brake dynamics of heavy-duty vehicles, reasonable enough for longitudinal control. The state equation for the truck velocity is then given as:

$$\dot{v} = \frac{F_t - F_a - F_r}{m}, \tag{2.15}$$

where

F_a = aerodynamic drag force,
F_r = force generated by the rolling resistance of the tires, and
m = vehicle mass.

Now, the force

$$F_a = c_a v^2, \tag{2.16}$$

where

c_a = aerodynamic drag coefficient,
v = vehicle speed.

Rolling resistance torque,

$$M_r = F_r h_\omega, \tag{2.17}$$

is a linear function of the vehicle mass,

$$M_r = c_r m g. \tag{2.18}$$

Now, using (2.16) and (2.18) in (2.15),

$$\dot{v} = \frac{F_t - c_a v^2}{m} - \frac{c_r g}{h_w} \tag{2.19}$$

is obtained. Then a first-order filter with a time constant τ_f is included in the vehicle dynamics of the fuel pump and the actuators which transmit the fuel command u to the injectors:

$$\dot{u_f} = \frac{(-u_f + u)}{\tau_f}, \tag{2.20}$$

where u_f is an index to maintain idle speed.
Then linearization is done to obtain a first-order linear model:

$$\frac{\delta v}{\delta u} = \frac{b}{s+a}. \tag{2.21}$$

Thus, they have used a model that although realistic and suitable for vehicle control is specifically a turbocharged diesel engine model, designed for heavy-duty vehicles.

2.3.6 Model 6

The paper by Mammar et al. [8] presents the design and simulation of an automated vehicle string longitudinal control. They have designed a vehicle model for a platoon consisting of a leader and three following vehicles. The acceleration of the vehicle is given by the equation:

$$a = \frac{1}{m}\left[F_{ex} + \frac{1}{r_e}(T_{rr} + \tau_e + \tau_b)\right], \tag{2.22}$$

where

m = vehicle mass,
F_{ex} = the external force which embeds the air drag and the gravitational force due to road slope,
r_e = the wheels' effective radius,
T_{rr} = rolling resistance torque,
t_e = engine torque, and
t_b = braking torque.

Vehicle longitudinal dynamics comprise very nonlinear components, especially when considering engine dynamics. The longitudinal control in such a case involves two levels. In one level, the nonlinear dynamics are compensated while the other will be responsible for the inter-vehicle distance tracking. Under such circumstances, the model for the *i*th vehicle is:

$$\dot{a_i}(t) = -\frac{1}{\tau_i} a_i(t) + \frac{g_i}{\tau_i} u_i^a(t), \tag{2.23}$$

where

a_i = acceleration of *i*th vehicle,
u_i^a = acceleration demand,
t_i and g_i denote the time constant and gain, respectively, of the actuator.

This model is thus simple, linear, and accounts for the forces resulting from road–tire interactions, but it has been assumed that the highly nonlinear components of vehicle longitudinal dynamics has already been completely taken care of.

2.3.7 Model 7

No and Chong [32], in their paper, derive a Lyapunov stability theorem-based control law to control a longitudinal platoon of vehicles. They use a third-order model for a platoon traveling with constant speed and direction:

$$\dot{x}_i = v_i, \tag{2.24}$$
$$\dot{v}_i = a_i, \tag{2.25}$$
$$\dot{a}_i = \frac{1}{\tau_i}(a_i^c - a_i), \tag{2.26}$$

where

x_i = absolute position,
v_i = absolute velocity, and
a_i = absolute acceleration of the *i*th vehicle in the platoon.

Jerk and acceleration limits are also considered with this model. The spacing error between the *i*th and the $(i-1)th$ vehicle is given as follows:

$$\delta_i = x_{i-1} - x_i - H_i \tag{2.27}$$

with H_i as the desired spacing.

So, a fairly simple model has been used, but it is a third-order model and thus has taken into account jerk apart from velocity and acceleration in the model.

2.3.8 Model 8

In their paper, Hedrick et al. [33] have used a longitudinal vehicle model to study the effects of communication delay on a vehicle platoon, and specifically on the string stability.
To linearize the highly nonlinear dynamics, certain assumptions have been made.

- The intake manifold dynamics are very fast compared with the vehicle dynamics.
- The torque converter is locked.
- There is negligible wheel slip.
- There is a rigid drive shaft.

As a result, a simple vehicle dynamics model is obtained:

$$\dot{v}_i = k_1 T_{net}(\alpha_i, v_i) - k_2 T_L(v_i), \tag{2.28}$$

where

T_net = net engine torque,
T_L = the load torque, comprising all external forces,
v_i = velocity of the ith vehicle,

α_i = throttle angle,
k_1 and k_2 = terms related to the vehicle's mass including moments of inertia and gear ratios.

Taking the assumptions into consideration:

- The engine speed can be directly related to the vehicle's velocity by the gear ratio as $v_i = r_i^* \omega_e$ where r_i^* is the gear ratio;
- The engine torque T_{net} can be produced exactly such that it offsets the load torques and so any desired v_i can be produced: $u_i = k_1 T_{net}(\alpha_i, v_i) - k_2 T_L(v_i)$.

Thus, the vehicle dynamics can be linearized and the system represented as follows:

$$\dot{x}_i = v_i \tag{2.29}$$

$$\dot{v}_i = u_i \tag{2.30}$$

Thus, it can be said that longitudinal vehicle dynamics being highly nonlinear, the authors, have linearized the system by considering a set of assumptions and appropriate feedback, resulting in a very simple second-order vehicle model. Here, the effect of communication delay on string stability was studied. It was assumed that the preceding vehicle's position, velocity, and acceleration can be obtained by local sensors via a wireless communication network. Time delay and packet loss, intrinsic characteristics for wireless communication networks, may cause instability of the formation controller and raise safety issues in platoon formation in AHS.

2.3.9 Model 9

All the models discussed above either consider longitudinal motion to be a constant or use a linearized model. The model needed for studying false data injection into vehicle platoons requires work on a longitudinal vehicle model, including its nonlinear behavior so as to be as near to a real scenario as possible. The model can then be linearized for further study.

Majdoub et al. [10] have designed a vehicle model that serves the purpose. The overall vehicle model turns out to be a combination of two nonlinear state space representations describing, respectively, the acceleration and deceleration longitudinal driving modes, as the slip coefficient depends on the current driving mode (acceleration or deceleration). The vehicle's longitudinal dynamics are characterized by two state variables, i.e., vehicle (chassis) speed V_v and front-wheel speed V_ω. Each representation describes the vehicle in the corresponding operation mode:

State space representation in deceleration mode ($V_\omega \leq V_v$):

$$\dot{V_\omega} = a_1 M_m + \left[a_2 + a_3 \frac{V_\omega}{V_v} + a_4 exp\left(a \frac{V_\omega}{V_v}\right)\right]^{-1} \left[a_5 + a_6 \frac{V_\omega}{V_v} + a_7 (V_v - V_a)^2 + a_8 \frac{V_\omega}{V_v} (V_v - V_a)^2 + a_g exp\left(a \frac{V_\omega}{V_v}\right) + a_{10} (V_v - V_a)^2 exp\left(a \frac{V_\omega}{V_v}\right)\right], \tag{2.31a}$$

$$\dot{V_v} = a_{11} + a_{12} (V_v - V_a)^2 \left[a_2 + a_3 \frac{V_\omega}{V_v} + a_4 exp\left(a \frac{V_\omega}{V_v}\right)\right]^{-1} \left[a_{13} + a_{14} \frac{V_\omega}{V_v} + a_{15} (V_v - V_a)^2 + a_{16} \frac{V_\omega}{V_v} (V_v - V_a)^2 + a_{17} exp\left(a \frac{V_\omega}{V_v}\right) + a_{18} (V_v - V_a)^2 exp\left(a \frac{V_\omega}{V_v}\right)\right] \tag{2.31b}$$

where

$\sum_{i=1}^{18}$ = various parameters,
M_m = couple that drives the wheel, and
V_a = wind speed.
Now, let:
$u = M_m$,
$x_1 = V_\omega$,
$x_2 = V_v$,

$$f_1(x_1, x_2) = \left[a_2 + a_3\frac{x_1}{x_2} + a_4 exp\left(a\frac{x_1}{x_2}\right)\right]^{-1}\left[a_5 + a_6\frac{x_1}{x_2} + a_7(x_2 - V_a)^2 + a_g exp\left(a\frac{x_1}{x_2}\right) + a_{10}(x_2 - V_a)^2 exp\left(a\frac{x_1}{x_2}\right)\right],$$

$$f_2(x_1, x_2) = a_{11} + a_{12}(x_2 - V_a)^2\left[a_2 + a_3\frac{x_1}{x_2} + a_4 exp\left(a\frac{x_1}{x_2}\right)\right]^{-1}\left[a_{13} + a_{14}\frac{x_1}{x_2} + a_{15}(x_2 - V_a)^2 + a_{16}\frac{x_1}{x_2}(x_2 - V_a)^2 + a_{17} exp\left(a\frac{x_1}{x_2}\right) + a_{18}(x_2 - V_a)^2 exp\left(a\frac{x_1}{x_2}\right)\right].$$

Thus, the model (Equations 2.31a and 2.31b) can be represented in compact form:

$$\dot{x_1} = a_1 u + f_1(x_1, x_2) \tag{2.32a}$$

$$\dot{x_2} = f_2(x_1, x_2) \tag{2.32b}$$

Similarly, *State space representation in deceleration mode* ($V_v < V_\omega$):

$$\dot{x_1} = a_{\acute{1}} u + f_{\acute{1}}(x_1, x_2) \tag{2.33a}$$

$$\dot{x_2} = f_{\acute{2}}(x_1, x_2), \tag{2.33b}$$

where

$$f_{\acute{1}}(x_1, x_2) = \left[\acute{a_2} + \acute{a_3}\frac{x_2}{x_1} + a_4 exp\acute{\left(\acute{a}\frac{x_2}{x_1}\right)}\right]^{-1}\left[\acute{a_5} + \acute{a_6}\frac{x_2}{x_1} + \acute{a_7}(x_2 - V_a)^2 + \acute{a_g} exp\left(a\frac{x_2}{x_1}\right) + a'_{10}(x_2 + V_a)^2 exp\left(\acute{a}\frac{x_2}{x_1}\right)\right],$$

$$f_{\acute{2}}(x_1, x_2) = a'_{11} + a'_{12}(x_2 - V_a)^2\left[\acute{a_2} + \frac{\acute{a_3}x_2}{x_1} + \acute{a_4}\exp\left(a\frac{\acute{x_2}}{x_1}\right)\right]^{-1}\left[a'_{13} + \frac{a'_{14}x_2}{x_1} + a'_{15}(x_2 - V_a)^2 + \frac{a'_{16}x_2}{x_1}(x_2 - V_a)^2 + a'_{17}\exp\left(a\frac{x_2}{x_1}\right) + a'_{18}(x_2 - V_a)^2\exp\left(a\frac{\acute{x_2}}{x_1}\right)\right],$$

where

$\sum_{i=1}^{18}$ = different parameters.

Now, combining Equations 2.32 and 2.33, the whole system is given in the following form:

$$\dot{x_1} = a_1^*(x_1, x_2)u + g_1(x_1, x_2) \tag{2.34a}$$

$$\dot{x_2} = g_2(x_1, x_2), \tag{2.34b}$$

Where 2.34 represents the vehicle model with the tire-road interactions taken into consideration with:

$$g_1(x_1, x_2) = \sigma(x_1, x_2) f_1(x_1, x_2) + \big(-\sigma(x_1, x_2)\big) f_1'(x_1, x_2),$$
$$g_2(x_1, x_2) = \sigma(x_1, x_2) f_2(x_1, x_2) + \big(-\sigma(x_1, x_2)\big) f_2'(x_1, x_2),$$
$$a_1^*(x_1, x_2) = \sigma(x_1, x_2) a_1 + \big(-\sigma(x_1, x_2)\big) a_1',$$
$$\sigma(x_1, x_2) = \frac{1 - sign(x_1 - x_2)}{2}.$$

Here, if road-tire contact is ignored, the immediate consequence is that $V_v = V_\omega$, i.e. $x_1 = x_2$, resulting in the equation:

$$\dot{V}_v = \frac{r_{eff}}{J + r_{eff}^2 M_v} M_m - \frac{r_{eff}^2 M_v}{J + r_{eff}^2 M_v} \left[g sin\theta + \frac{1}{2M_v} \rho S C_x (x_2 - V_a)^2 \right]. \quad (2.35)$$

Now, let:

$$\xi = \frac{r_{eff}}{J + r_{eff}^2 M_v}$$

and

$$f(x_2) = \frac{r_{eff}^2 M_v}{J + r_{eff}^2 M_v} \left[g sin\theta + \frac{1}{2M_v} \rho S C_x (x_2 - V_a)^2 \right].$$

Hence, the vehicle model can be represented as follows:

$$\dot{x_1} = \xi u + f(x_2), \quad (2.36)$$

where

r_{eff} = effective wheel radius,
J = inertia resulting from the wheel, transmission shaft, and driving motor,
M_v = vehicle mass,
θ = road slope,
ρ = air density depending on atmospheric pressure and ambient temperature,
S = frontal projection area of vehicle,
C_x = aerodynamic drag coefficient, and
g = acceleration due to gravity.

The model represented by 2.36 gives a compact form of the whole idea.

The authors also developed another model that is a more realistic vehicular longitudinal model that structurally enforces the state variables (x_1, x_2) so as to maintain them within a domain. Controllers are designed based on the models 2.34 and 2.36 and tested on the realistic model.

2.4 Discussion

The bicycle model has been used in many papers other than by Brennan and Alleyne [28] and Will and Zak [29] (ignoring the longitudinal dynamics), like Nalecz and Biendemann [34], who used it as a special case. Mohajerpoor et al. [35], in their work, used the model as the framework to extract the equations of

motion for their work; while Ramanata [36] in his thesis derived and validated the bicycle model with three degrees of freedom (utilizing both the lateral and longitudinal dynamics).

Biral et al. [37] utilized the model given by Tai and Tomizuka [9] but reduced it to a simpler second-order model for their work. Although their control algorithm has been referred to a number of times, the model used by Tai and Tomizuka [9] has not been used much in other papers.

The model described in the work by Sheikholeslam and Desoer [30] has been used in multiple works [38–42]. In Nieuwenhuijze's work [43], there is a combination of the models used by Sheikholeslam and Desoer [30] and Liu et al. [33]. The linearization techniques used by Sheikholeslam and Desoer [30] have been used by Ploeg et al. [44].

The paper by Yanakiev and Kanellakopoulos [31] has been referred to in a number of papers, but the model has been reused only in the papers by the same authors [45–50]. Meanwhile, their approach for studying longitudinal control in heavy-duty vehicles has been utilized in other works but not the model. The work done by Mammar et al. [8] has not been used or referred to in any other work as of yet, nor has the model used by them been validated anywhere.

He and Lu [51] have used the third-order model defined in the work done by Chong et al. [32] for trafficability analysis at traffic crossings by optimizing parameters to reduce platoon spacing. The idea of the model by Chong et al. [32] has also been used by Junaid et al. [52] in their work.

The control algorithm used by Liu et al. [33] has been referred to more often in others' works than the model used by them. Nieuwenhuijze [43] and Xiao et al. [53], have used the assumptions provided as well as the vehicle model by Liu et al. [33], along with other works.

Attia et al. [54] used the same approach to design a vehicle model as done by Majdoub et al. [10] and based the tire model on the work done by Kiencke and Nielsen [55]. They have also used the same approach in another of their works that deals with lateral and longitudinal control of an automotive vehicle [56]. Giri et al. [57] have also used the model given by Majdoub et al. [10] to study the tire effect in longitudinal vehicle control. In their book, Kiencke et al. [55] have the complete description and the validation of the tire model that has been extensively used by many others in their works.

Most of the previous works on longitudinal control were based on simple models neglecting important nonlinear aspects of the vehicle such as rolling resistance, aerodynamic effects, and road load. A convenient model is one that is sufficiently accurate but remains simple enough to be utilizable in control design.

But, for more accuracy, control design relies on a more complete model that accounts for most vehicle nonlinear dynamics, including tire-road interaction. The models given by Majdoub et al. [10] are more realistic as they include the nonlinearities associated with longitudinal motion. Also, they can be used as and when necessary depending on the extent of simplicity and realisticity needed. The model dynamics is based on the well-known and validated bicycle model, and the tire model used is also Kiencke's validated and widely used model. Thus, overall, the model defined in the work by Majdoub et al. [10] is a suitable choice for studying longitudinal vehicle motion.

In this work, the model by Majdoub et al. [10] has been used although it has been completely linearized, as a simple model was to be used for the study, ignoring all nonlinearities.

The following table gives an overall idea about the vehicle models.

Table 2.1 Summary of vehicle models.

Model	Paper/Citation	Main idea	Shortcoming	Experimental validation
Model-1 (Bicycle model)	Brennan and Alleyne [28]	To develop a scaled version of a vehicle and a roadway for safe and economic testing of controller strategies	Although validation for "bicycle" model is there, longitudinal motion is ignored.	Yes
Model -2 (Bicycle model)	Will and Zak [29]	To particularly predict the dynamics for steering and braking maneuvers	Although validation for "bicycle" model is there, longitudinal motion is ignored	Yes
Model - 3	Tai and Tomizuka [9]	Addressing the longitudinal velocity tracking problem	Control algorithm more commonly used than the model; model not experimentally validated	No
Model - 4	Sheikholeslam and Desoer [30]	Evaluated the performance of longitudinal control laws with no communication of lead vehicle information, in a vehicle platoon	Model used in a number of other papers, but, presence of jerk complicates the system	No
Model - 5	Yanakiev and Kanellakopoulos [31]	Adaptive longitudinal control design for heavy-duty vehicles	A turbocharged diesel engine model, designed specifically for heavy-duty vehicles. Also, model reused by same authors only.	No
Model - 6	Mammar et al. [8]	Presents the design and simulation of an automated vehicle string longitudinal control.	Unidirectional platoon strategy used. Model not referred to in any other work as of yet.	No
Model - 7	No and Chong [32]	Derive a Lyapunov stability theorem–based control law to control a longitudinal platoon of vehicles.	Presence of jerk complicates the system; model used only in 2 papers	No
Model - 8	Hedrick et al. [33]	Used a longitudinal vehicle model to study the effects of communication delay on a vehicle platoon, and specifically on the string stability.	Control algorithm has been more in use than the model	No
Model - 9	Majdoub et al. [10]	Designing a nonlinear model that will be useful in the study of vehicle longitudinal motion control, based on "bicycle" model and Kiencke's model, both of which are validated.	Retains nonlinearity	Yes

3. VEHICLE AND STRING MODELING

3.1 Vehicle Model

The vehicle model used is a simple and nonlinear model and has been obtained ignoring the tire dynamics of the system, as done by Majdoub et al. [10] in their work. The model is given as follows:

$$\dot{x}_i = v_i$$
$$\dot{v}_i = c_1 w - c_2 (v_i - c_3)^2,$$

where x_i is the position (with i = 1, 2, 3...n), v_i is the velocity, c_1, c_2, and c_3 are constants depending on the effective wheel radius, inertia resulting from the wheel, transmission shaft and driving motor, vehicle mass, road slope, air density, frontal projection area of the vehicle, aerodynamic drag coefficient, and acceleration due to gravity, and ω is the control input.

Using feedback linearization technique [58]:

Let

$$w = \frac{c_2}{c_1}((v_i - c_3)^2) + \frac{u}{c_1}.$$

Thus, the following model is obtained:

$$\dot{x}_i = v_i,$$
$$\dot{v}_i = u,$$

where u is the new control input.

3.2 String Model

In this work, it is assumed that the vehicles travel in the same direction at all times on a horizontal road surface, using bidirectional inter-vehicle communication, in which the controller receives relative position and velocity information from both the preceding and following vehicles. The model is based on the mass-spring-damper system as can be seen in Figure 3.1, in which x_n is the position of the first mass, representing the leading vehicle, k is the spring constant that represents the proportional gain, and c is the damper constant that represents the derivative gain [4]. This model is used as it is easier to implement into a physical model.

The state space representation of the string model in absolute and error dynamics are given as follows.

3.2.1 Absolute Dynamics Model

Assuming the variables used for the model as:

x_i = position of the vehicles,
v_i = velocity of the vehicles,
d = desired spacing,
K_p = proportional gain, and
K_v = derivative gain,

where x_n and v_n are the position and velocity of the lead vehicle while x_1 and v_1 are the position and velocity of the last vehicle.

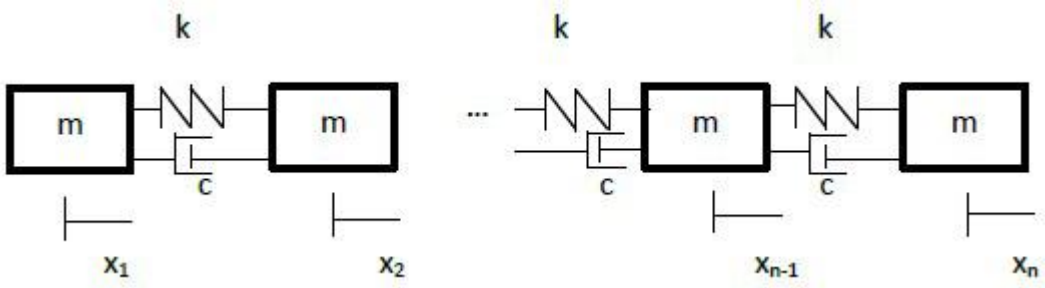

Figure 3.1 Mass-spring-damper system emulating a vehicle platoon.

The absolute-dynamics model for n number of vehicles is given as follows:

$$\dot{x_1} = v_1 \tag{3.1a}$$
$$\dot{v_1} = K_p(x_2 - x_1 - d) + K_v(v_2 - v_1) \tag{3.1b}$$

$$\dot{x_2} = v_2 \tag{3.2a}$$
$$\dot{v_2} = K_p(x_3 - x_2 - d) + K_v(v_3 - v_2) + K_p(x_1 - x_2 + d) + K_v(v_1 - v_2), \tag{3.2b}$$

$$\dot{x_3} = v_3 \tag{3.3a}$$
$$\dot{v_3} = K_p(x_4 - x_3 - d) + K_v(v_4 - v_3) + K_p(x_2 - x_3 + d) + K_v(v_2 - v_3), \tag{3.3b}$$

$$\dot{x_{m-1}} = v_{m-1} \tag{3.4a}$$
$$\dot{v_{m-1}} = K_p(x_m + -x_{m-1} - d) + K_v(v_m - v_{m-1}) + K_p(x_{m-2} - x_{m-1} + d) + K_v(v_{m-2} - v_{m-1}), \tag{3.4b}$$

$$\dot{x_m} = v_m \tag{3.5a}$$
$$\dot{v_m} = K_p(x_{m+1} - x_m - d) + K_v(v_{m+1} - v_m) + K_p(x_{m-1} - x_m + d) + K_v(v_{m-1} - v_m), \tag{3.5b}$$

$$\dot{x_{m+1}} = v_{m+1} \tag{3.6a}$$
$$\dot{v_{m+1}} = K_p(x_{m+2} - x_{m+1} - d) + K_v(v_{m+2} - v_{m+1}) + K_p(x_m + -x_{m+1} + d) + K_v(v_m - v_{m+1}), \tag{3.6b}$$

$$\vdots$$

$$\dot{x_{n-1}} = v_{n-1} \tag{3.7a}$$
$$\dot{v_{n-1}} = K_p(x_n - x_{n-1} - d) + K_v(v_n - v_{n-1}) + K_p(x_{n-2} - x_{n-1} + d) + K_v(v_{n-2} - v_{n-1}), \tag{3.7b}$$

$$\dot{x_n} = v_n \tag{3.8a}$$
$$\dot{v_n} = 0 \tag{3.8b}$$

As can be seen, the leader has a fixed velocity and thus always moves with *zero* acceleration. It is thus understood that the attacker or any other vehicle will have no effect on the leader.

3.2.2 Error Dynamics Model

To obtain the error dynamics model, the following variables are first chosen:

$$z_i = x_{i+1} - x_i - d,$$

and

$$y_i = v_{i+1} - v_i,$$

where

z_i = difference between the relative positions $(x_{i+1} - x_i)$, and desired spacing d,
y_i = relative velocity, which is also the derivative of z_i.

Implementing these variables on Equations 3.1 to 3.8, the following are obtained:

$$\dot{z_1} = y_1 \quad (3.9a)$$
$$\dot{y_1} = K_p z_2 + K_v y_2 - 2K_p z_1 - 2K_v y_1, \quad (3.9b)$$
$$\dot{z_2} = y_2 \quad (3.10a)$$
$$\dot{y_2} = K_p z_1 + K_v y_1 - 2K_p z_2 - 2K_v y_2 + K_p z_3 + K_v y_3, \quad (3.10b)$$
$$\vdots$$
$$\dot{z_{n-2}} = y_{n-2} \quad (3.11a)$$
$$\dot{y_{n-2}} = K_p z_{n-3} + K_v y_{n-3} - 2K_p z_{n-2} - 2K_v y_{n-2} + K_p z_{n-1} + K_v y_{n-1}, \quad (3.11b)$$

$$\dot{z_{n-1}} = y_{n-1} \quad (3.12a)$$
$$\dot{y_{n-1}} = K_p z_{n-1} + K_v y_{n-1} - K_p z_{n-2} - K_v y_{n-2}. \quad (3.12b)$$

In the error dynamics form, $2(n-2)$ equation for n number of vehicles are given. The error dynamics is needed to study the string stability of the vehicle platoon.

4. FALSE DATA INJECTION-LINEAR MODEL

Here, a vehicle platoon with a bidirectional-constant spacing platooning strategy has been used (as it provides string stability in automated vehicle control [59]). In this strategy, information from both the preceding and following vehicles are taken into consideration while making control decisions to maintain constant spacing between the vehicles. Also, the controller used is the proportional-derivative (PD) controller, with K_p as the proportional gain and K_v as the derivative gain, throughout.

Considering that there is one attacker in the platoon who can send false information to the vehicle that is immediately preceding and/or following it, the following cases can be analyzed:

4.1 Addition of Constant Errors

4.1.1 Case 1

The last vehicle in the platoon (3.1) is the attacker, and it provides inaccurate position and velocity information to the preceding vehicle.

Theorem 1. When the attacker is at the end of the vehicle platoon, and it sends false position ($\mathrm{d_e}$) and velocity data ($\mathrm{v_e}$) to the preceding vehicle, there is a shift in the position error ($\pm \mathrm{K_e d_e} \pm \mathrm{K_v v_e}$) from 0, of all the vehicles except the attacking vehicle, although all the vehicles reach the desired velocity (leader velocity $\mathrm{v_n}$). Thus, the attacker set the inter-vehicle separation for the entire platoon.

Proof. With the false data injected into the second last vehicle (3.2), by the last vehicle (3.1), which is the attacker, (3.2) is affected as follows:

$$\dot{x_2} = v_2 \tag{4.1a}$$
$$\dot{v_2} = K_p(x_3 - x_2 - d) + K_v(v_3 - v_2) + K_p(x_1 - x_2 + d + d_e) + K_v(v_1 - v_2 + v_e). \tag{4.1b}$$

As can be seen, the affected vehicle given by 4.1 has d_e as the false position data and v_e as the false velocity data injected into it.

Now, it is first shown that all the velocities eventually reach the desired velocity. The vehicles are represented by the equation:

$$\dot{x_i} = v_i \tag{4.2a}$$
$$\dot{v_i} = u. \tag{4.2b}$$

Considering the velocity components from the system of equations given by 4.2b, they can be represented in the following matrix:

$$A_v = \begin{bmatrix} -K_v & K_v & 0 & 0 & \cdots & 0 & 0 & 0 \\ K_v & -2K_v & K_v & 0 & \cdots & 0 & 0 & 0 \\ 0 & K_v & -2K_v & K_v & \cdots & 0 & 0 & 0 \\ 0 & 0 & K_v & -2K_v & \cdots & 0 & 0 & 0 \\ \vdots & \vdots & \vdots & \vdots & \ddots & \vdots & \vdots & \vdots \\ 0 & 0 & 0 & 0 & \cdots & K_v & -2K_v & K_v \\ 0 & 0 & 0 & 0 & \cdots & 0 & K_v & -K_v \end{bmatrix},$$

which, as can be seen, is an $n \times n$ Laplacian matrix[1]. Now, to get the equilibrium[2] points of the system, the stationary equation is solved:

$$A_v v_i = 0$$

Solving which, the following is obtained:

$$v_1 = v_2 = \cdots = v_n.$$

And it is also seen that all the eigenvalues of A, the system matrix of the whole platoon (4.2) are negative(< 0), where A is given as follows:

$$A = \begin{bmatrix} 0 & 1 & 0 & 0 & 0 & 0 & \cdots & 0 & 0 & 0 & 0 \\ -K_p & -K_v & K_p & K_v & 0 & 0 & \cdots & 0 & 0 & 0 & 0 \\ 0 & 0 & 0 & 1 & 0 & 0 & \cdots & 0 & 0 & 0 & 0 \\ K_p & K_v & -2K_p & -2K_v & K_p & K_v & \cdots & 0 & 0 & 0 & 0 \\ 0 & 0 & 0 & 0 & 0 & 1 & \cdots & 0 & 0 & 0 & 0 \\ 0 & 0 & K_p & K_v & -2K_p & -2K_v & \cdots & 0 & 0 & 0 & 0 \\ \vdots & \vdots & \vdots & \vdots & \vdots & \vdots & \ddots & \vdots & \vdots & \vdots & \vdots \\ 0 & 1 & 0 & 0 & 0 & 0 & \cdots & 0 & 1 & 0 & 0 \\ 0 & 0 & 0 & 0 & 0 & 0 & \cdots & -2K_p & -2K_v & K_p & K_v \\ 0 & 1 & 0 & 0 & 0 & 0 & \cdots & 0 & 0 & 0 & 1 \\ 0 & 0 & 0 & 0 & 0 & 0 & \cdots & K_p & K_v & -K_p & -K_v \end{bmatrix}.$$

Thus, it suffices to say that the system eventually goes to a stable[3] equilibrium point [63].

And so, the system gradually goes to v_n, which is the desired velocity. And as the whole platoon goes to a constant velocity, it can be said that the platoon eventually goes to zero acceleration. So, the velocity of any *i*th vehicle v_i goes to v_n:

$$\Rightarrow v_i = v_{i+1} = v_n,$$

where $i = 1 \ldots (n-1)$, thus making all

$$(v_i - v_{i-1}) = (v_i - v_{i+1}) = 0.$$

So at zero acceleration, from 3.1b, the following is obtained:

$$K_p(x_2 - x_1) = K_p d. \tag{4.3}$$

[1] In a Laplacian matrix, the sum of the rows and the sum of the columns is zero [60].

[2] Equilibrium point: A point x_o in the state space is an equilibrium point of the autonomous system $\dot{x} = Ax$ if, when the state x reaches x_0 for all future times. That is, for a linear time invariant (LTI) system, the equilibrium point is the solution of the equation: $Ax_0 = 0$ [61].

[3] Stability: The homogeneous LTI system $\dot{x} = Ax$ is said to be marginally asymptotically stable if, for every initial condition $x(t_0 = x_0)$ the homogeneous state-space response $x(t) = \phi(t, t_0)x_0 \; \forall t \geq 0$, where $\phi(t, t_0)$ is the state transition matrix, is uniformly bounded. The system is asymptotically stable if $x(t) \to 0$ as $t \to \infty$. The homogenous LTI system is both asymptotically and marginally stable if all the eigen values of A have negative real part. Thus, the system $\dot{x} = Ax$ is stable if $Re[\lambda_i] < 0$ for $i \in [1, n]$, where λ_i are eigenvalues of the system [62].

Using 4.3 in 3.2b the following is obtained:

$$K_p(x_3 - x_2) = K_p d - K_p d_e - K_v v_e, \tag{4.4}$$

Again, using 4.4 in 3.3b yields 4.5 and so on

$$\begin{aligned} K_p(x_4 - x_3) &= K_p d - K_p d_e - K_v v_e, \\ &\vdots \\ K_p(x_n - x_{n-1}) &= K_p d - K_p d_e - K_v v_e. \end{aligned} \tag{4.5}$$

Thus, all the inter-vehicular spacings are shifted by a value of $\left(- K_p d_e - K_v v_e\right)$ instead of being $K_p d$ in case of the predecessor spacing error, and by a value of $\left(K_p d_e + K_v v_e\right)$ in the follower spacing error. In the following figures (Figures 4.1, 4.2 and 4.3), where a platoon of 10 vehicles, with $d_e = 5$ and $v_e = 5$ have been considered, it can be seen that the position error has a shift of $\pm$ 43.5 with K_p taken to be 1 and K_v considered to be 7.7, while all the vehicles reached the desired velocity.

So, in this scenario, the attacker is able to create a huge distance between the second last vehicle of the platoon and the rest of the vehicles preceding it. Thus, it might eventually result in the victim gradually moving out of the effective region of the sensors.

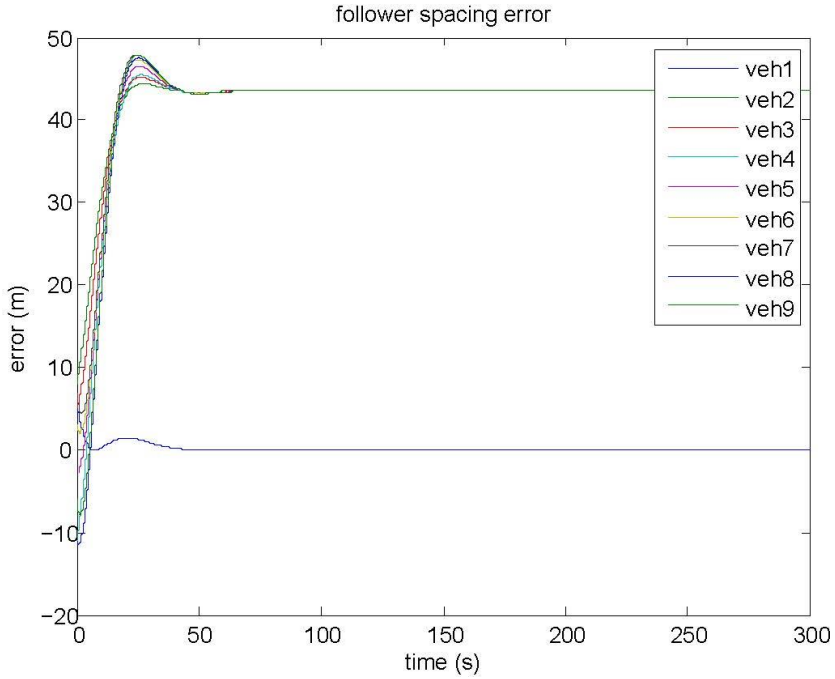

Figure 4.1 In a platoon of 10 vehicles, the follower spacing error is 43.5.

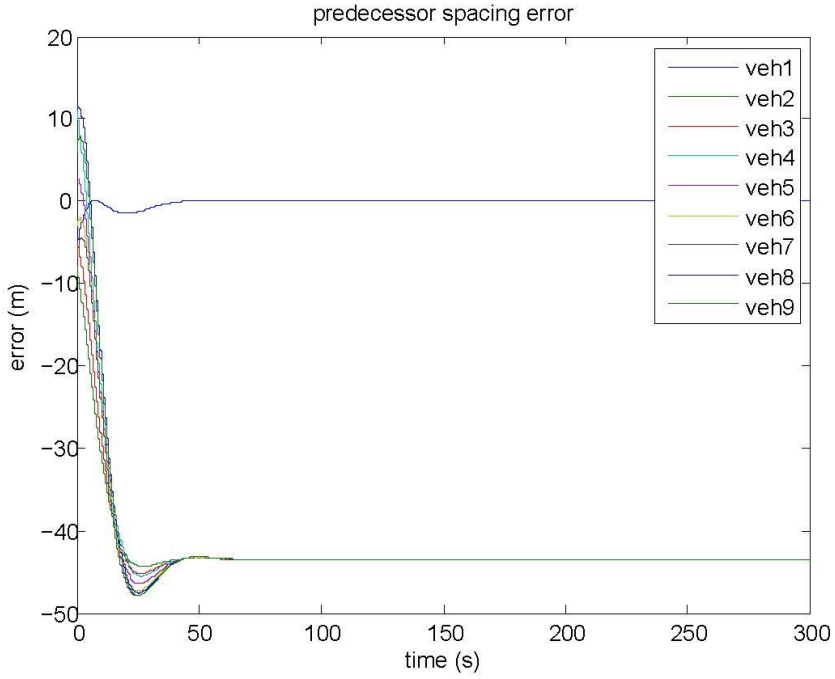

Figure 4.2 In a platoon of 10 vehicles, the predecessor spacing error is -43.5.

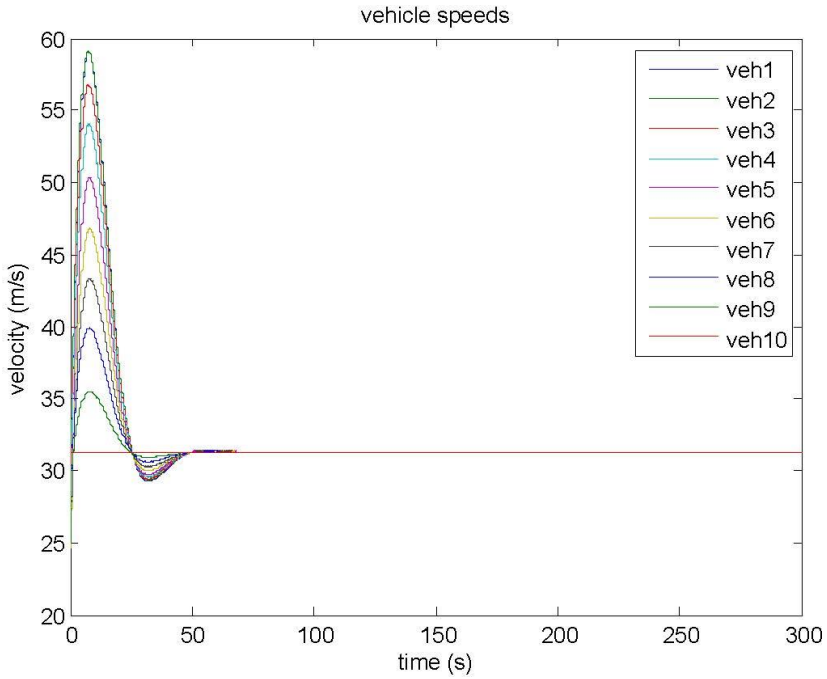

Figure 4.3 In spite of the false data injected, the velocities go to the desired value of 31.29 (in this case).

4.1.2 Case 2

The attacker is at the center of the vehicle platoon, and it sends false position and velocity information to both the preceding and following vehicles.

Theorem 2. When a vehicle platoon has an attacker at the center that provides false position and velocity information to both preceding and following vehicles, although the velocities reach the desired value, there are varied spacing errors throughout the platoon. Thus, the attacker gains control over only the positions of the vehicles.

Proof. In an *n*-vehicle platoon, considering the *m*th vehicle to be the vehicle in the middle, as defined under Chapter 3, Absolute Dynamics Model, Equations 3.4 and 3.6 can be rewritten with the added position error (d_e) and velocity error (v_e) as:

$$\dot{x_{m-1}} = v_{m-1} \tag{4.6a}$$

$$\dot{v_{m-1}} = K_p(x_m + d_e - x_{m-1} - d) + K_v(v_m + v_e - v_{m-1}) + K_p(x_{m-2} - x_{m-1} + d) + K_v(v_{m-2} + v_{m-1}), \tag{4.6b}$$

$$\dot{x_m} = v_m \tag{4.7a}$$

$$\dot{v_m} = K_p(x_{m+1} - x_m - d) + K_v(v_{m+1} - v_m) + K_p(x_{m-1} - x_m + d) + K_v(v_{m-1} - v_m), \tag{4.7b}$$

$$\dot{x_{m+1}} = v_{m+1} \tag{4.8a}$$

$$\dot{v_{m+1}} = K_p(x_{m+2} - x_{m+1} - d) + K_v(v_{m+2} - v_{m+1}) + K_p(x_m + d_e - x_{m+1} + d) + K_v(v_m + v_e - v_{m+1}). \tag{4.8b}$$

where Equation 4.7 is the attacker, at the center. The other equations for the platoon remain the same. Under this scenario, it is seen that the system matrix *A* and the matrix comprising the velocity components from 4.2b are not affected by the false data added and hence remain the same as in the previous case. Thus, it can be said that even in this case, the equilibrium point is given as follows: $v_1 =$

$v_2 = \cdots v_{m-1} = v_m = v_{m+1} = \cdots v_n$. The eigenvalues of the system remain the same and are all < 0. Thus, the system eventually goes to a stable equilibrium point.

So the velocities reach the desired value (leader velocity v_n) eventually, i.e., zero acceleration, making the velocity of any *i*th vehicle to be v_n. Thus any $(v_i - v_{i-1}) = (v_i - v_{i+1} = 0)$.

Now, at zero acceleration, from Equation 3.1b,

$$K_p(x_2 - x_1) = K_p d.$$

From 3.2b,

$$K_p(x_3 - x_2) = K_p d,$$

And the same continues up to the first victim (Equation 4.6). From Equation 4.6b, the position spacing between 4.6 and the attacker (4.7) is given, which as can be seen, instead of $K_p d$, becomes:

$$K_p(x_m - x_{m-1}) = K_p d - K_p d_e - K_v v_e.$$

And the same is seen for the spacing between the attacker (4.7) and the next victim (4.8).

$$K_p(x_{m+1} - x_m) = K_p d - K_p d_e - K_v v_e \tag{4.9}$$

While for the rest of the inter-vehicular spacings, instead of $K_p d$ they become:

$$K_p(x_{m+2} - x_{m+1}) = K_p d - 2K_p d_e - 2K_v v_e, \tag{4.10}$$

$$\vdots$$

$$K_p(x_n - x_{n-1}) = K_p d - 2K_p d_e - 2K_v v_e. \tag{4.11}$$

Had the attacker been in any other arbitrary *i*th position instead of being at the center of the platoon, except for the last position (which is discussed in Case 1), the same results as above are seen.
In the following figures (Figures 4.4 and 4.5), it has been shown that in a platoon of 10 vehicles, when the attacker is the 5th vehicle, and it sends false position and velocity data to the 4th and 6th vehicles, the velocities reach the desired value (which in this example is 31.29 m/s) while all the inter-vehicular spacing errors are not at zero. Instead, the inter-vehicular spacing errors are shifted by factors of $(K_p d - K_p d_e - K_v v_e)$ and $(K_p d - 2K_p d_e - 2K_v v_e)$, where, in the example, $K_p = 1$, $K_v = 7.7$, $d_e = 10$, and $v_e = 10$. From Figure 4.6 it can be graphically inferred that, although the velocities reach the desired value, the platoon no longer remains string stable.[4]

In this scenario the attacker is able to create a huge gap between the vehicles instead of the desired spacing. The platoon gets divided into three regions with three different spacings. This scenario does result in collisions among the vehicles in a very short span of time.

[4] String Stability: Let $z_1 = x_1 - x_{1+1}$, where z_1 is the spacing error between the *i*th and the $(i+1)^{th}$ vehicles. Then the string stability criterion is given as: $|G_i(s))| = \left|\frac{z_i}{z_{i+1}}\right| < 1$, for $i = 1 \ldots n-2$, where $s = j\omega$ and ω is the angular frequency, and $|G_i(s))|$ represents the magnitude of the (error) transfer function between the *i*th and $(i+1)^{th}$ vehicles [4].

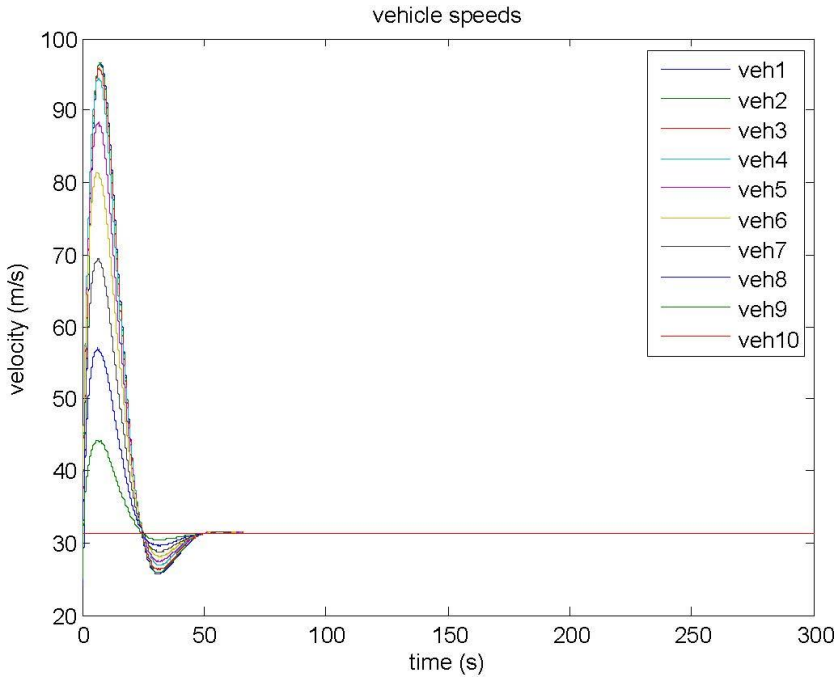

Figure 4.4 In a platoon of 10 vehicles, where vehicle 5 ("veh5") is the attacker, and vehicles 4 and 6 are the victims, all the vehicles reach the desired velocity.

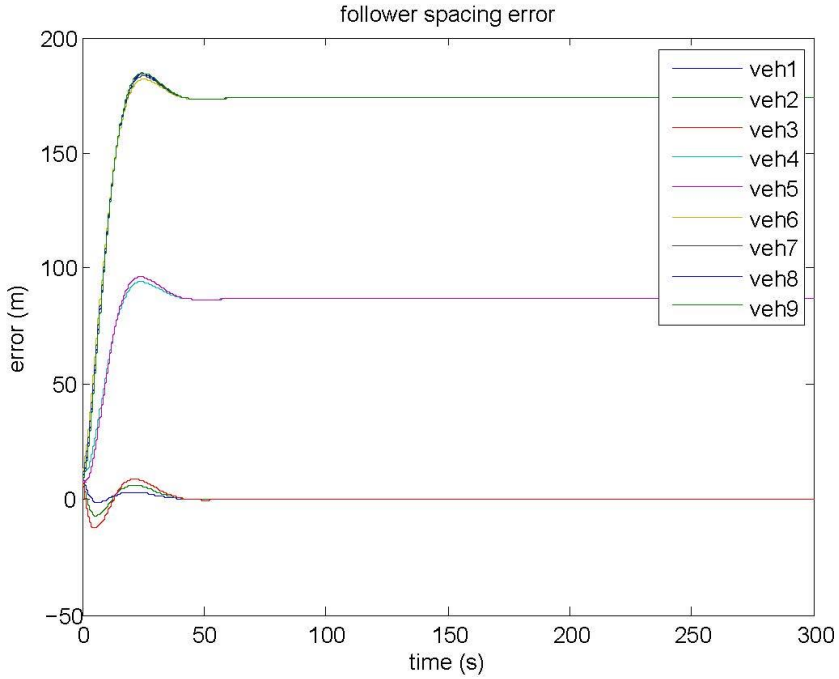

Figure 4.5 In a platoon of 10 vehicles, where vehicle 5 ("veh5") is the attacker, and vehicles 4 and 6 are the victims, the varying spacing error can be seen.

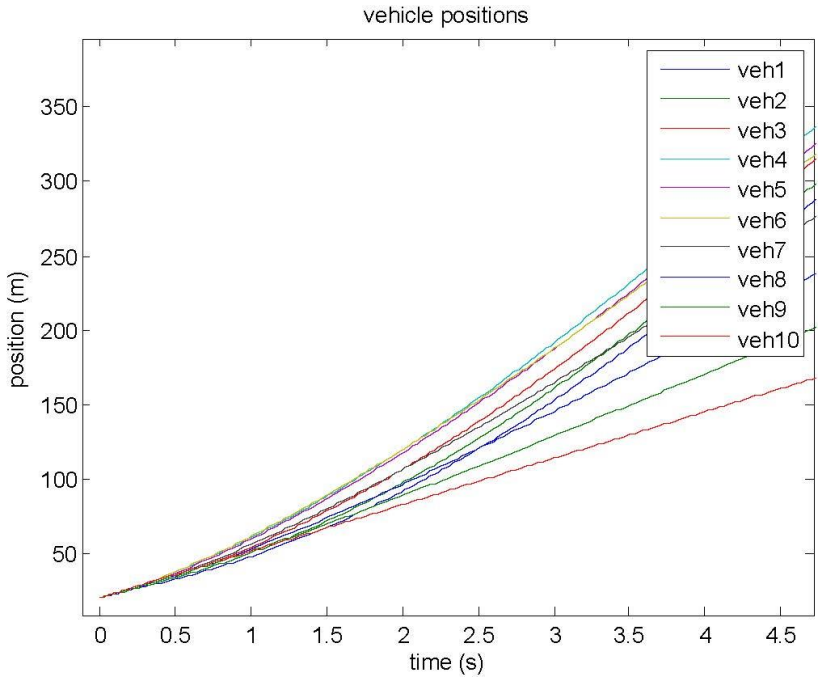

Figure 4.6 In a platoon of 10 vehicles, where vehicle 5 ("veh5") is the attacker, the vehicles 4 and 6 are the victims, the platoon does not remain string stable.

Thus, in the above two cases, the attacker is able to gain some control over the positions of the vehicles, but not the velocity, no matter if it be in the last position (where it affects one vehicle) or any other arbitrary position (where it affects two vehicles).

4.2 Attacker Has Access to Victim's States and Manipulates Its Acceleration

4.2.1 Case 1

The attacker is in an arbitrary *i*th position, and it has access to the states of the vehicle preceding it and it sends false information such that the acceleration of the victim is set to 0.

Theorem 3. When a vehicle platoon has an attacker in an arbitrary *i*th position that sets the acceleration of the preceding vehicle (the victim) to zero, i.e., sets a fixed velocity to it, results in all the vehicles up to the victim attaining the velocity of the victim while the vehicles between the victim and the leader attain velocities such that the difference between them is constant.

Proof. Assuming an *n*-vehicle platoon, where the nth vehicle is the leader, with the attacker in an arbitrary *i*th position, that sets the preceding vehicle's velocity to a new velocity v_v and its acceleration to zero, then the platoon can be written as:

$$\dot{x_1} = v_1 \tag{4.12a}$$
$$\dot{v_1} = K_p(x_2 - x_1 - d) + K_v(v_2 - v_1), \tag{4.12b}$$

$$\dot{x_2} = v_2 \tag{4.13a}$$
$$\dot{v_2} = K_p(x_3 - x_2 - d) + K_v(v_3 - v_2) + K_p(x_1 - x_2 + d) + K_v(v_1 - v_2), \tag{4.13b}$$

$$\vdots$$

$$\dot{x_i} = v_i \tag{4.14a}$$
$$\dot{v_1} = K_p(x_{i+1} - x_i - d) + K_v(v_{i+1} - v_i) + K_p(x_{i-1} - x_i + d) + K_v(v_{i-1} - v_i), \tag{4.14b}$$

$$\dot{x_{i+1}} = v_v \tag{4.15a}$$
$$\dot{v_v} = 0, \tag{4.15b}$$

$$\dot{x_{i+2}} = v_{i+2} \tag{4.16a}$$
$$\dot{v_{i+2}} = K_p(x_{i+3} - x_{i+2} - d) + K_v(v_{i+3} - v_{i+2}) + K_p(x_v - x_{i+2} + d) + K_v(v_v - v_{i+2}), \tag{4.16b}$$

$$\vdots$$

$$\dot{x_{n-1}} = v_{n-1} \tag{4.17a}$$
$$\dot{v_{n-1}} = K_p(x_n - x_{n-1} - d) + K_v(v_n - v_{n-1}) + K_p(x_{n-2} - x_{n-1} + d) + K_v(v_{n-2} - v_{n-1}), \tag{4.17b}$$

$$\dot{x_n} = v_n \tag{4.18a}$$
$$\dot{v_n} = 0. \tag{4.18b}$$

For simplicity, let us assume, $i = 2$, i.e., the 2nd vehicle is the attacker, making the 3rd vehicle the victim. So, the corresponding system matrix is given as follows:

$$A = \begin{bmatrix} 0 & 1 & 0 & 0 & 0 & 0 & \cdots & 0 & 0 & 0 & 0 \\ -K_p & -K_v & K_p & K_v & 0 & 0 & \cdots & 0 & 0 & 0 & 0 \\ 0 & 0 & 0 & 1 & 0 & 0 & \cdots & 0 & 0 & 0 & 0 \\ K_p & K_v & -2K_p & -2K_v & K_p & K_v & \cdots & 0 & 0 & 0 & 0 \\ 0 & 0 & 0 & 0 & 0 & 1 & \cdots & 0 & 0 & 0 & 0 \\ 0 & 0 & 0 & 0 & 0 & 0 & \cdots & 0 & 0 & 0 & 0 \\ \vdots & \vdots & \vdots & \vdots & \vdots & \vdots & \ddots & \vdots & \vdots & \vdots & \vdots \\ 0 & 1 & 0 & 0 & 0 & 0 & \cdots & 0 & 1 & 0 & 0 \\ 0 & 0 & 0 & 0 & 0 & 0 & \cdots & -2K_p & -2K_v & K_p & K_v \\ 0 & 1 & 0 & 0 & 0 & 0 & \cdots & 0 & 0 & 0 & 1 \\ 0 & 0 & 0 & 0 & 0 & 0 & \cdots & K_p & K_v & -K_p & -K_v \end{bmatrix}.$$

It is seen that except the eigenvalues of the victim, which are *zero*, all the rest are < 0, making the system marginally stable. But the system has no positive eigenvalues, thus the system does not become unstable. Now, considering the matrix comprising the velocity components, the following is obtained:

$$A_v = \begin{bmatrix} -K_v & K_v & 0 & 0 & \cdots & 0 & 0 & 0 \\ K_v & -2K_v & K_v & 0 & \cdots & 0 & 0 & 0 \\ 0 & 0 & 0 & 0 & \cdots & 0 & 0 & 0 \\ 0 & 0 & K_v & -2K_v & \cdots & 0 & 0 & 0 \\ \vdots & \vdots & \vdots & \vdots & \ddots & \vdots & \vdots & \vdots \\ 0 & 0 & 0 & 0 & \cdots & K_v & -2K_v & K_v \\ 0 & 0 & 0 & 0 & \cdots & 0 & K_v & -K_v \end{bmatrix}.$$

It can be seen, the row in the matrices corresponding to the acceleration of the victim (the 3rd vehicle) is *zero*. As a system approaches stability, it moves toward the equilibrium point. The equilibrium point for this scenario is obtained by solving

$$A_v v_i = 0.$$

Solving the above, it is seen that the vehicles from the end of the platoon up to the victim attain the victim's velocity while the rest achieve velocities that are equally spaced and follow a pattern:

$$\begin{aligned} v_1 &= v_2, \\ v_2 &= v_3, \\ v_4 &= \frac{v_5+v_3}{2}, \\ v_5 &= \frac{v_6+v_4}{2}, \\ v_6 &= \frac{v_7+v_5}{2}, \\ &\vdots \\ v_{n-1} &= \frac{v_n+v_{n-2}}{2}. \end{aligned}$$

And it is known that v_n is the fixed velocity of the leader.

The above phenomena can be seen in the following two figures. In Figure 4.7, in a platoon of 10 vehicles, the last vehicle (vehicle 1) is the attacker and vehicle 2 the victim. As a result, the velocities up to the victim are the same while from vehicle 3 to vehicle 9, the velocities are equally distributed between the victim and the leader.

In Figure 4.8, vehicle 4 is the victim, and as a result, all vehicles up to the 4th vehicle attain the velocity of the victim and the rest get equally divided between the victim and the leader.

In both the cases, the leader has a fixed velocity, which in these examples is taken to be 31:29 m/s. Since the velocities do not remain the same for all the vehicles, they no longer maintain a constant spacing between them. As some velocities are equal while the rest differ, with one greater than the previous, it is graphically shown that the inter-vehicular spacings gradually keep increasing, thus making the system string unstable (Figure 4.9).

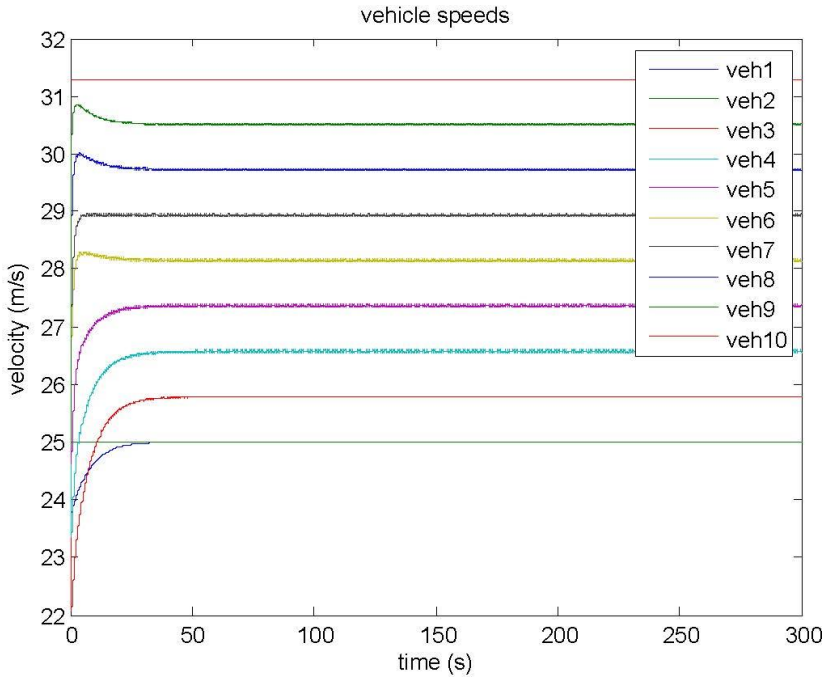

Figure 4.7 In a platoon of 10 vehicles, where vehicle 2 ("veh2") is the victim, all the vehicles between the victim and the leader ("veh10") obtain velocities that are equally varied.

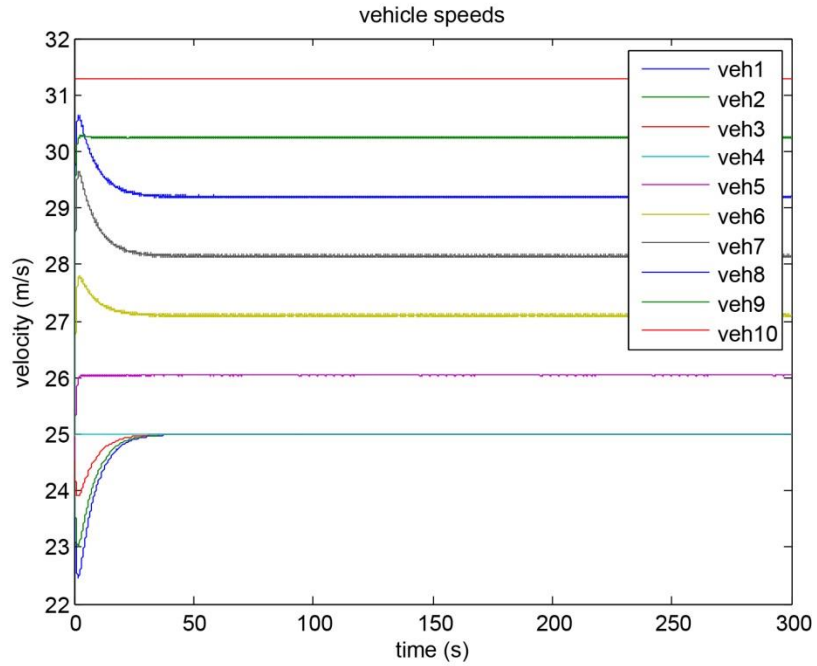

Figure 4.8 In a platoon of 10 vehicles, where vehicle 4 ("veh4") is the victim, all the vehicles up to the 4th vehicle obtain the velocity of the victim.

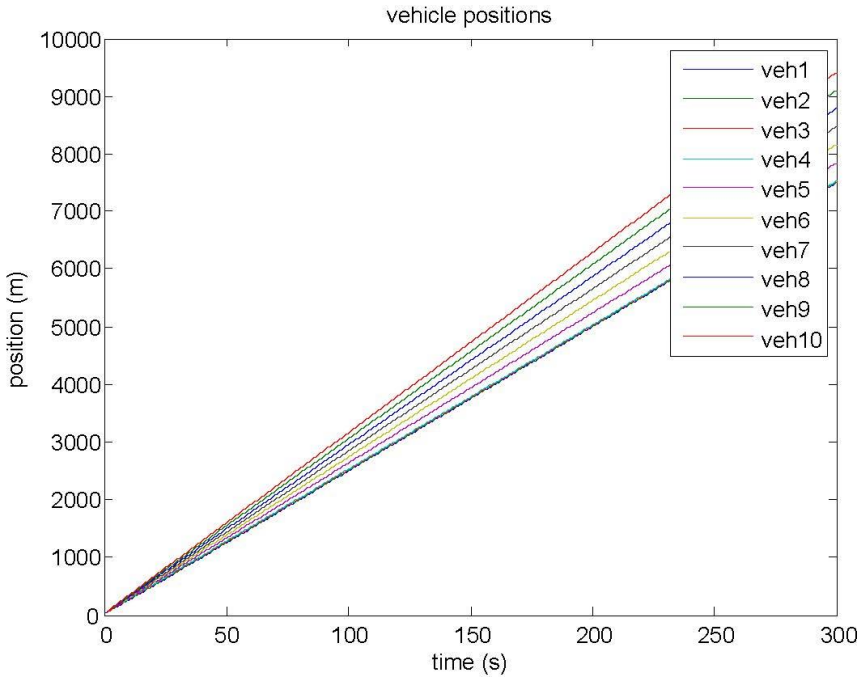

Figure 4.9 In a platoon of 10 vehicles, where vehicle 4 ("veh4") is the victim, the inter-vehicular spacings are no longer equal, making the system string unstable.

In this case, the attacker manages to change the speeds of some vehicles in the platoon, thus disrupting the string stability.

4.2.2 Case 2

The attacker is in an arbitrary *i*th position, and having access to the states of its preceding vehicle, it sends false information such that it eliminates all information of the victim's predecessor.

Theorem 4. When a vehicle platoon has an attacker at an arbitrary *i*th position, and it sends false data to the preceding vehicle such that it removes any information related to the victim's predecessor, all the vehicles up to the victim attain the same velocity as that of the victim while the vehicles between the victim and the leader, attain velocities that have a constant difference between them.

Proof. In a platoon of n vehicles represented by Equations (3.1)–(3.8), let an arbitrary *i*th vehicle be the attacker, making the $(i + 1)$*th* vehicle the victim, and $(i + 2)$*th* vehicle the predecessor of the victim:

$$\dot{x_i} = v_i \tag{4.19a}$$

$$\dot{v_i} = K_p(x_{i+1} - x_i - d) + K_v(v_{i+1} - v_i) + K_p(x_{i-1} - x_i + d) + K_v(v_i - v_{i+1}), \tag{4.19b}$$

$$\dot{x_{i+1}} = v_{i+1} \tag{4.20a}$$

$$\dot{v_{i+1}} = K_p(x_i - x_{i+1} + d) + K_v(v_i - v_{i+1}), \tag{4.20b}$$

$$\dot{x_{i+2}} = v_{i+2} \tag{4.21a}$$

$$\dot{v_{i+2}} = K_p(x_{i+3} - x_{i+2} - d) + K_v(v_{i+3} - v_{i+2}) + K_p(x_{i+1} - x_{i+2} + d) + K_v(v_{i+1} - v_{i+2}). \tag{4.21b}$$

where $v_{v+1} = v_v\ (say)$, i.e., the velocity of the victim.

For simplicity, if the *i*th vehicle is assumed to be the 2nd vehicle, thus making the 3rd vehicle the victim, the corresponding systems matrix in this scenario is:

$$A = \begin{bmatrix} 0 & 1 & 0 & 0 & 0 & 0 & \cdots & 0 & 0 & 0 & 0 \\ -K_p & -K_v & K_p & K_v & 0 & 0 & \cdots & 0 & 0 & 0 & 0 \\ 0 & 0 & 0 & 1 & 0 & 0 & \cdots & 0 & 0 & 0 & 0 \\ K_p & K_v & -2K_p & -2K_v & K_p & K_v & \cdots & 0 & 0 & 0 & 0 \\ 0 & 0 & 0 & 0 & 0 & 1 & \cdots & 0 & 0 & 0 & 0 \\ 0 & 0 & K_p & K_v & -K_p & -K_v & \cdots & 0 & 0 & 0 & 0 \\ \vdots & \vdots & \vdots & \vdots & \vdots & \vdots & \ddots & \vdots & \vdots & \vdots & \vdots \\ 0 & 1 & 0 & 0 & 0 & 0 & \cdots & 0 & 1 & 0 & 0 \\ 0 & 0 & 0 & 0 & 0 & 0 & \cdots & -2K_p & -2K_v & K_p & K_v \\ 0 & 1 & 0 & 0 & 0 & 0 & \cdots & 0 & 0 & 0 & 1 \\ 0 & 0 & 0 & 0 & 0 & 0 & \cdots & K_p & K_v & -K_p & -K_v \end{bmatrix}.$$

It is seen that the eigenvalues of this matrix are < 0, making the system a stable system. Now, as a system attains stability, it approaches its equilibrium point. To find the equilibrium points, the matrix comprising the velocity components of the system is considered:

$$A_v = \begin{bmatrix} -K_v & K_v & 0 & 0 & \cdots & 0 & 0 & 0 \\ K_v & -2K_v & K_v & 0 & \cdots & 0 & 0 & 0 \\ 0 & K_v & -K - v & 0 & \cdots & 0 & 0 & 0 \\ 0 & 0 & K_v & -2K_v & \cdots & 0 & 0 & 0 \\ \vdots & \vdots & \vdots & \vdots & \ddots & \vdots & \vdots & \vdots \\ 0 & 0 & 0 & 0 & \cdots & K_v & -2K_v & K_v \\ 0 & 0 & 0 & 0 & \cdots & 0 & K_v & -K_v \end{bmatrix}.$$

Solving $A_v v_i = 0$, the following is obtained:

$$\begin{aligned} v_1 &= v_2, \\ v_2 &= v_v, \\ v_4 &= \tfrac{v_5+v_3}{2}, \\ v_5 &= \tfrac{v_6+v_4}{2}, \\ v_6 &= \tfrac{v_7+v_5}{2}, \\ &\vdots \\ v_{n-1} &= \tfrac{v_n+v_{n-2}}{2}. \end{aligned}$$

Thus, it is seen that all vehicles up to the victim achieve the same velocity as that of the victim while the rest achieve velocities that are equally spaced and follow a pattern. As the predecessor information is removed by the attacker, the link between the 3rd and 4th vehicles, in this case, is broken. So $v_3 \neq v_4$. And thus the response is as seen.

As the vehicles move with different velocities instead of the desired velocity, the platoon no longer remains string stable, as the distance between the vehicles keeps increasing.

In the following figures, a platoon of 10 vehicles has been considered, assuming the 5th vehicle is the attacker, all the vehicles leading up to the 6th vehicle attain the same velocity as that of the 6th, which is the victim, while the 7th, 8th, and, 9th vehicles have velocity equally spaced between the victim and the leader (Figure 4.10). And, as a result of the differing velocities, the vehicles gradually move away from each other (Figure 4.11), thus showing string instability in the system.

Thus, under this scenario as well, the attacker makes some of the vehicles (all the vehicles leading up to the victim) travel at a different velocity instead of the desired value, thus making the platoon string unstable.

Due to constant increase in the spacing between the vehicles, eventually a point of time might come when the vehicles are not in the range of the sensor of the next vehicle.

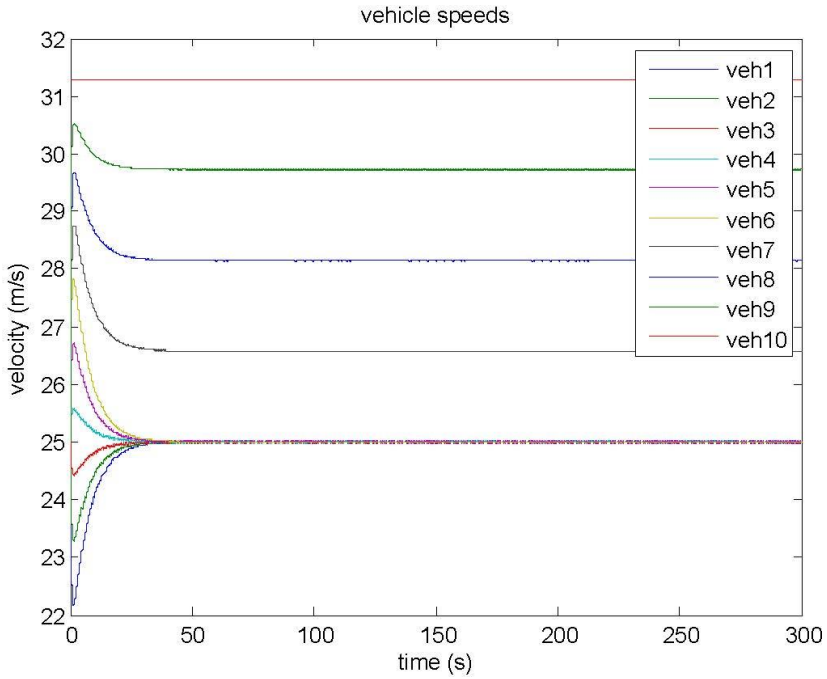

Figure 4.10 Due to false data injection, vehicles do not attain the desired velocity.

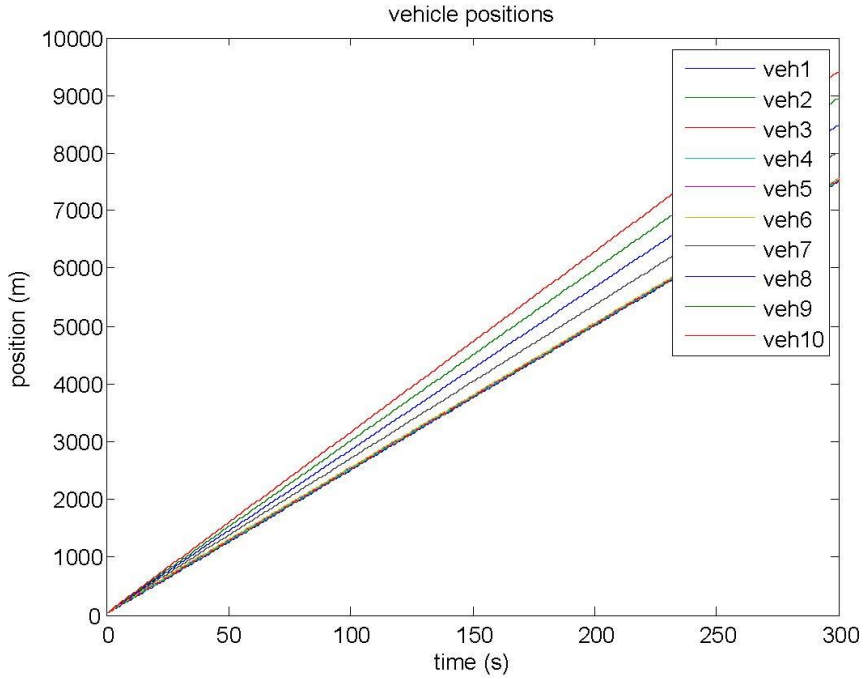

Figure 4.11 Due to false data injection, vehicles are no longer string stable.

4.2.3 Case 3

The attacker is in an arbitrary ith position, and having access to the states of its preceding vehicle, it sends false information such that it eliminates all the information about the victim's follower.

Theorem 5. When a vehicle platoon has an attacker at an arbitrary position, and it sends false data to its preceding vehicle such that it removes any information related to the victim's follower, i.e., about the

attacker itself, all the vehicles still reach the desired velocity, and they also are string stable, as there is no position error.

Proof. In a platoon of *n* vehicles represented by Equations 3.1 through 3.8, let an arbitrary *i*th vehicle be the attacker, making the (*i* + 1)*th* vehicle the victim, and (i + 2)*th* vehicle the predecessor of the victim:

$$\dot{x_i} = v_i \tag{4.22a}$$

$$\dot{v_i} = K_p(x_{i+1} - x_i - d) + K_v(v_{i+1} - v_i) + K_p(x_{i-1} - x_i + d) + K_v(v_{i-1} - v_i), \tag{4.22b}$$

$$\dot{x_{i+1}} = v_{i+1} \tag{4.23a}$$

$$\dot{v_{i+1}} = K_p(x_{i+2} - x_{i+1} - d) + K_v(v_{i+2} - v_{i+1}), \tag{4.23b}$$

$$\dot{x_{i+2}} = v_{i+2} \tag{4.24a}$$

$$\dot{v_{i+2}} = K_p(x_{i+3} - x_{i+2} - d) + K_v(v_{i+3} - v_{i+2}) + K_p(x_{i+1} - x_{i+2} + d) + K_v(v_{i+1} - v_{i+2}). \tag{4.24b}$$

Where $v_{i+1} = v_v\ (say)$, i.e., the velocity of the victim. For simplicity, if the *i*th vehicle is assumed to be the 2nd vehicle, thus making the 3rd vehicle the victim, the corresponding systems matrix in this scenario is:

$$A = \begin{bmatrix} 0 & 1 & 0 & 0 & 0 & 0 & 0 & 0 & \cdots & 0 & 0 \\ -K_p & -K_v & K_p & K_v & 0 & 0 & 0 & 0 & \cdots & 0 & 0 \\ 0 & 0 & 0 & 1 & 0 & 0 & 0 & 0 & \cdots & 0 & 0 \\ K_p & K_v & -2K_p & -2K_v & K_p & K_v & 0 & 0 & \cdots & 0 & 0 \\ 0 & 0 & 0 & 0 & 0 & 1 & 0 & 0 & \cdots & 0 & 0 \\ 0 & 0 & 0 & 0 & -K_p & -K_v & K_p & K_v & \cdots & 0 & 0 \\ \vdots & \vdots & \vdots & \vdots & \vdots & \vdots & \vdots & \vdots & \ddots & \vdots & \\ 0 & 1 & 0 & 0 & 0 & 0 & 0 & 0 & \cdots & 0 & 0 \\ 0 & 0 & 0 & 0 & 0 & 0 & 0 & -2K_p & \cdots & K_p & K_v \\ 0 & 1 & 0 & 0 & 0 & 0 & 0 & 0 & \cdots & 0 & 1 \\ 0 & 0 & 0 & 0 & 0 & 0 & 0 & 0 & \cdots & -K_p & -K_v \end{bmatrix}.$$

It is seen that the eigenvalues of this matrix are < 0, making the system a stable system. Now, as a system attains stability, it approaches its equilibrium point. To find the equilibrium points, the matrix comprising the velocity components of the system is considered:

$$A_v = \begin{bmatrix} -K_v & K_v & 0 & 0 & \cdots & 0 & 0 & 0 \\ K_v & -2K_v & K_v & 0 & \cdots & 0 & 0 & 0 \\ 0 & 0 & -K_v & K_v & \cdots & 0 & 0 & 0 \\ 0 & 0 & K_v & -2K_v & \cdots & 0 & 0 & 0 \\ \vdots & \vdots & \vdots & \vdots & \ddots & \vdots & \vdots & \vdots \\ 0 & 0 & 0 & 0 & \cdots & K_v & -2K_v & K_v \\ 0 & 0 & 0 & 0 & \cdots & 0 & K_v & -K_v \end{bmatrix}.$$

Solving $A_v v_i = 0$, the following is obtained:

$$\begin{aligned} v_1 &= v_2, \\ v_2 &= v_v, \\ v_v &= v_4, \\ v_4 &= v_5, \\ &\vdots \\ v_{n-1} &= v_n. \end{aligned}$$

Thus, it is seen that all vehicles attain the same velocity as that of the leader, despite the fact that the attacker removes information about itself (the victim's follower), because the link between the victim and its predecessor and follower is never completely broken. So the velocity information is passed on, and thus the response is as seen.

In the following graphs, a 10-vehicle platoon is considered with the attacker in the 5th position, making the 6th vehicle the victim.

As all the velocities are equal to the desired velocity or the leader velocity, the system in this case shows no error in velocity (Figure 4.12) or in the inter-vehicular spacings (Figure 4.13) and is thus string stable (Figure 4.14).

As can be seen from the graphs, this kind of attack does not bring forth any challenging situations for the platoon, thus this attack should not be a feasible option for an attacker.

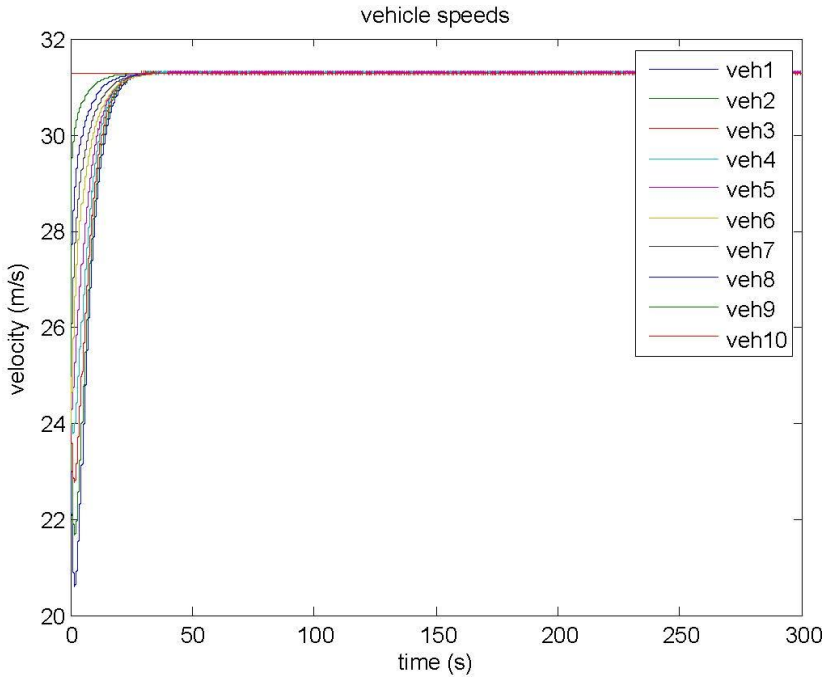

Figure 4.12 All the vehicles reach desired value when the attacker omits information about itself.

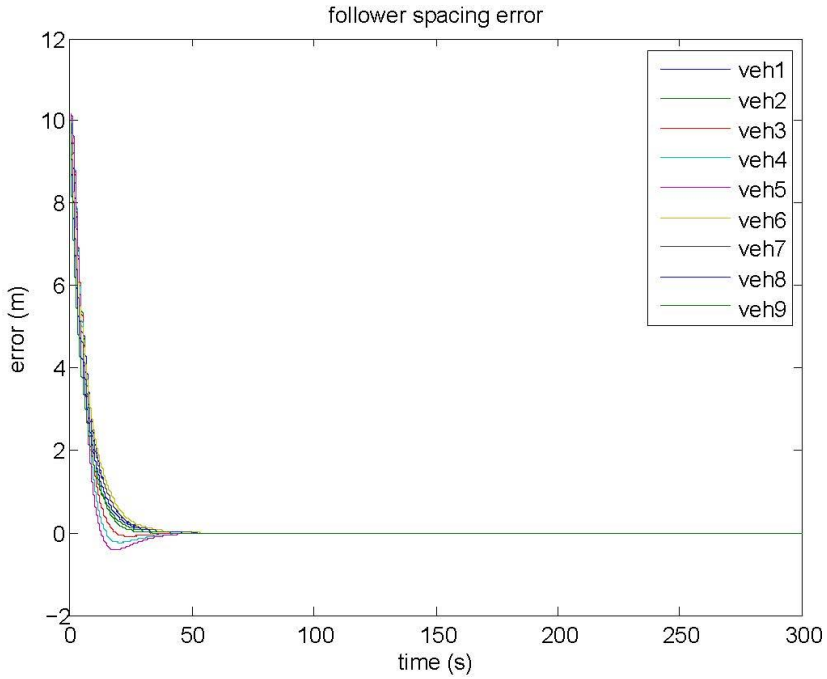

Figure 4.13 There is no spacing error when the attacker provides false data in which it removes information about itself.

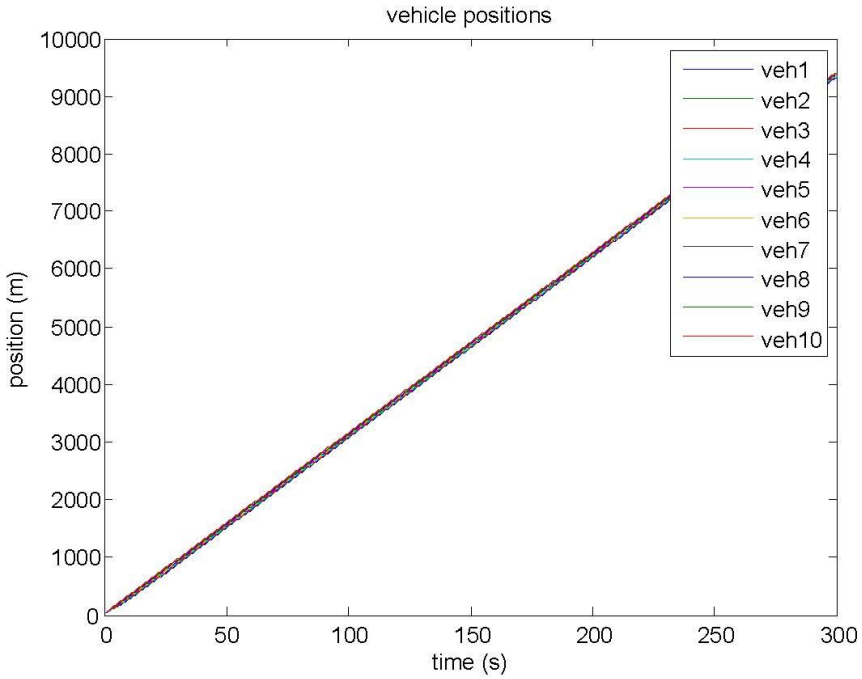

Figure 4.14 Due to absence of spacing error, the platoon is string stable.

5. FALSE DATA INJECTION-NONLINEAR MODEL

In the previous chapter, the model was considered a simple, linear model, and studied the effects of FDI (false data injection) on the whole platoon. Here, the FDI was implemented on the nonlinear model in order to study how it affects a more realistic model so that a clearer idea can be obtained as to how FDI can affect the vehicle in a real-life scenario. Thus, a nonlinear model is used that has inherent nonlinearities such as delay and rate limits or saturations.

The vehicle platoon uses a bidirectional-constant spacing platooning strategy in which information from both the preceding and following vehicles are taken into consideration while making control decisions to maintain constant spacing between the vehicles. And the controller used is the proportional-derivative (PD) controller.

Throughout, the desired (lead vehicle) velocity was considered to be 31:29m/s and the limitation applied on the velocity was: upper limit = 35m/s and lower limit = 0m/s. For the acceleration $\pm$1m/s2, and for the jerk (rate of change of acceleration), the threshold was considered 0:05m/s3, although in the literature varying limitations were used. The velocity upper limit was chosen as 25.4m/s; the acceleration, deceleration, and jerk limits were chosen to be 6m/s^2, 8m/s^2, and 4m/s^3, respectively, in their work by Mammar et al. [8]. Sheikholeslam et al. [30] used 21.9m/s as the desired velocity and 0.5m/s^3 and 1m/s^2 as the limitation on jerk and acceleration, respectively. While Godbole et al. [64] used -5m/s^2, 2m/s^2, and $\pm$5m/s^3 as the limits on deceleration, acceleration, and jerk, respectively, Jensen et al. [65] used 31.305m/s as the maximum speed limit and 4.46m/s^2, 9.22m/s^2, and 3m/s^3 as the acceleration, deceleration, and jerk limits, respectively.

Considering that there is one attacker in the platoon who can send false information to the vehicle that is immediately preceding and/or following it, in the following figures, the effects of time delay (present within the system) and rate limits on a platoon of 10 vehicles can be seen, with and without FDI.

5.1 System with Delay and Rate Limits with No FDI

5.1.1 Case 1: Delay Constant 0:01

Figures 5.1 and 5.2 depict the effect of the scenario when the system has a delay with delay constant 0.01. As can be seen, the system remains stable. All the vehicles reach desired velocity and are string stable, i.e., the spacing and velocity errors are zero. Thus, when the delay in the system has delay constant $\leq$ 0.01, it does not affect the system and is stable (when there is no FDI).

5.1.2 Case 2: Delay Constant > 0:01

Figures 5.3 and 5.4 depict the effect of the scenario when the system has a delay, with delay constant greater than 0.01 (in this case 0.1).

Thus, it is seen that with the delay constant > 0.01, the system becomes unstable. Even in the absence of any FDI, all the vehicles do not reach the desired velocity and are string unstable, i.e., the spacing and velocity errors are not zero, and it was seen that when the delay constant is even 0.02 the system has instability, although there is no FDI present. Thus, any value > 0.01 will destabilize the platoon.

5.2 System with Time Delay and Rate Limits with FDI

In this scenario, addition of FDI to the realistic system model, which has time delays (with delay constant 0.1) and rate limits, is considered.

5.2.1 Addition of Constant Errors

False position and velocity information is added by the attacker to the victim's states, when the system has time delay and rate limits.

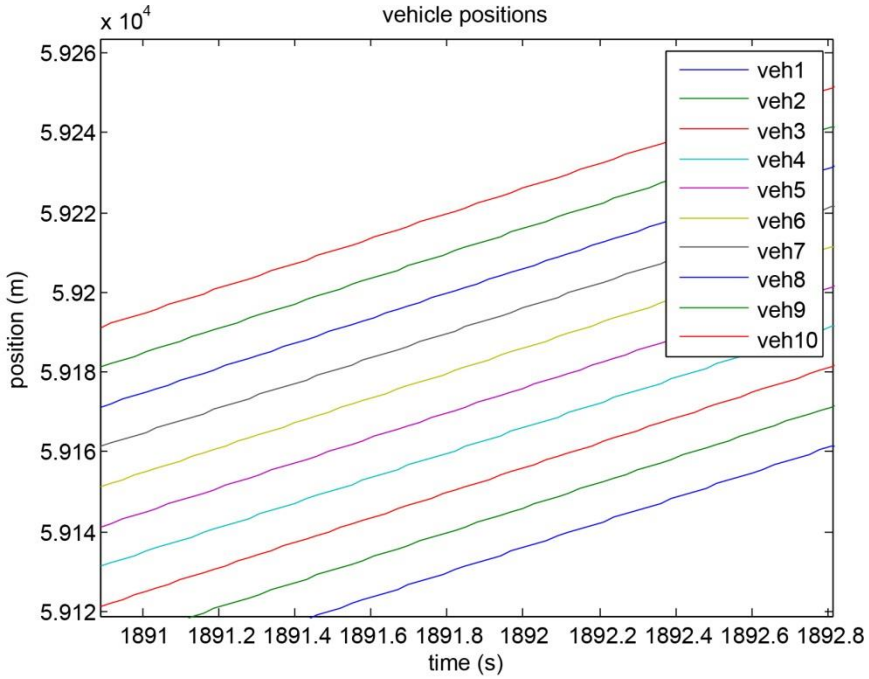

Figure 5.1 All the vehicles are string stable, i.e., they have the desired (and constant) spacing between them, in spite of the delay.

Case 1

The system has a time delay with delay constant 0:1, rate limits on the velocity, acceleration and jerk, and the last vehicle in the platoon is the attacker that provides inaccurate position and velocity information to the preceding vehicle. Figures 5.5 - 5.9 show the effects of the aforementioned scenario.

As can be seen from the above figures, the vehicles do not reach the desired velocity, the velocity error does not go to zero, and the spacing error gradually increases, thus the system is string unstable.

Case 2

The system has a time delay with delay constant 0:1, rate limits on velocity, acceleration, and jerk, and the attacker is at the center of the vehicle platoon, and it sends false position and velocity information to both the preceding and following vehicles.

Figures 5.10 - 5.14 show the effects of the aforementioned scenario. From the above figures, it is seen that, again, the vehicles do not reach the desired velocity, the velocity error does not go to zero, and the

spacing error gradually increases, thus the system is string unstable. In this case, the variation of the speeds from the desired value is more than the previous case.

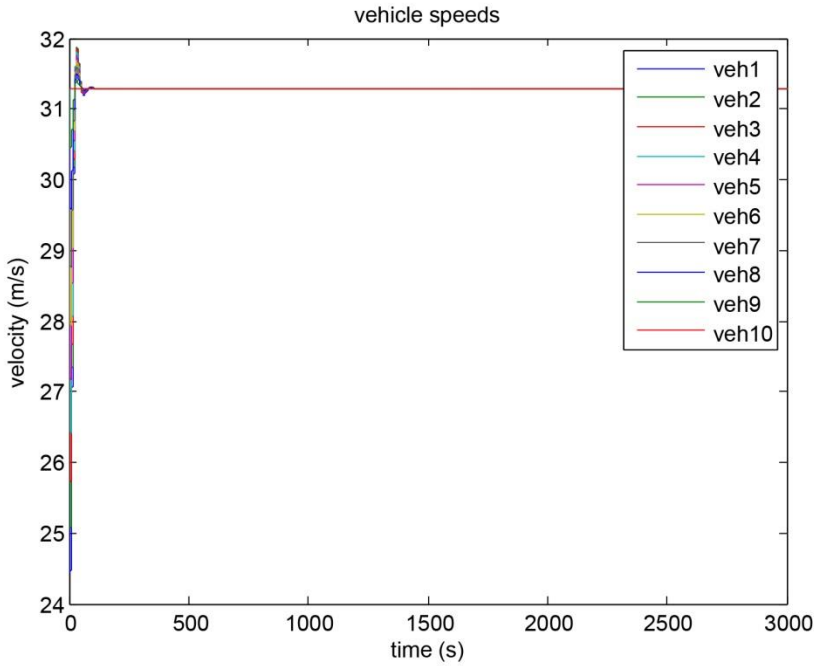

Figure 5.2 All the vehicles reach desired velocity, although the system has an inherent delay.

5.2.2 Attacker Has Access to Victim's States and Manipulates Its Acceleration

Case 1

The attacker is in an arbitrary *i*th position and has access to the states of the vehicle preceding it, and it sends false information such that the acceleration of the victim is set to 0, along with the system having time delay and rate limits.

Figures 5.15 - 5.17 show the effects of the aforementioned scenario (here, the *4th* vehicle is the victim). From Figures 5.15 - 5.17, it can be seen that, again, the vehicles do not reach the desired velocity, the velocity error does not go to zero (as all the vehicles do not achieve the desired velocity), and the spacing error gradually increases. Thus, the system is string unstable. The vehicles up to the victim attain the velocity of the victim, and the ones between the victim and the leader attain velocities such that the difference between them is constant.

On increasing the delay constant to 0:5, it is seen that the system becomes unstable, with the gradual increase in the inter-vehicle spacing even more than the case with a lower delay constant (Figure 5.18). Also, it is seen that the vehicles attain different speeds (Figure 5.19).

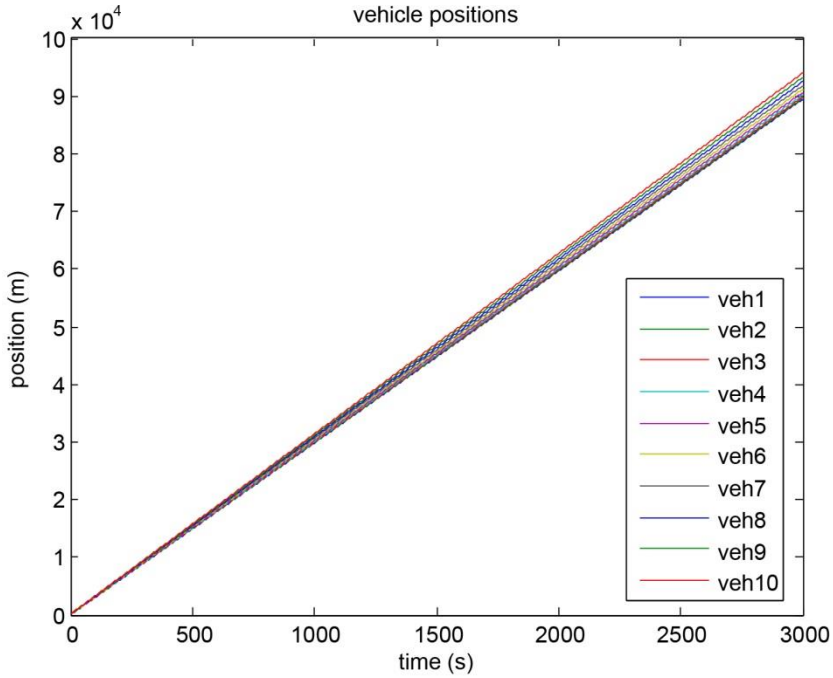

Figure 5.3 The vehicles are not string stable, which means that the vehicles gradually move away from each other and the spacing between them is no longer as desired and not a constant.

Case 2

The attacker is in an arbitrary *i*th position, and having access to the states of its preceding vehicle, it sends false information such that it eliminates all information of the victim's predecessor, along with the system having time delay and rate limits.

Figures 5.20 - 5.24 show the effects of the aforementioned scenario (here, the *6th* vehicle is the victim).

Case 3

The attacker is in an arbitrary ith position, and having access to the states of its preceding vehicle, it sends false information such that eliminates all information of the victim's follower, along with the system having time delay and rate limits.

Figures 5.25 - 5.27 show the effects of the aforementioned scenario (with the *6th* vehicle as the victim). Thus, in this case it is seen that in comparison to Figures 4.12 and 4.14, due to the presence of delay, the platoon is no longer reaching desired velocities and thus no longer remaining string stable.

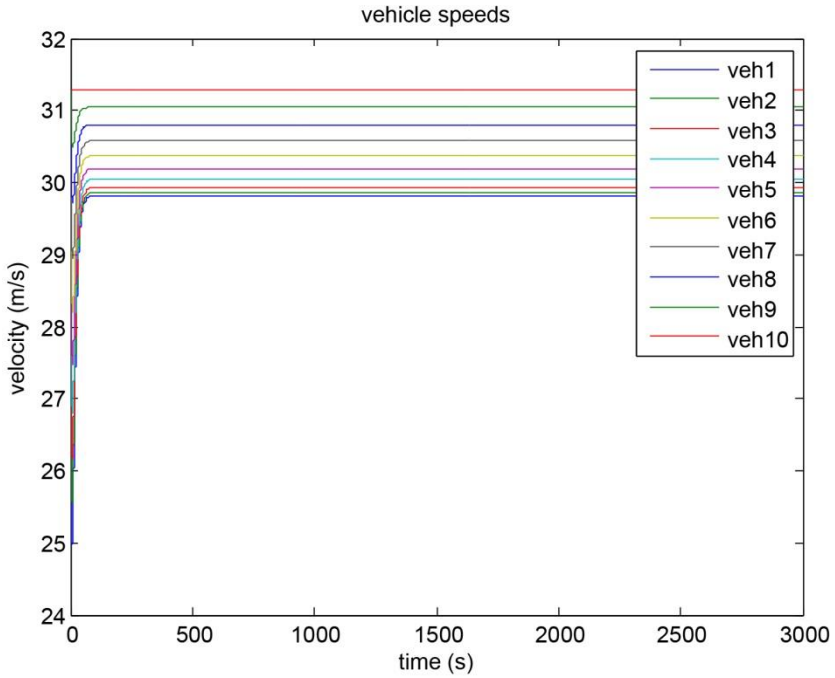

Figure 5.4 All the vehicles do not reach the desired velocity. Except for the leader, all the vehicles attain velocities less than the desired value.

5.3 Discussion

Here, it is seen that when the proportional-derivative (PD) control is implemented on the nonlinear model with rate limits and time delays with delay constant less than 0.01, the system is still able to cope and the controller can do its work. But when the delay constant is any greater than 0.01, even in the absence of any FDI, the controller is unable to maintain stability in the system. Vehicles do not reach the desired velocity, and they become increasingly string unstable as the delay constant is increased. Thus, when PD control is implemented on a more realistic model, it is seen that the control fails to have as much control over the platoon as in the linear model. With the delay present as an inherent factor in the system, the controller falters.

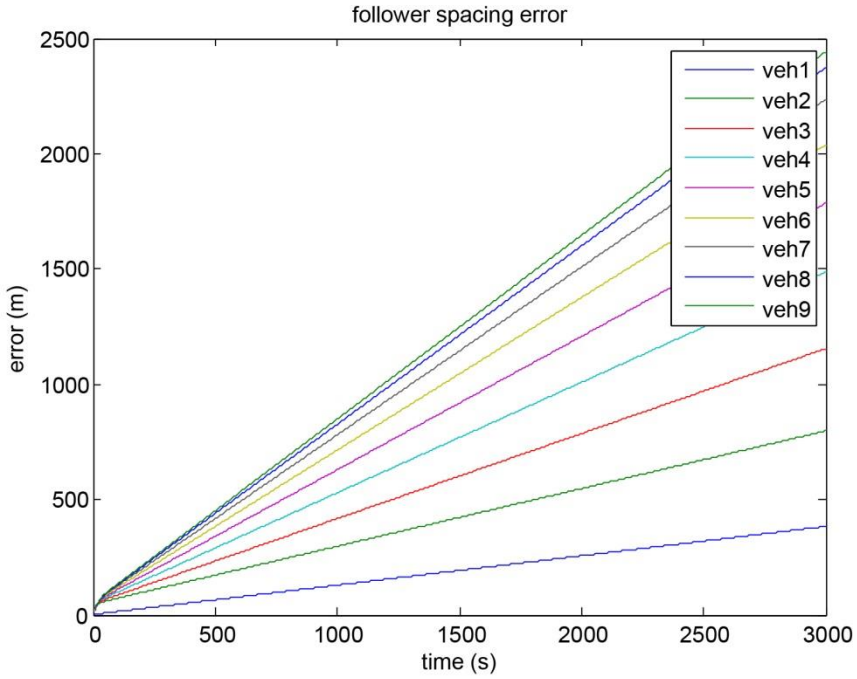

Figure 5.5 Spacing error increases with time, thus all vehicles are moving away from each other.

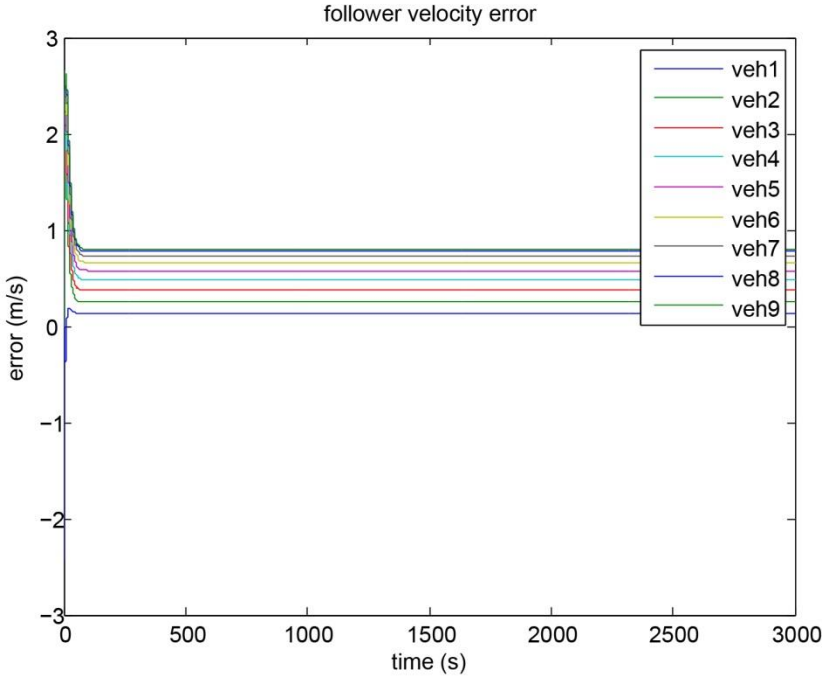

Figure 5.6 The velocity error is not zero, i.e., all the vehicles do not reach desired value.

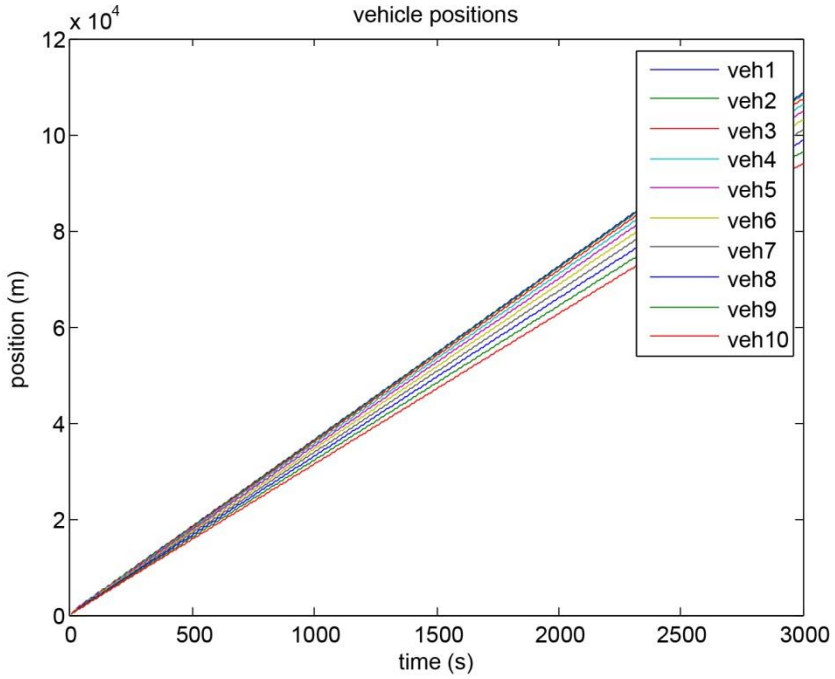

Figure 5.7 The vehicles are not string stable.

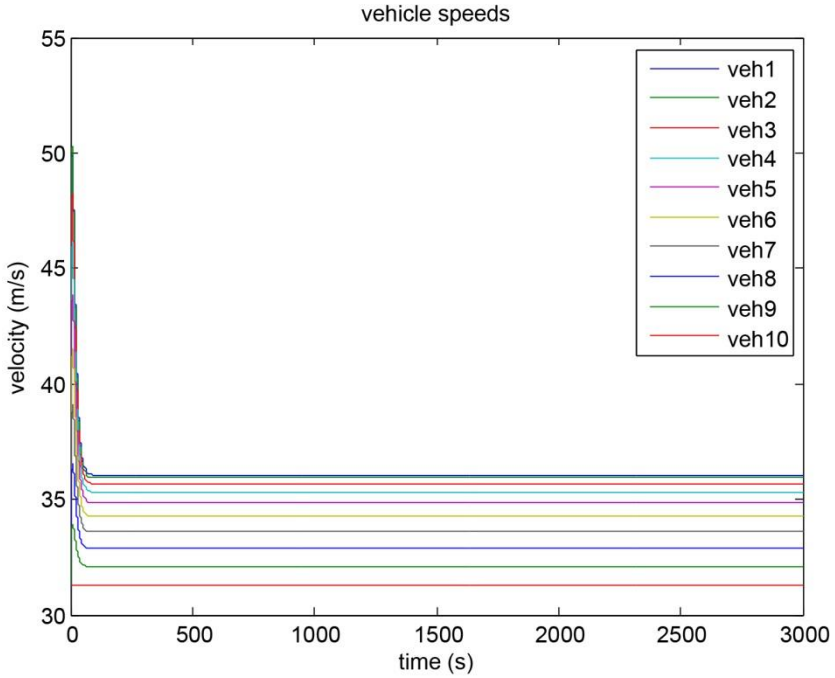

Figure 5.8 All the vehicles do not reach the desired velocity. Except the leader, all the other vehicles attain velocities greater than the desired value.

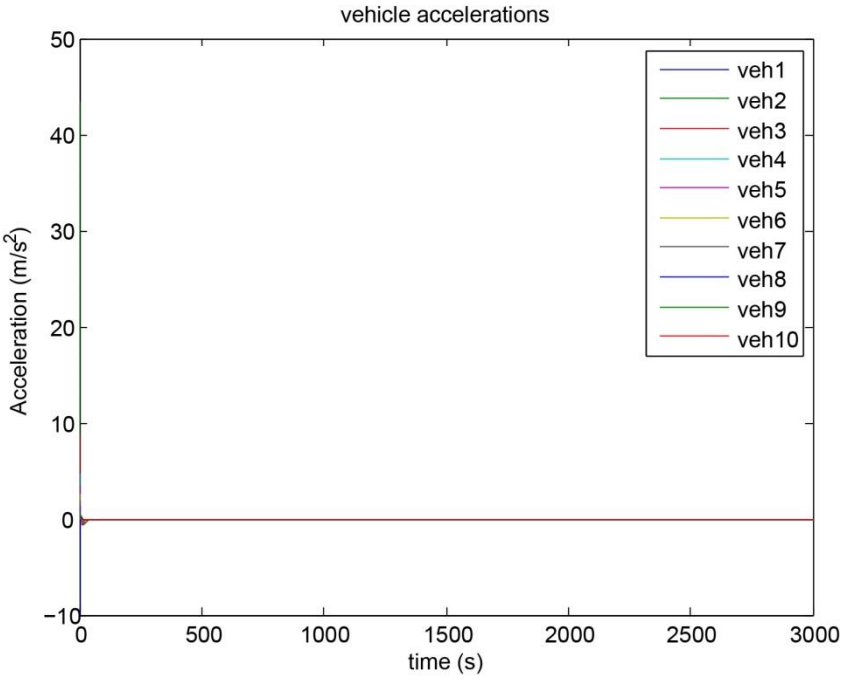

Figure 5.9 As the rate limit on acceleration and jerk is implemented, the acceleration eventually goes to zero.

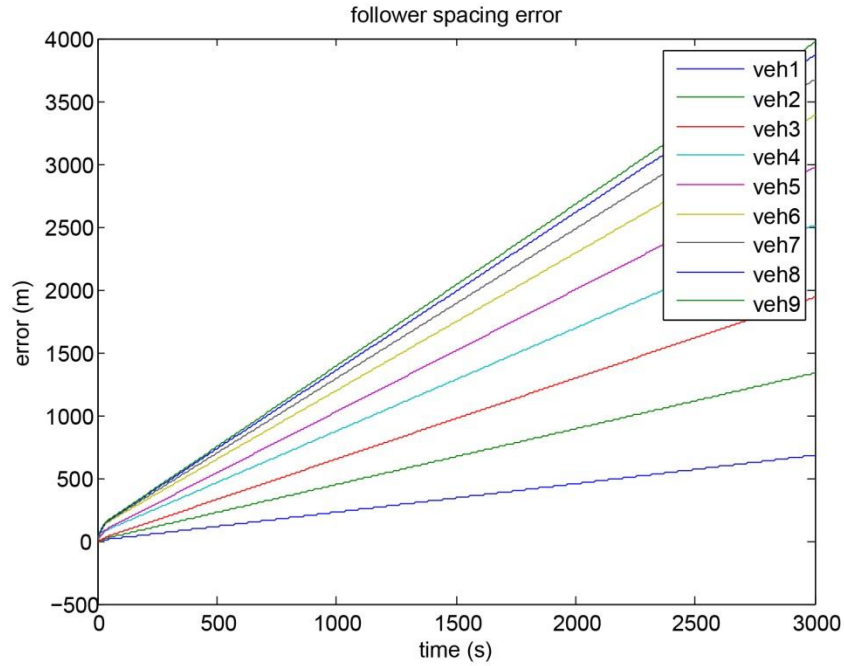

Figure 5.10 Spacing error is present. Also, the gradual increase is greater than in the previous case.

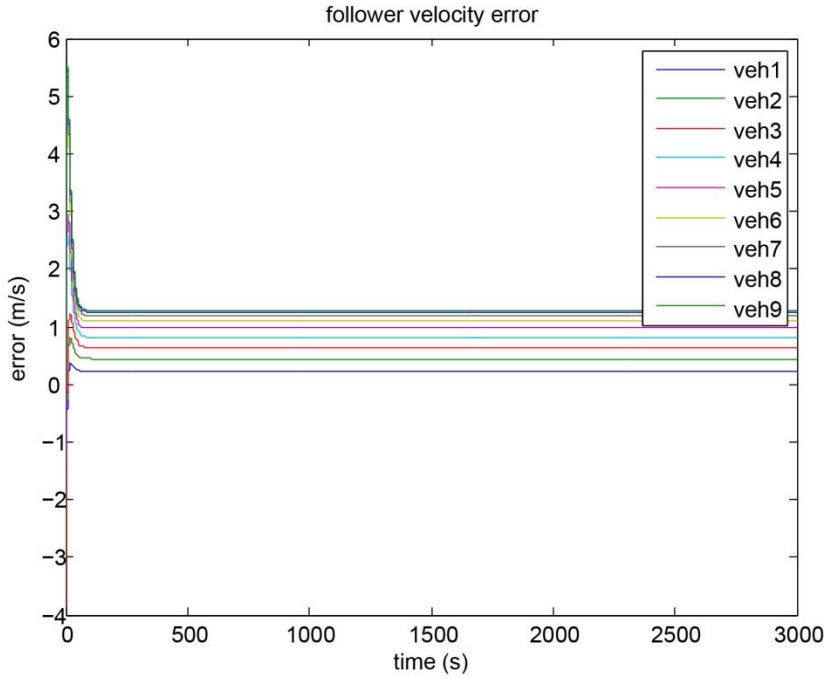

Figure 5.11 The velocity error is not zero, thus all the vehicles do not reach desired velocity.

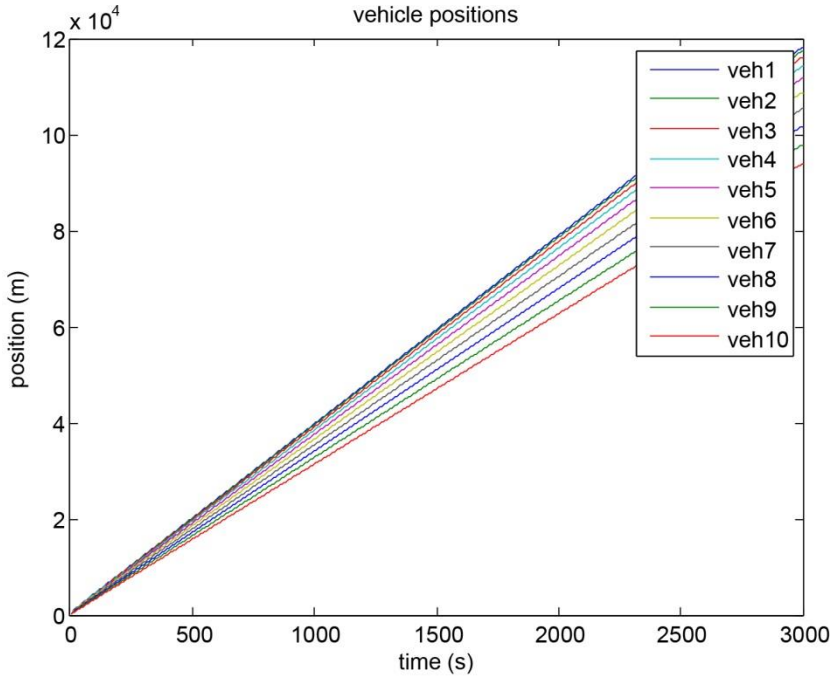

Figure 5.12 The vehicles are not string stable.

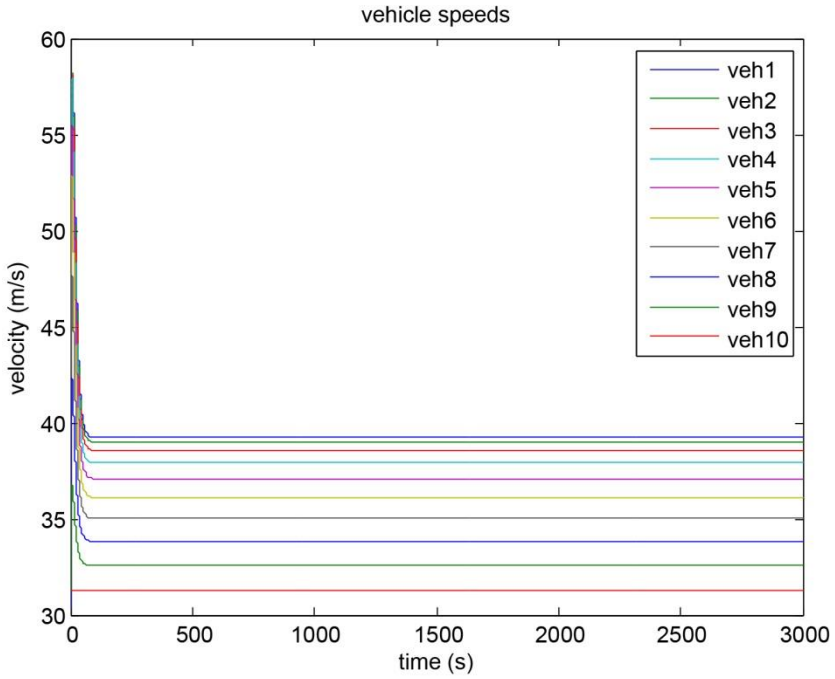

Figure 5.13 All the vehicles attain velocities greater than the leader's velocity.

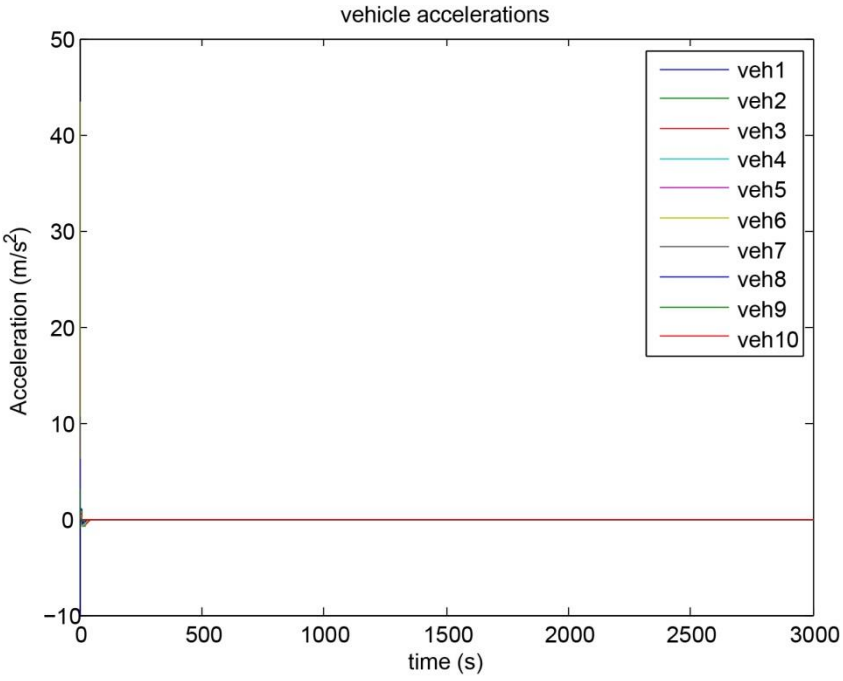

Figure 5.14 The acceleration eventually goes to zero, as rate limits are present.

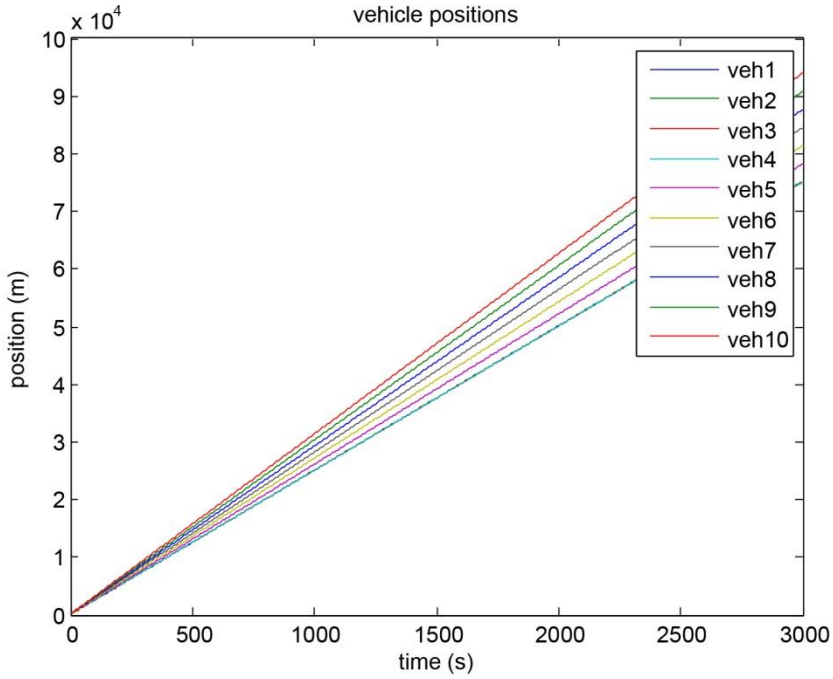

Figure 5.15 The vehicles are moving away from each other, thus they do not have constant spacing between them.

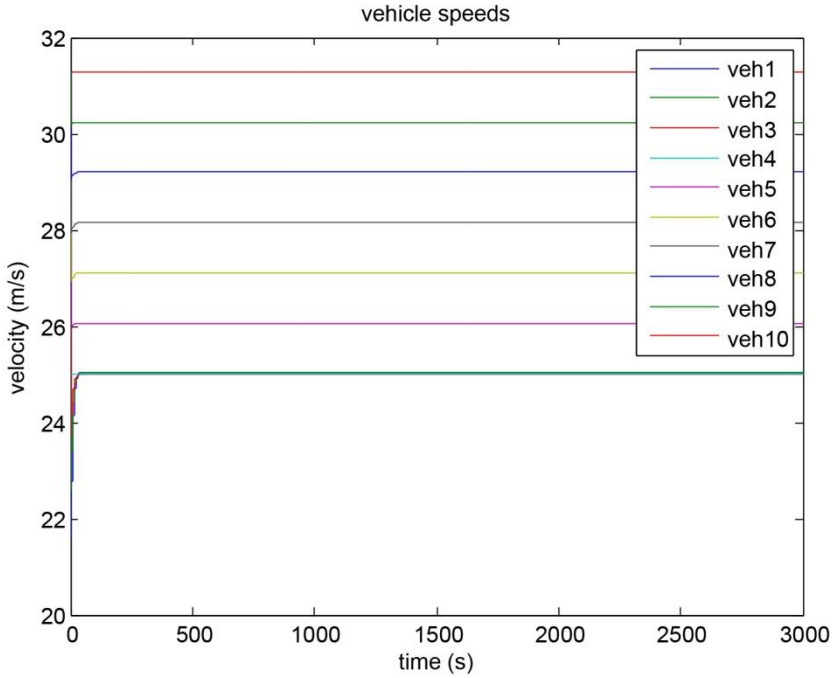

Figure 5.16 Vehicles up to the victim ("veh4") attain its velocity while the rest attain velocities equally dispersed between the victim's and the leader's.

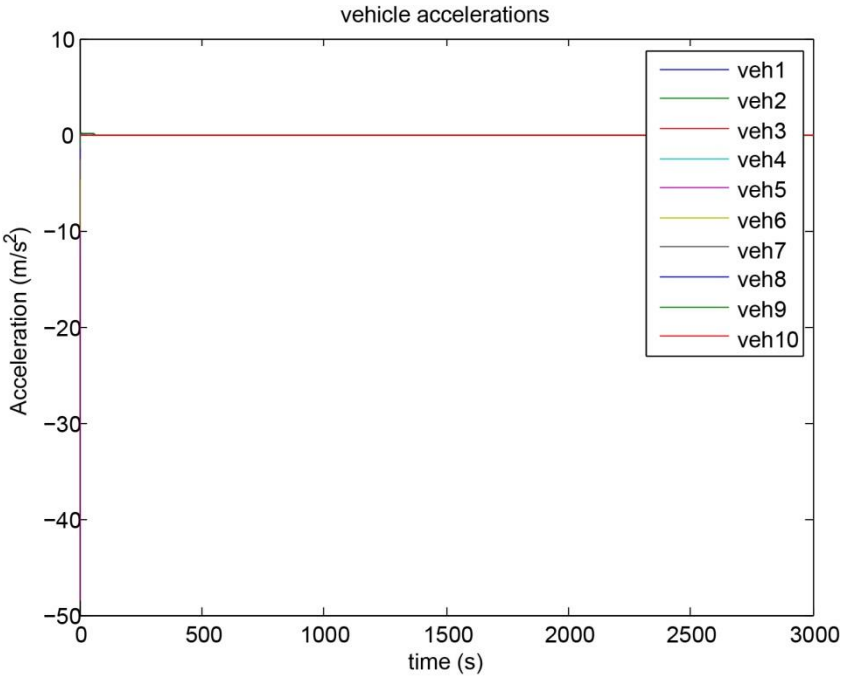

Figure 5.17 Acceleration eventually goes to zero.

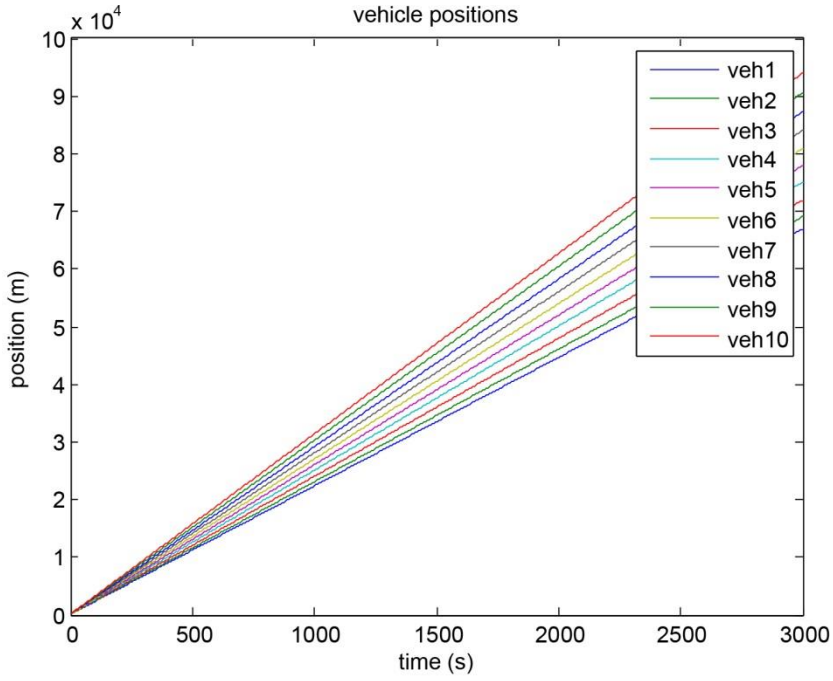

Figure 5.18 The vehicles are string unstable.

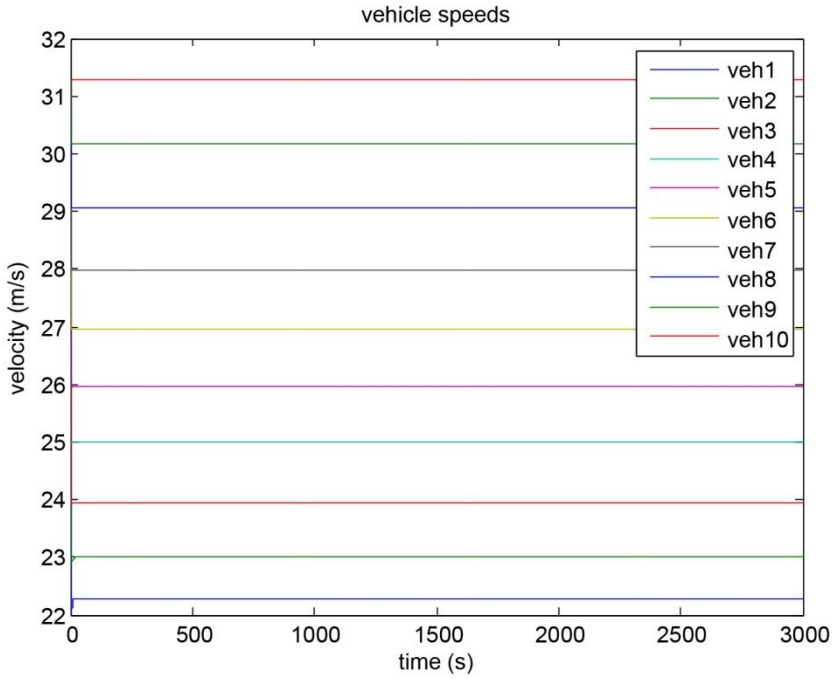

Figure 5.19 Vehicles attain varying speeds.

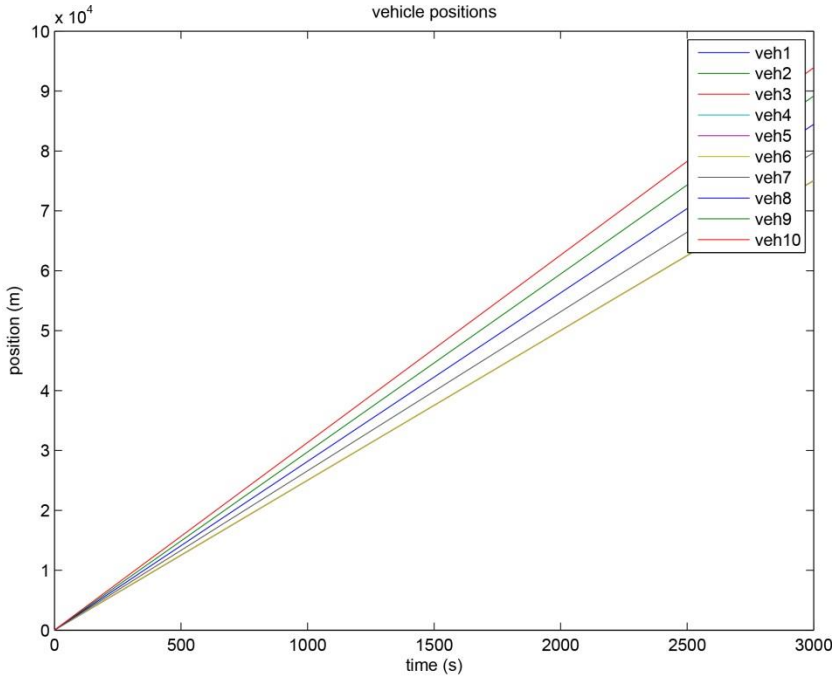

Figure 5.20 The vehicles up to the victim have constant spacing between them while the rest have their respective spacings gradually increase with time.Thus, the platoon is string unstable.

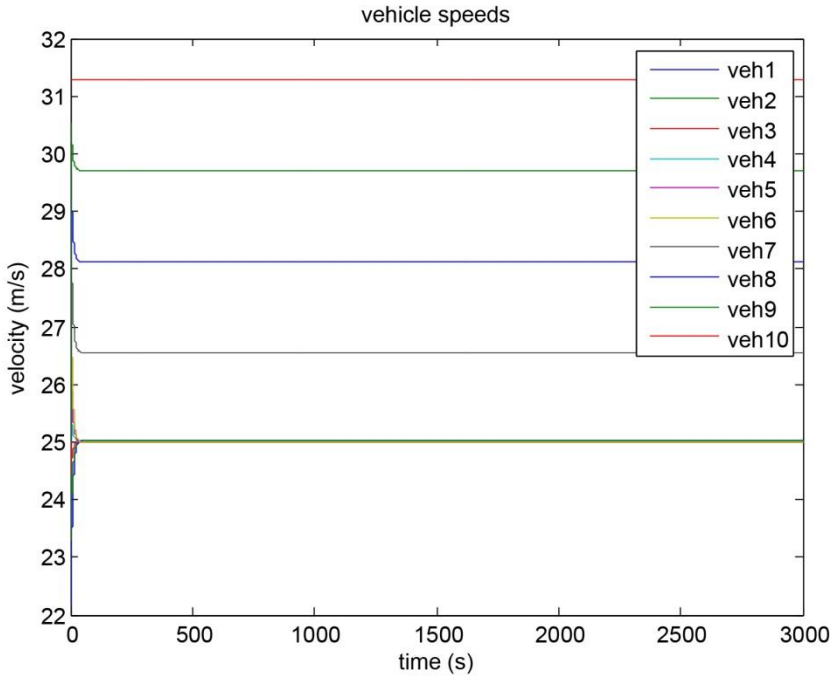

Figure 5.21 Vehicles up to the victim ("veh6") attain its velocity.

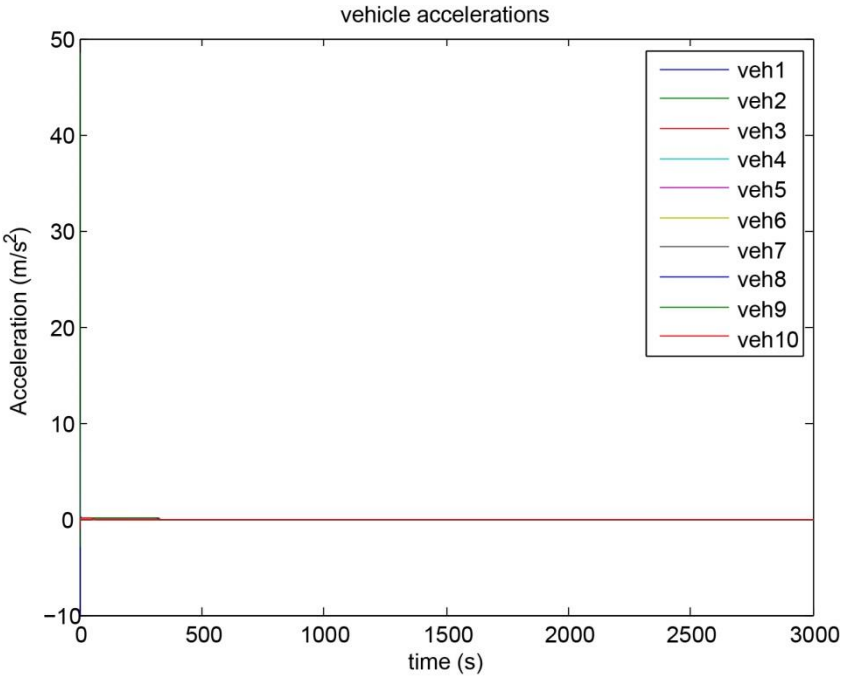

Figure 5.22 Acceleration eventually goes to zero.

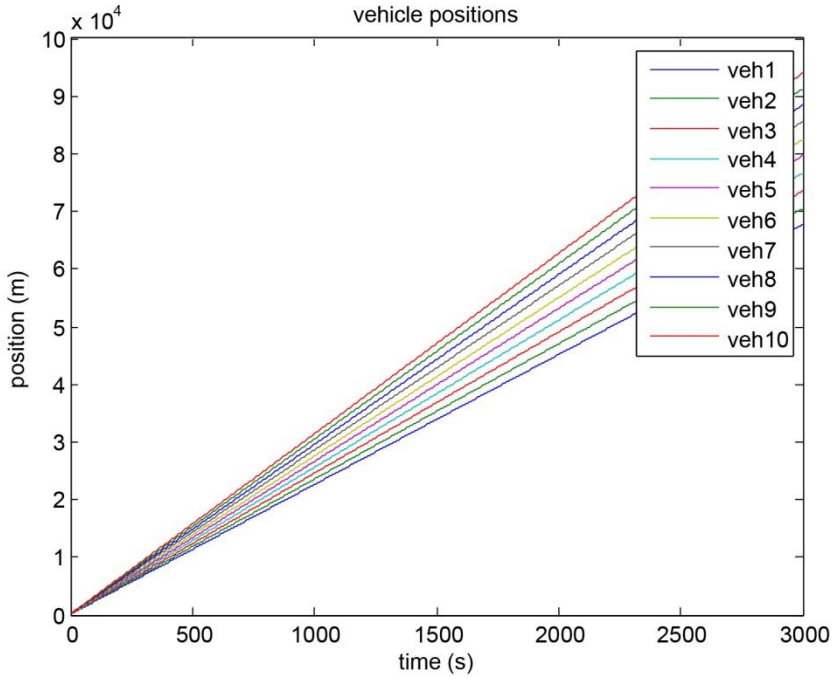

Figure 5.23 More prominent effect with delay constant '1' – the vehicles are not string stable and none of the vehicles have constant spacing between them.

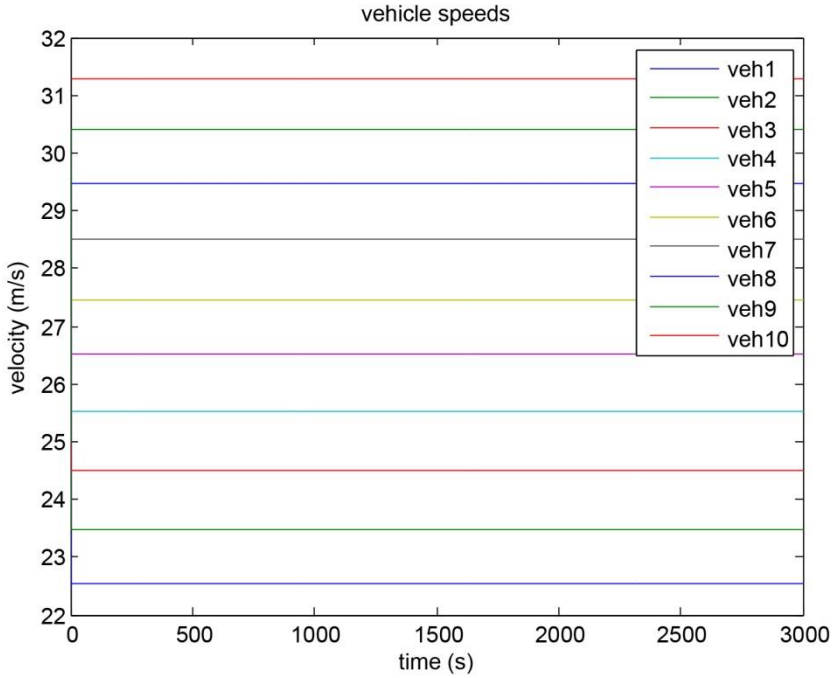

Figure 5.24 More prominent effect with delay constant '1' – the vehicles attain varying velocities.

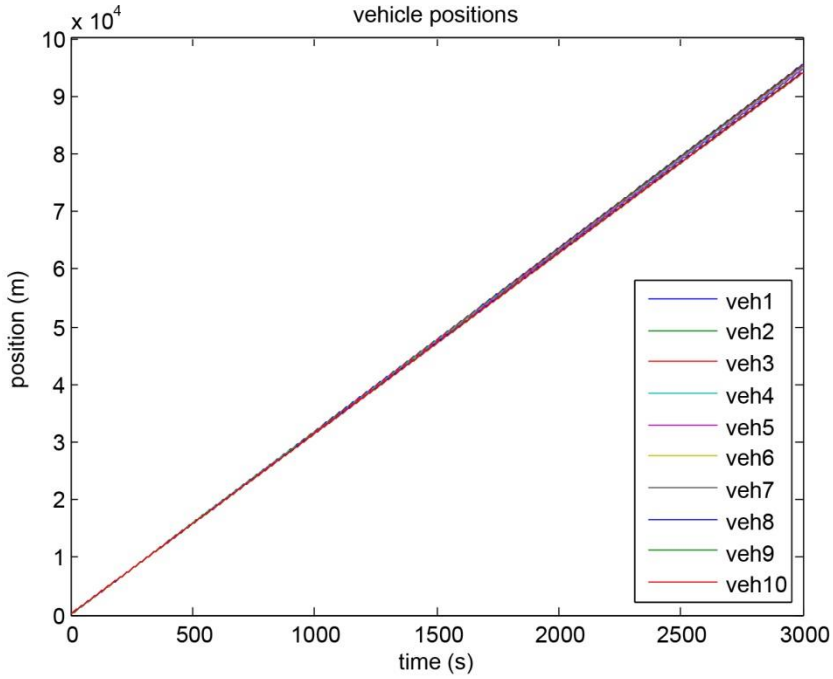

Figure 5.25 The vehicles are not string stable.

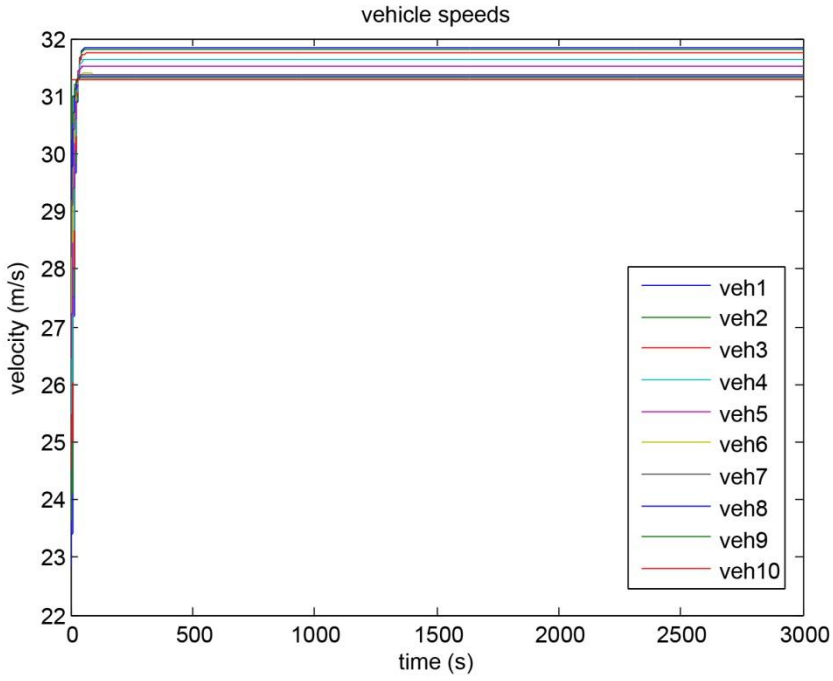

Figure 5.26 Vehicles do not reach the desired velocity, as it would have in case there was no delay in the system.

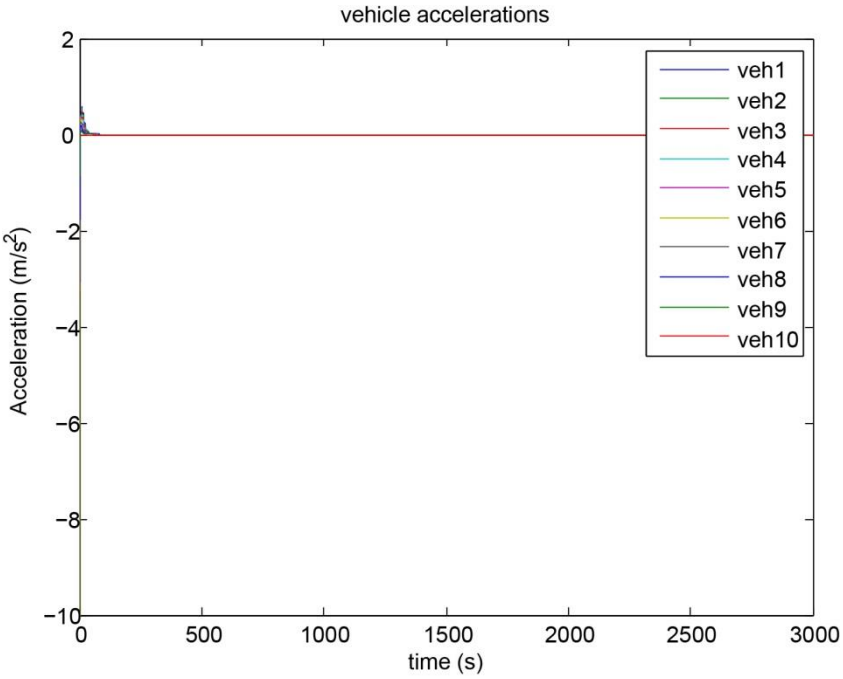

Figure 5.27 Acceleration eventually goes to zero.

6. FALSE DATA INJECTION-WITH PID CONTROL AND OSCILLATIONS

In this section, we see how the use of Proportional-Integral-Derivative (PID) control influences the vehicle platoon with false data injection (FDI), and how the system copes with the presence of oscillations in it.

6.1 Using Proportional-Integral-Derivative (PID) Control

Here again, a vehicle platoon with bidirectional-constant spacing platooning strategy has been used, where information from both the preceding and following vehicles are taken into consideration while making control decisions to maintain constant spacing between the vehicles. And the controller used is the PID controller, with K_p as the proportional gain, K_i as the integral gain, and K_v as the derivative gain, and their corresponding values have been chosen as 1, 1, and 7.7, respectively.

Thus, in this case, the absolute dynamics model for *n* number of vehicles is given as:

$$\dot{x_1} = v_1 \tag{6.1a}$$
$$\dot{v_1} = K_p(x_2 - x_1 - d) + K_i(x_2 - x_1 - d)T_s + K_v(v_2 - v_1), \tag{6.1b}$$

$$\dot{x_2} = v_2 \tag{6.2a}$$
$$\dot{v_2} = K_p(x_3 - x_2 - d) + K_i(x_3 - x_2 - d)T_s + K_v(v_3 - v_2) + K_p(x_1 - x_2 + d) + K_i(x_1 - x_2 + d)T_s + K_v(v_1 - v_2), \tag{6.2b}$$

$$\dot{x_3} = v_3 \tag{6.3a}$$
$$\dot{v_3} = K_p(x_4 - x_3 - d) + K_i(x_4 - x_3 - d)T_s + K_v(v_4 - v_3) + K_p(x_2 - x_3 + d) + K_i(x_2 - x_3 + d)T_s + K_v(v_2 - v_3), \tag{6.3b}$$

$$\dot{x_{m-1}} = v_{m-1} \tag{6.4a}$$
$$\dot{v_{m-1}} = K_p(x_m + -x_{m-1} - d) + K_i(x_m + -x_{m-1} - d)T_s + K_v(v_m - v_{m-1}) + K_p(x_{m-2} - x_{m-1} + d) + K_i(x_{m-2} - x_{m-1} + d)T_s + K_v(v_{m-2} - v_{m-1}), \tag{6.4b}$$

$$\dot{x_m} = v_m \tag{6.5a}$$
$$\dot{v_m} = K_p(x_{m+1} - x_m - d) + K_i(x_{m+1} - x_m - d)T_s + K_v(v_{m+1} - v_m) + K_p(x_{m-1} - x_m + d) + K_i(x_{m-1} - x_m + d)T_s + K_v(v_{m-1} - v_m), \tag{6.5b}$$

$$\dot{x_{m+1}} = v_{m+1} \tag{6.6a}$$
$$\dot{v_m} = K_p(x_{m+2} - x_{m+1} - d) + K_i(x_{m+2} - x_{m+1} - d)T_s + K_v(v_{m+2} - v_{m+1}) + K_p(x_m - x_{m+1} + d) + K_i(x_m - x_{m+1} + d)T_s + K_v(v_m - v_{m+1}), \tag{6.6b}$$

$$\dot{x_{n-1}} = v_{n-1} \tag{6.7a}$$
$$\dot{v_{n-1}} = K_p(x_n - x_{n-1} - d) + K_i(x_n - x_{n-1} - d)T_s + K_v(v_n - v_{n-1}) + K_p(x_{n-2} - x_{n-1} + d) + K_i(x_{n-2} - x_{n-1} + d)T_s + K_v(v_{n-2} - v_{n-1}), \tag{6.7b}$$

$$\dot{x_n} = v_n \tag{6.8a}$$
$$\dot{v_n} = 0. \tag{6.8b}$$

Considering that there is one attacker in a platoon of 10 vehicles who can send false information to the vehicle that is immediately preceding and/or following it, the following cases can be analyzed.

6.2 Addition of Constant Errors

6.2.1 Case 1

The last vehicle in the platoon is the attacker and it provides inaccurate position and velocity information to the preceding vehicle.

In a platoon of 10 vehicles, the last vehicle *(vehicle 1)* is the attacker and it sends position and velocity error to *vehicle 2*.

As can be seen in Figures 6.1–6.4, except for the inter-vehicle spacing between the attacker and the victim, which is as desired, all the other spacings have increased by the value, which is equal to the false data added to the system, although all the vehicles do reach desired velocity.

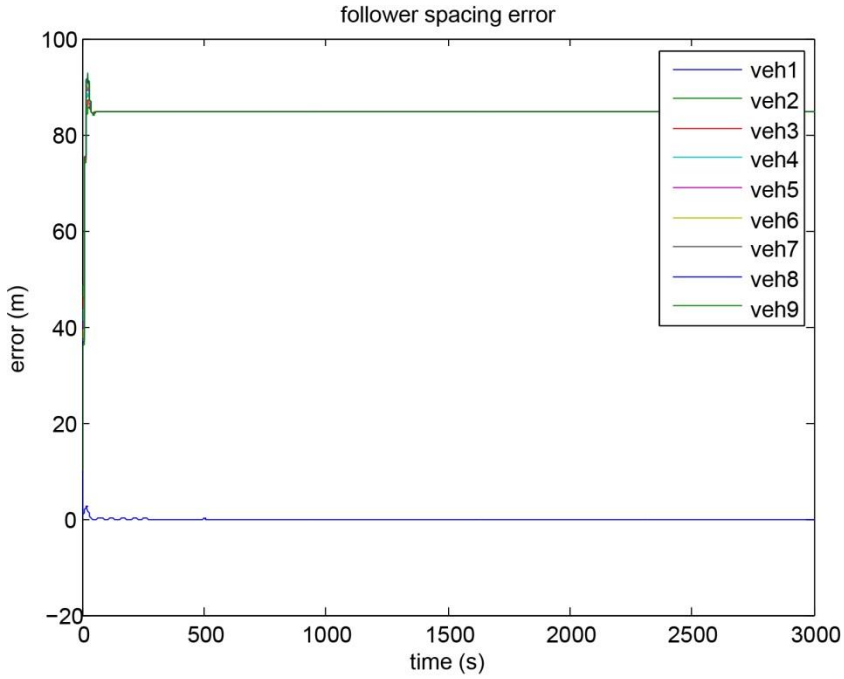

Figure 6.1 Spacing error between attacker and victim is 0, while the rest attain a value that depends on the error added by the attacker.

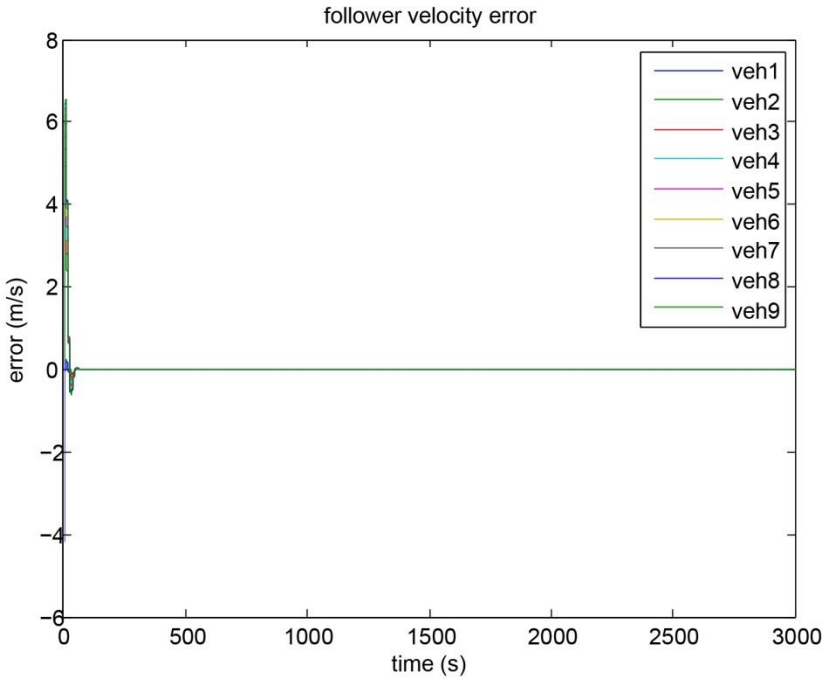

Figure 6.2 The velocity error goes to zero.

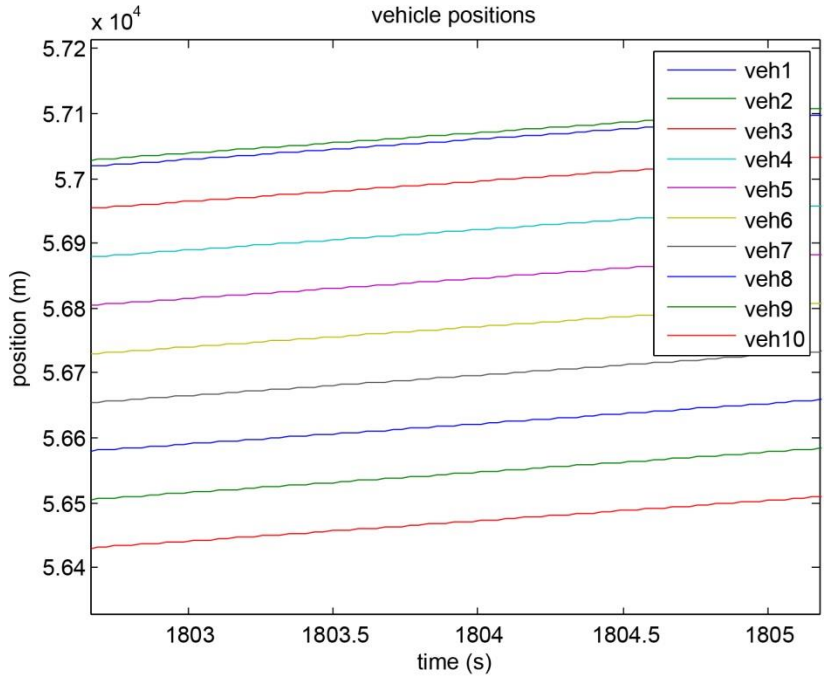

Figure 6.3 The whole platoon is not string stable.

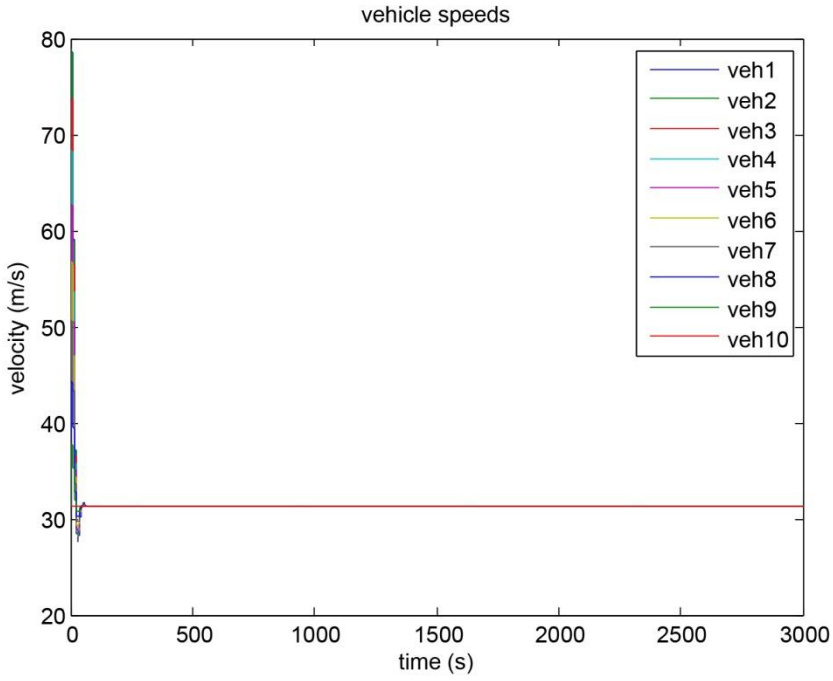

Figure 6.4 All the vehicles reach desired velocity.

6.2.2 Case 2

The attacker is at the center of the vehicle platoon, and it sends false position and velocity information to both the preceding and following vehicles.

In the platoon of 10 vehicles, the *5th* vehicle is considered here to be the attacker.

Here it is seen that the platoon gets divided into three parts as far as the spacing is concerned. Up to the first victim, the spacing error is at zero. In the platoon of 10 vehicles, when the attacker is the *5th* vehicle, and it sends false position and velocity data to the *4th* and *6th* vehicles, the velocities reach the desired value (which in this example is 31.29m/s), while all the inter-vehicular spacing errors are not at zero. Instead, the inter-vehicular spacing errors are shifted by factors of $(K_p d - K_p d_e - K_i d_e T - K_v v_e)$ and $(K_p d - 2K_p d_e - 2K_i d_e T - 2K_v v_e)$, where, in the example, $K_p = 1$, $K_i = 1$, $K_v = 7.7$, $T = 0.03$, $d_e = 10$, and $v_e = 10$. Also, although the velocities reach the desired value, the platoon no longer remains string stable (Figures 6.5 - 6.8).

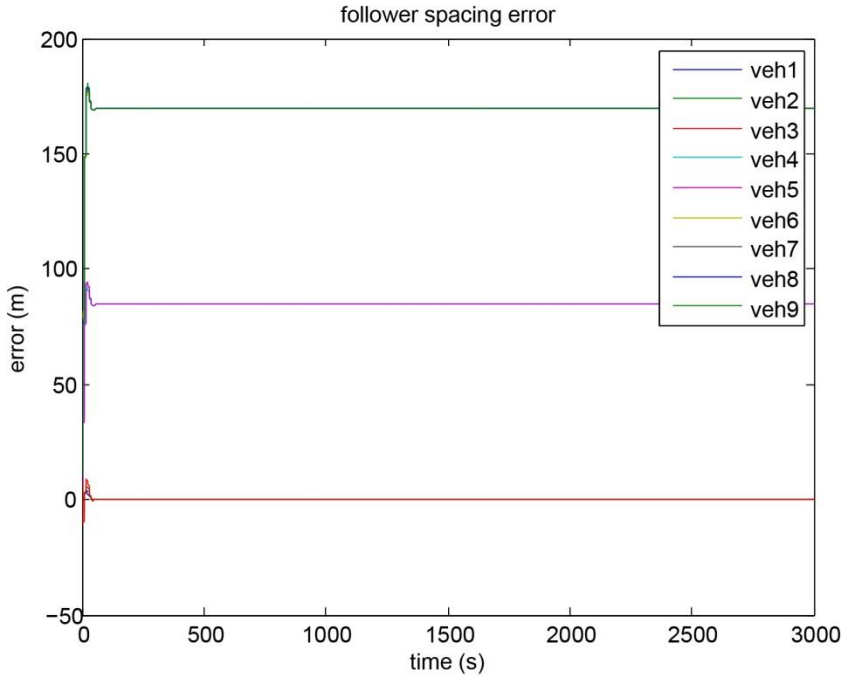

Figure 6.5 The spacing error varies into three regions due to the error added by the attacker.

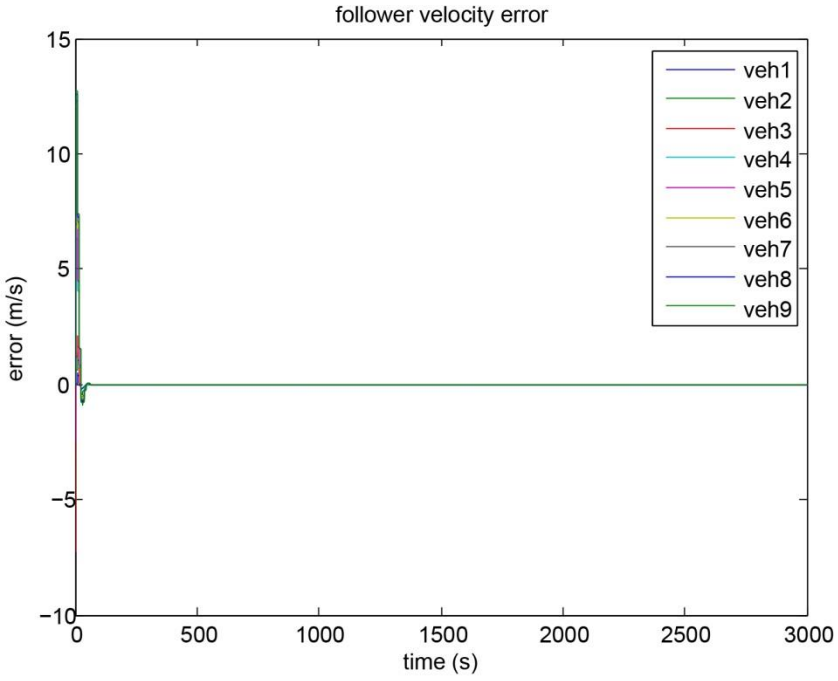

Figure 6.6 The velocity error goes to zero.

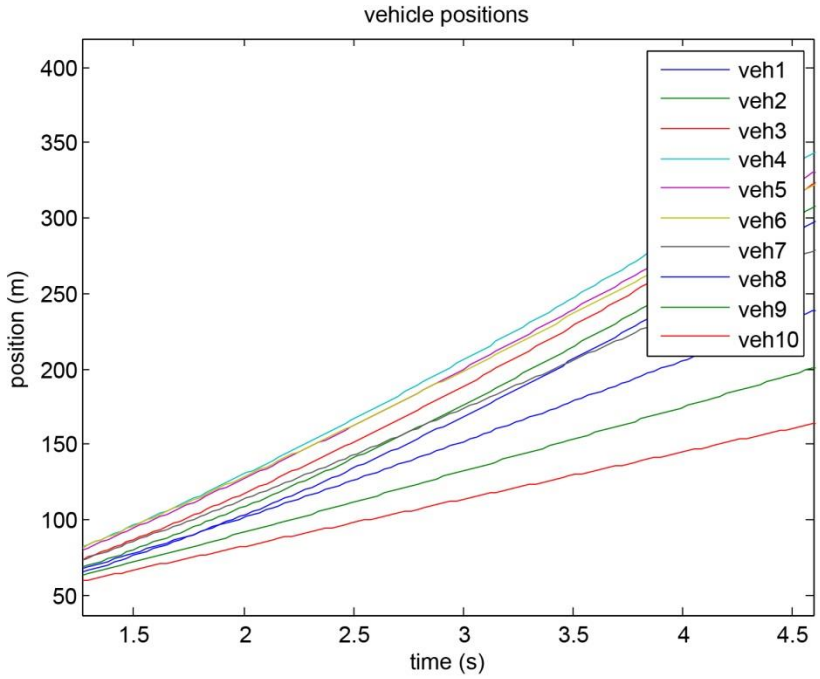

Figure 6.7 There are collisions at a very early point of time. The platoon is thus string unstable.

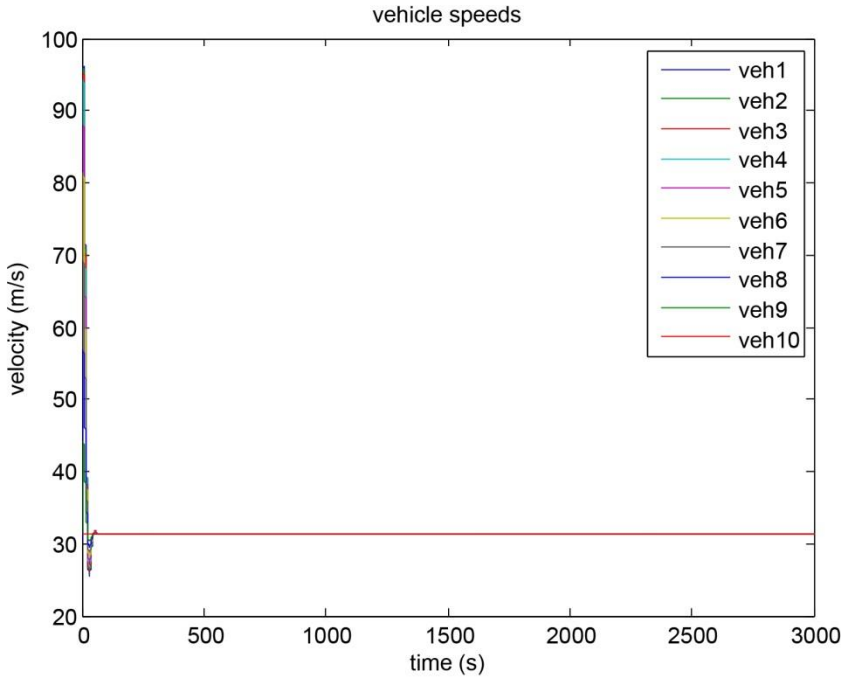

Figure 6.8 All the vehicles reach desired velocity.

6.3 Attacker Has Access to Victim's States and Manipulates Its Acceleration

6.3.1 Case 1

The attacker is in an arbitrary *i*th position and it has access to the states of the vehicle preceding it and it sends false information such that the acceleration of the victim is set to 0.

Since the velocities do not remain the same for all the vehicles, they no longer maintain a constant spacing between them. As some velocities are equal while the rest differ, with one greater than the previous, it is seen that the vehicles are string unstable (Figures 6.9 and 6.10).

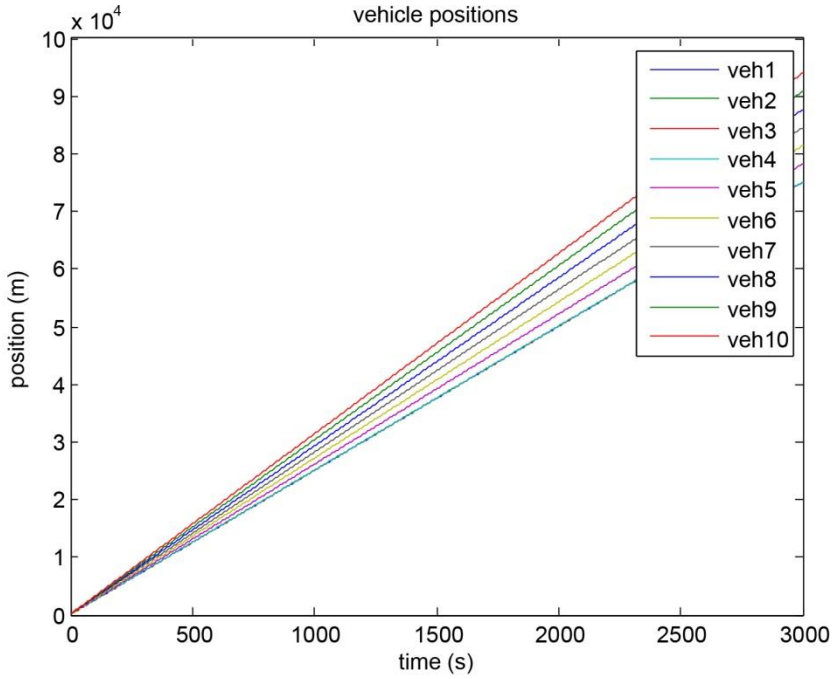

Figure 6.9 The vehicles are not string stable.

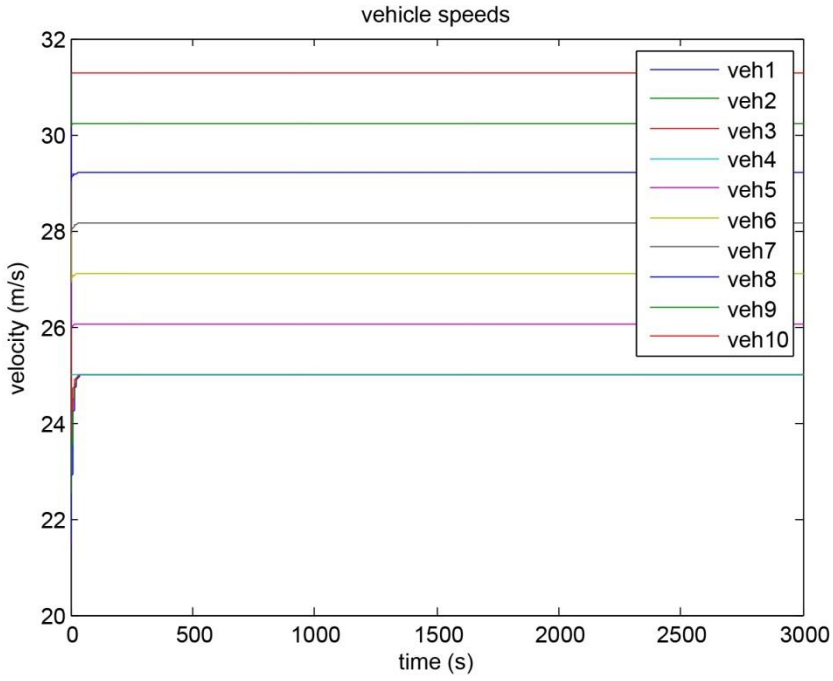

Figure 6.10 All the vehicles up to the victim reach the velocity of the victim.

6.3.2 Case 2

The attacker is in an arbitrary *i*th position, and having access to the states of its preceding vehicle, it sends false information such that all information of the victim's predecessor is eliminated.

It is seen that all vehicles up to the victim achieve the same velocity as that of the victim while the rest achieve velocities that are equally spaced between the leader and the victim. As the predecessor information is removed by the attacker, the link between the victim and its predecessor is broken, and thus the response (Figures 6.11 and 6.12).

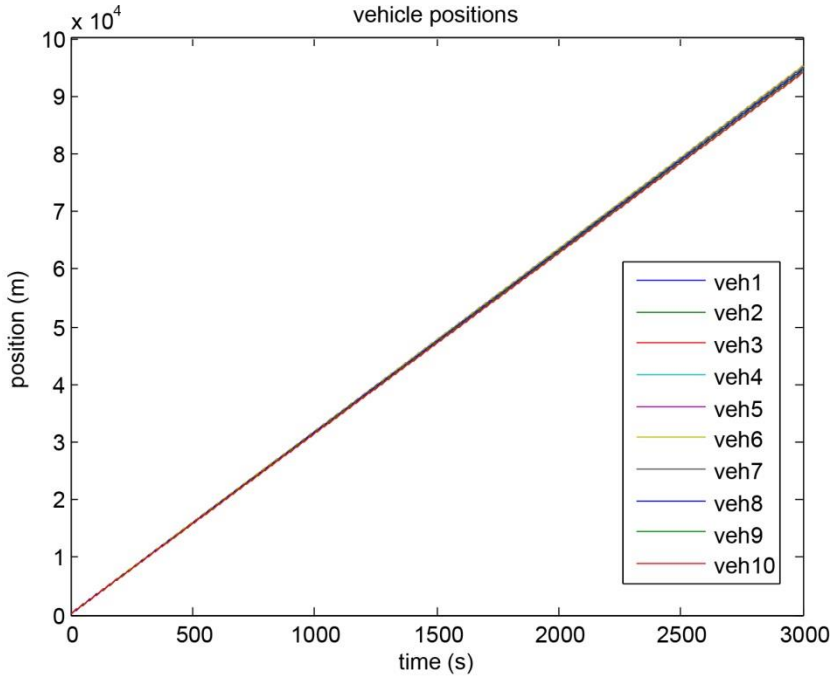

Figure 6.11 The vehicles are not string stable.

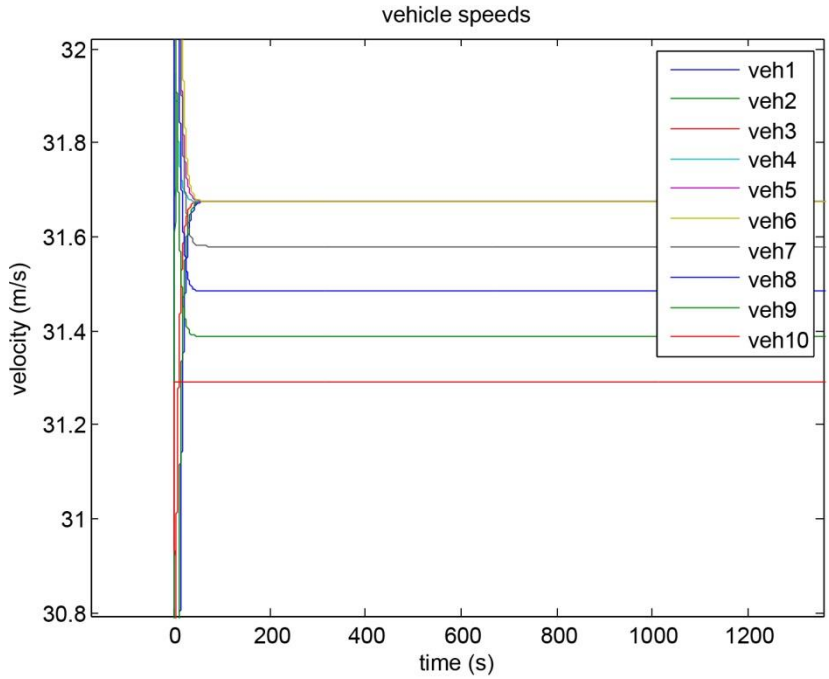

Figure 6.12 All the vehicles attain varying velocities.

6.3.3 Case 3

The attacker is in an arbitrary *i*th position, and having access to the states of its preceding vehicle, it sends false information such that it eliminates all the information about the victim's follower.

In spite of the follower information being eliminated, it is seen that the vehicles reach desired velocity and are string stable. This happens because the link between the victim, its predecessor, and its follower is never broken in spite of the FDI, in this case (Figures 6.13 and 6.14).

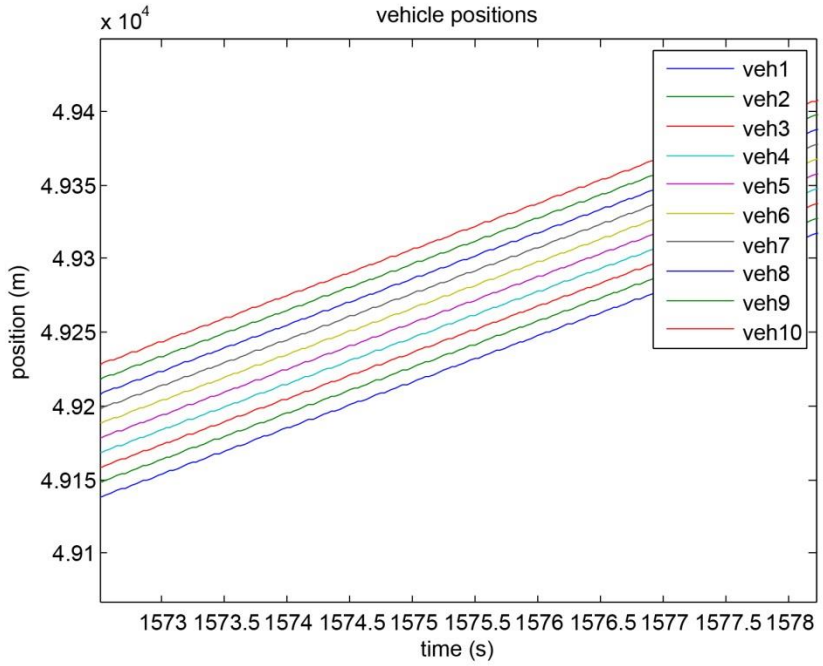

Figure 6.13 The vehicles are string stable.

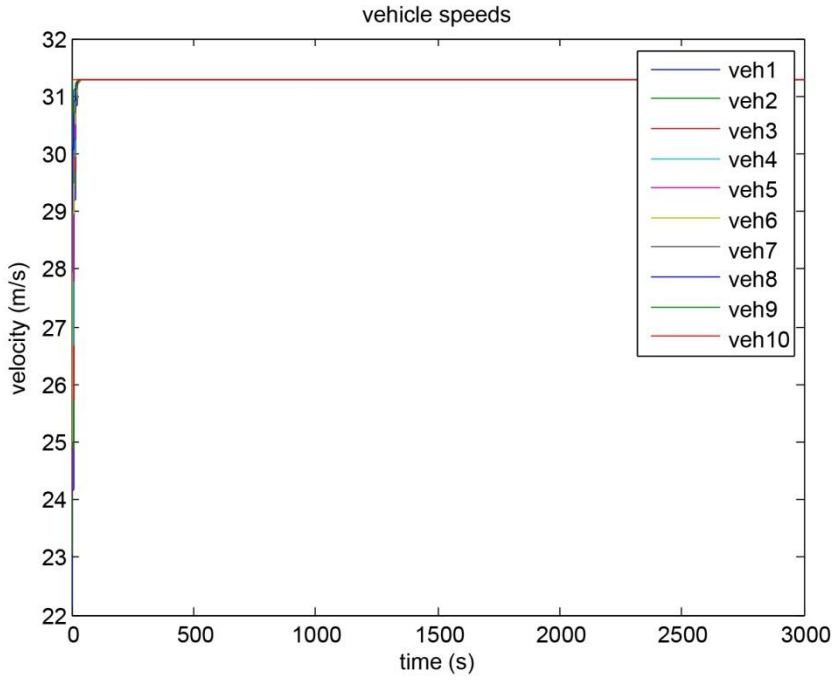

Figure 6.14 All the vehicles reach the desired velocity.

6.4 Oscillations and FDI

In this section we observe the effect of oscillations in the vehicle platoon. Three scenarios are considered.

- Oscillations present in the system without any False Data Injection (FDI)
- Oscillation present in the system for a certain period of time followed by FDI
- Oscillation and FDI together

Again, considering a platoon of 10 vehicles, the above mentioned cases are seen as follows.

6.4.1 Oscillations Present in the System without Any FDI

Figures 6.15 and 6.16 show the effect of oscillations of amplitude $1m$ and frequency $1Hz$ on the vehicle speeds and positions.

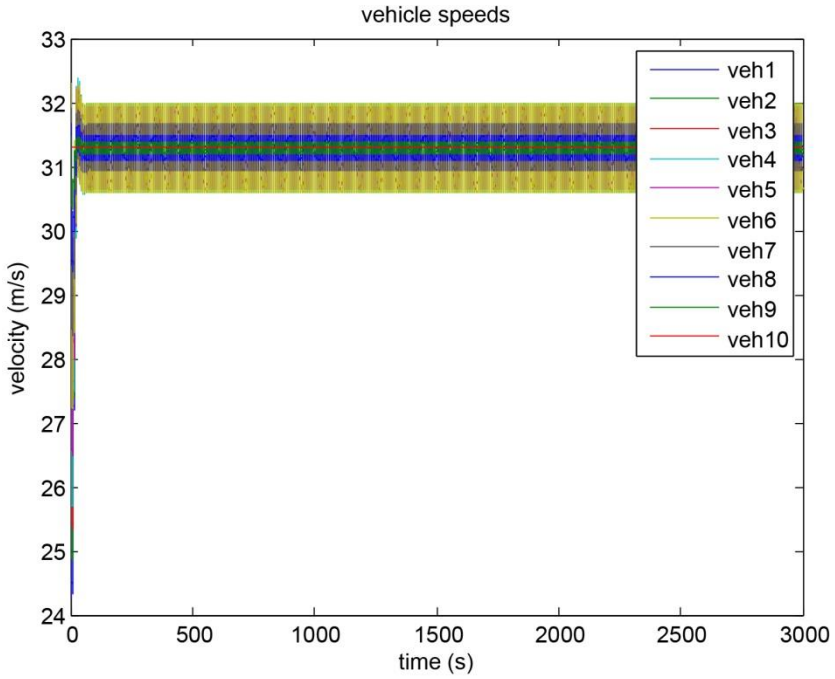

Figure 6.15 The vehicle speeds when the oscillation in the system has frequency and amplitude of magnitude 1: Forced oscillations in the system but not stable.

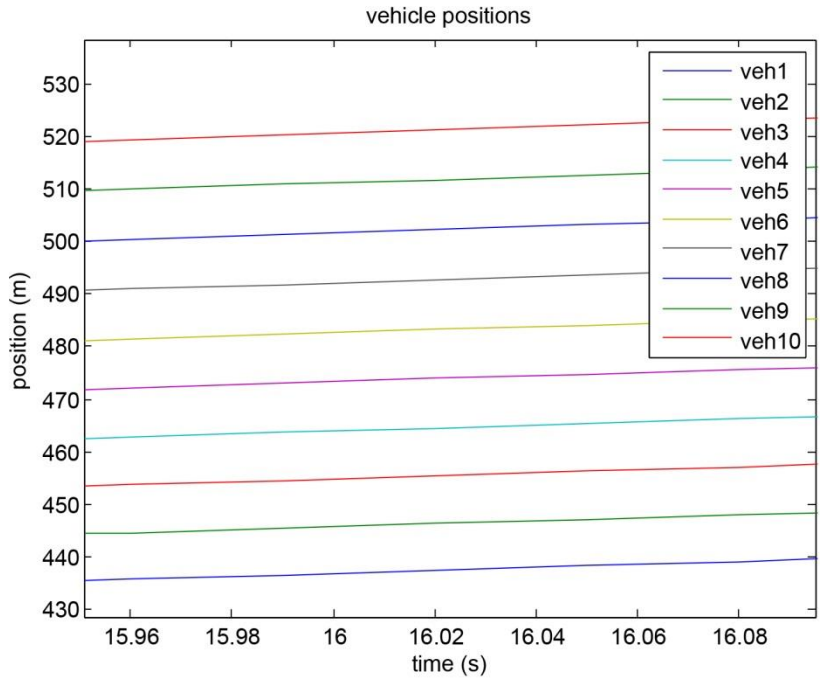

Figure 6.16 The vehicle positions when the oscillation in the system has frequency and amplitude of magnitude 1: String stable.

Figures 6.17 and 6.18 show the effect of oscillations of amplitude $10m$ and frequency $1Hz$ on the vehicle speeds and positions.

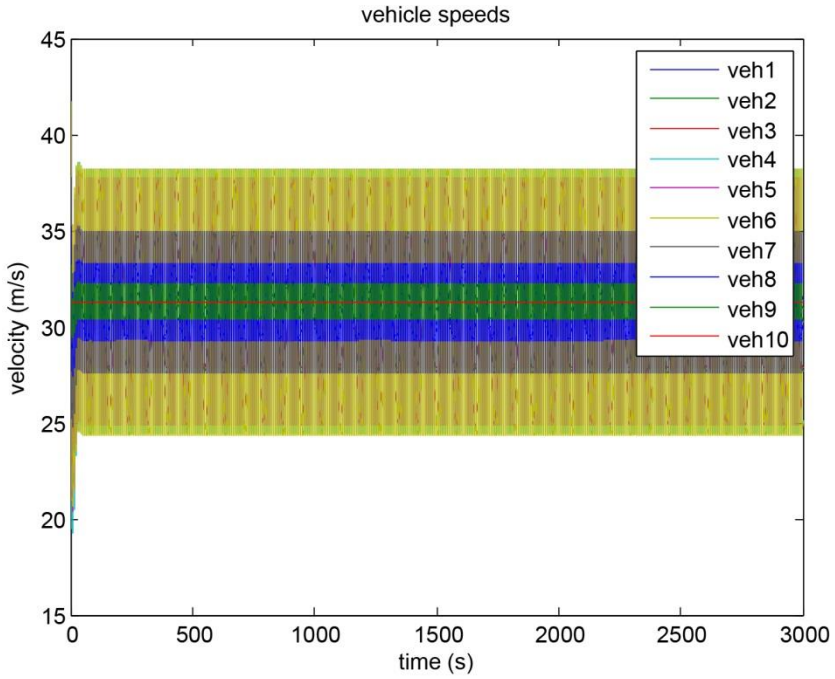

Figure 6.17 The vehicle speeds when the oscillation frequency is 1Hz and the amplitude has magnitude 10.

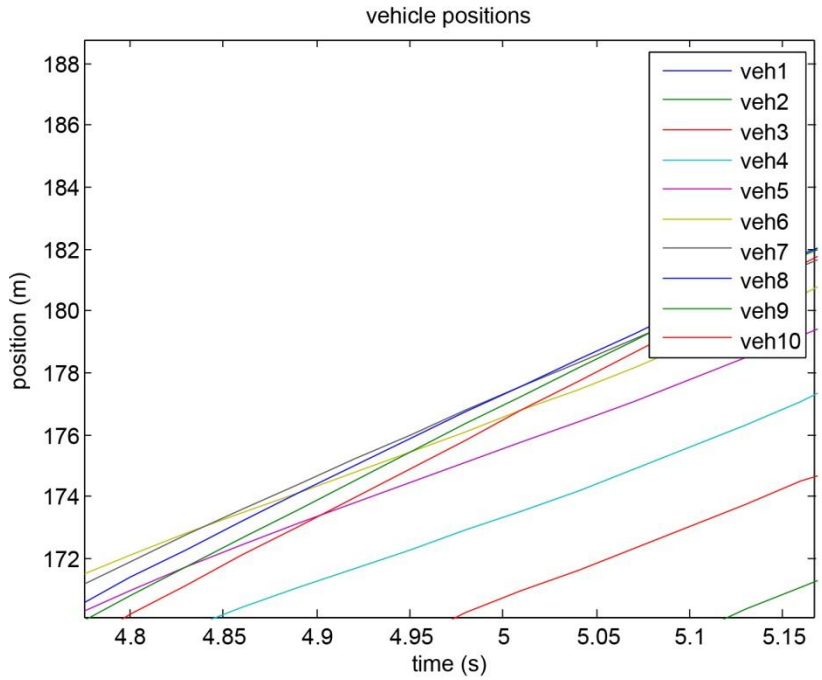

Figure 6.18 The vehicle positions when the oscillation frequency is 1Hz and the amplitude has magnitude 10: There are collisions, i.e., not string stable.

Figures 6.19 and 6.20 show the effect of oscillations of amplitude $1m$ and the natural frequency of the system ($0.131Hz$) on the vehicle speeds and positions.

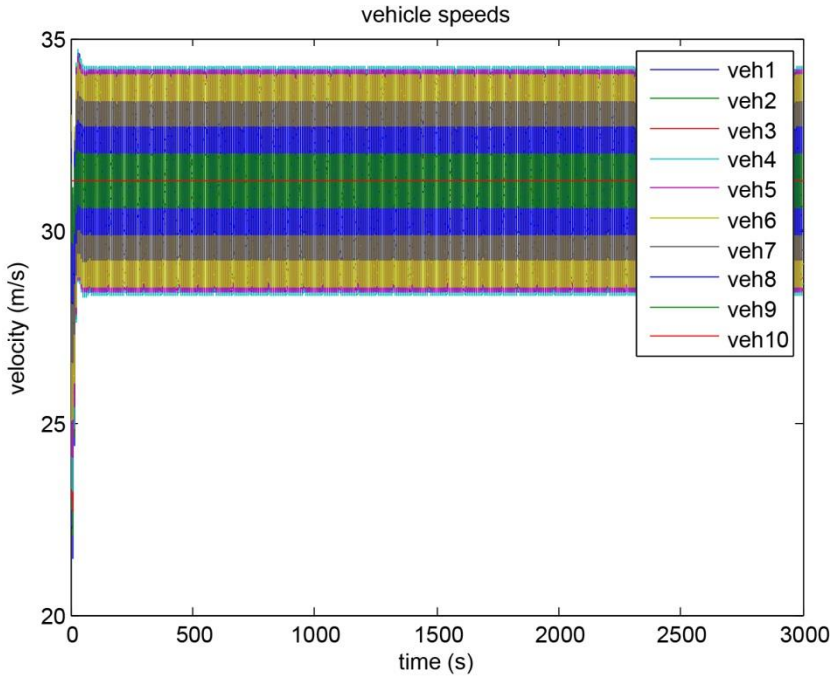

Figure 6.19 The vehicle speeds when the oscillation is at the natural frequency and the amplitude has magnitude 1.

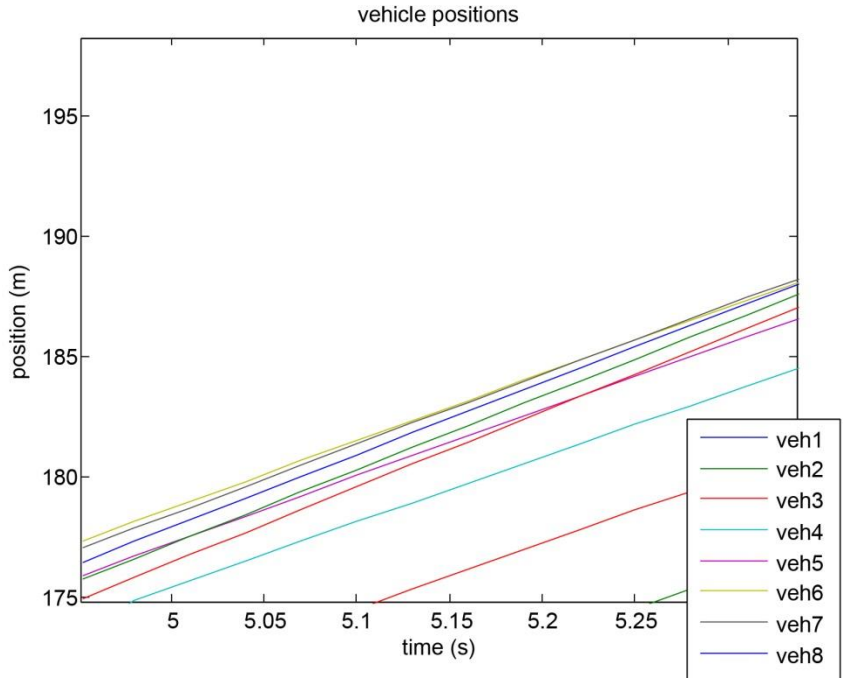

Figure 6.20 The vehicle positions when the oscillation is at the natural frequency and the amplitude has magnitude 1: Collisions occur, hence string unstable.

Thus, we see that when there is no FDI, if the amplitude of the oscillation is too high or if the frequency of the oscillation is at the natural frequency of the system, then there are collisions, hence the platoon becomes unstable.

6.4.2 Oscillation Present in the System for a Certain Period of Time Followed by FDI

Here, we consider that the system has oscillations for time = 0 to 50 seconds, and then the attacker at the center of the platoon (*vehicle 5*) sends false position and velocity error to both the preceding (*vehicle 6*) the following (*vehicle 4*) vehicles.

Figures 6.21 and 6.22 thus show the effect of oscillations (amplitude 10*m* and frequency 1*Hz*) for the first 50 seconds, followed by FDI, on the vehicle speeds and positions.

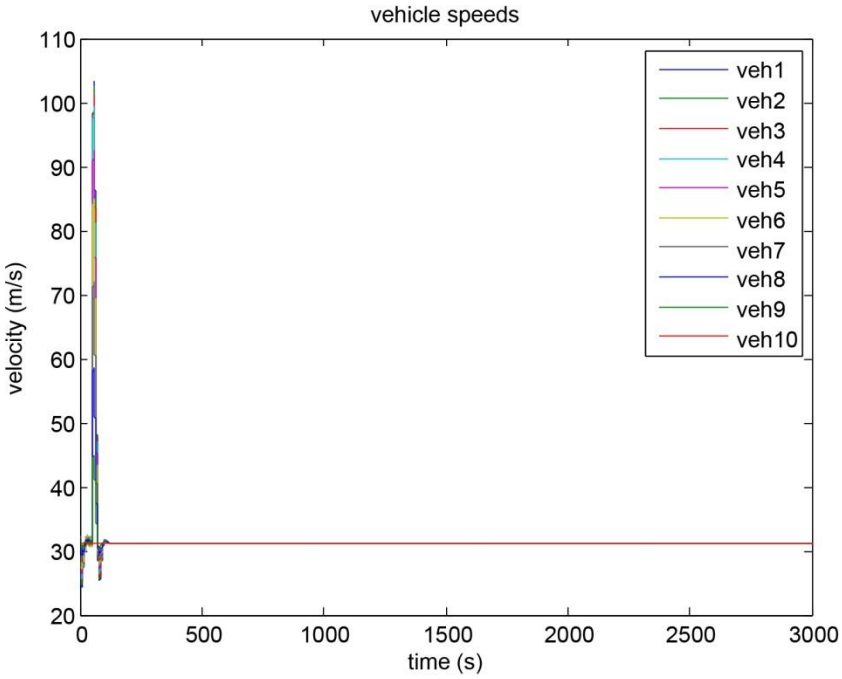

Figure 6.21 The vehicle speeds when the oscillation frequency is 1Hz and the amplitude has magnitude 10: Vehicles reach desired value.

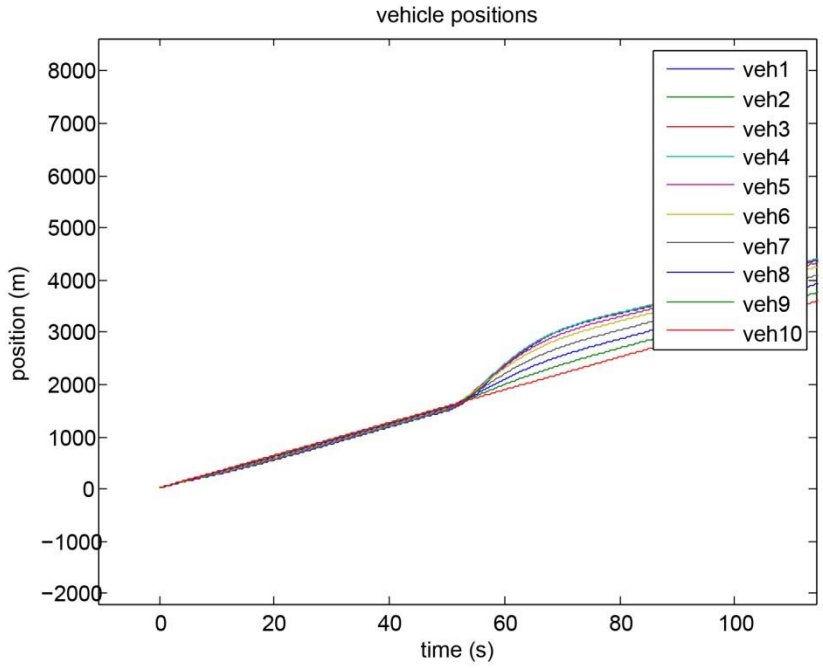

Figure 6.22 The vehicle positions when the oscillation frequency is 1Hz and the amplitude has magnitude 10: There are collisions, i.e., not string stable.

6.4.3 Oscillation and FDI Together

In this case, we consider that the oscillation and the FDI are acting on the system together. And again, in the platoon of 10 vehicles, the attacker at the center of the platoon (*vehicle 5*) sends false position and velocity error to both the preceding (*vehicle 6*) the following (*vehicle 4*) vehicles.

In this case, we see that the platoon has collisions and thus is string unstable at frequencies $1Hz$ or the natural frequency and amplitude $1m$ or $10m$. Thus, with both oscillations and FDI present, the system is not stable (Figures 6.23 - 6.25).

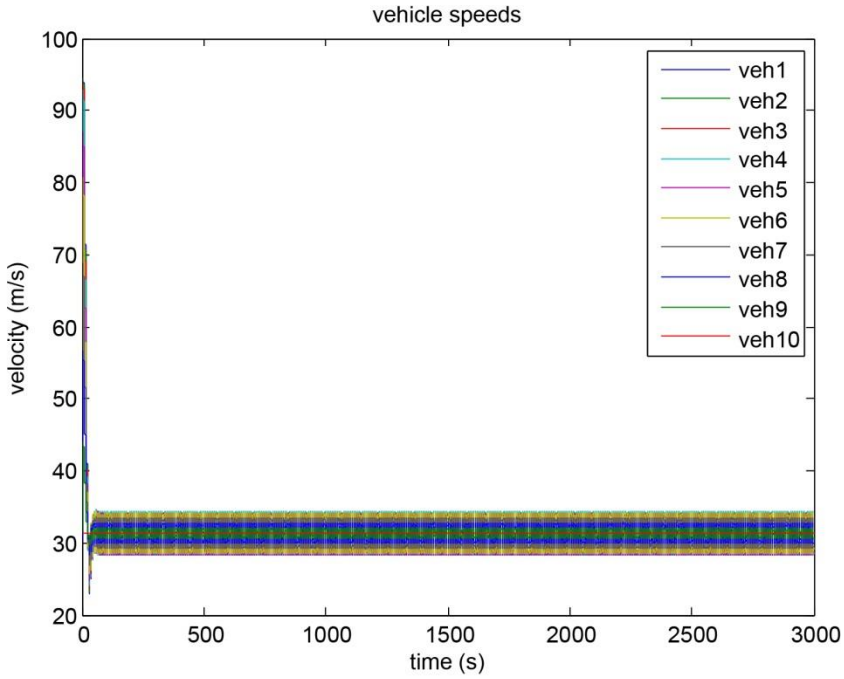

Figure 6.23 The vehicle speeds when there is oscillation (frequency is 1Hz and the amplitude has magnitude 1) as well as FDI.

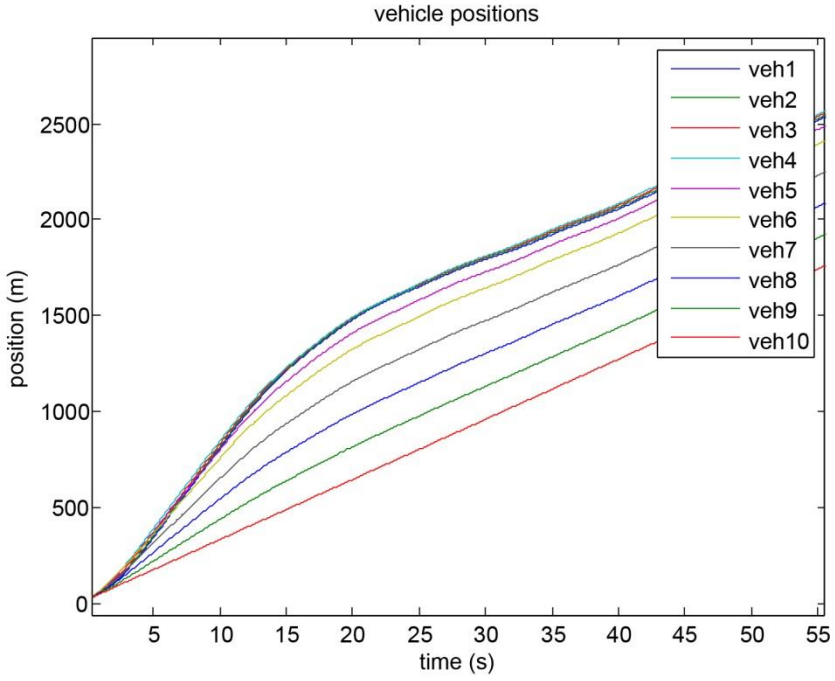

Figure 6.24 The vehicle positions when the oscillation frequency is 1Hz and the amplitude has magnitude 1: There are collisions, i.e., not string stable.

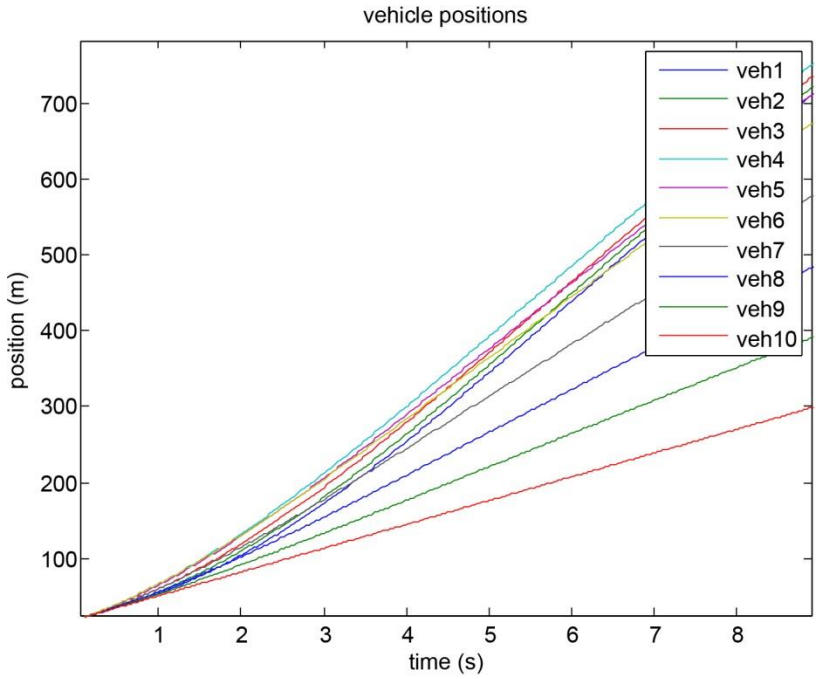

Figure 6.25 The vehicle positions when the oscillation frequency is the natural frequency (0.131Hz) and the amplitude has magnitude 10: There are collisions, i.e., not string stable.

7. CONCLUSION AND FUTURE WORK

7.1 Conclusion

In this report, various vehicle models particularly designed for longitudinal motion were analyzed as to their viable usage in different research relevant to longitudinal motion control. Then using a simple linearized vehicle model as a proving ground, analysis of scenarios where varied false data was injected into the system was done. It has been seen so far, that the attacks were able to make the system string unstable as the vehicles cross paths considerably before they reach a state of stability, when the attacker has access to information on the vehicles that are immediately following or preceding it. The attacker is capable of gaining control over the positions and velocities of the platoon in one way or the other.

7.2 Future Work

The following scenarios can be further studied.

- When considering the nonlinear model with inherent nonlinearities, the system goes unstable as spacing errors occur and early collisions in vehicles happen. In particular, with respect to the time delay, it is seen that the system remains stable as long as the delay constant is <= 0.01. Also, the limitations used on the acceleration and jerk values have been based on the work done here. Thus, a way to optimize the control such that the system can be under control in spite of nonlinearities should be looked into, taking into consideration the more realistic jerk and acceleration limitation and higher delay constants.
- Using PID control has more or less the same control effect in comparison to PD control in this work. Thus, further work can be done so as to understand the limitations of both the control efforts.
- Given the presence of oscillations with a high magnitude of the amplitude and at the natural frequency of the system, the platoon goes unstable, even in the absence of any FDI (false data injection). With FDI and oscillations together the system also goes unstable. Further work can thus be done to understand how such a situation can be controlled.
- In this work, all the scenarios considered have one attacker in the platoon. Multiple-attacker scenarios can also be studied further. For example, let us consider in a platoon of 10 vehicles, the 3rd and 6th vehicles are the attackers and have access to the states of the corresponding preceding vehicles (*vehicle* 4 and *vehicle* 7, respectively), so they send false information such that they set the accelerations of the victims to a new value. In this case, assuming the new accelerations for vehicles 4 and 7 are $20/=s^2$ and $25m/s^2$, respectively, the effects can be seen in the Figures (7.1 - 7.4) as the platoon going completely unstable. Thus, this kind of scenario can be studied further.
- Various other frameworks that can lead the longitudinal platoon of vehicles into complete instability, where the attack can override the controller and gain complete control over the platoon, should also be studied.

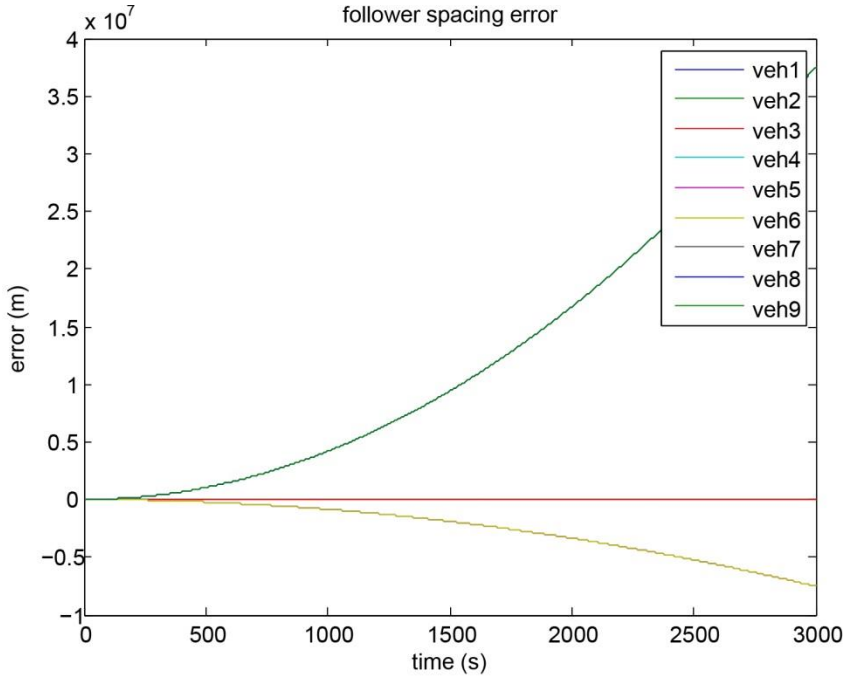

Figure 7.1 Spacing error increases with time.

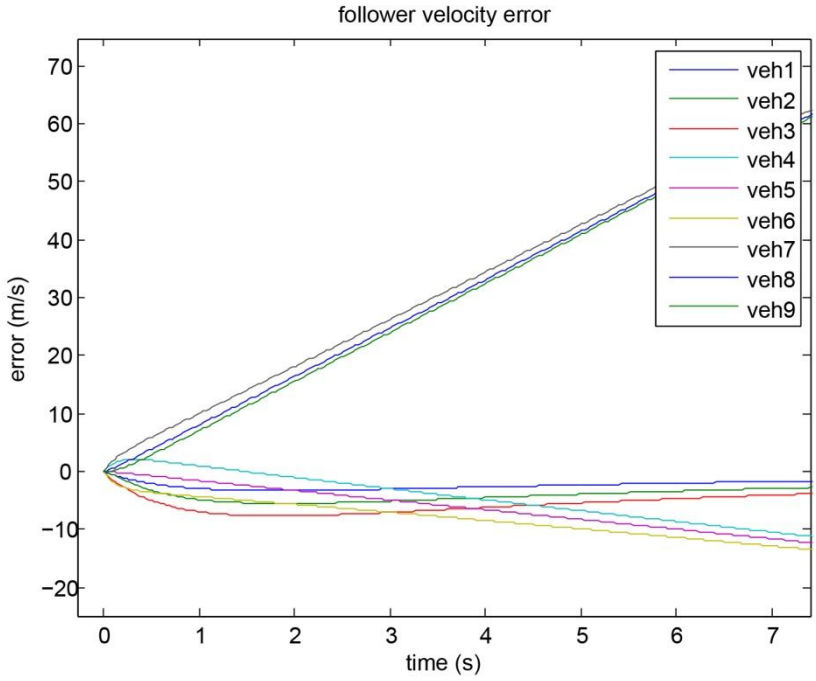

Figure 7.2 Velocity error is not zero.

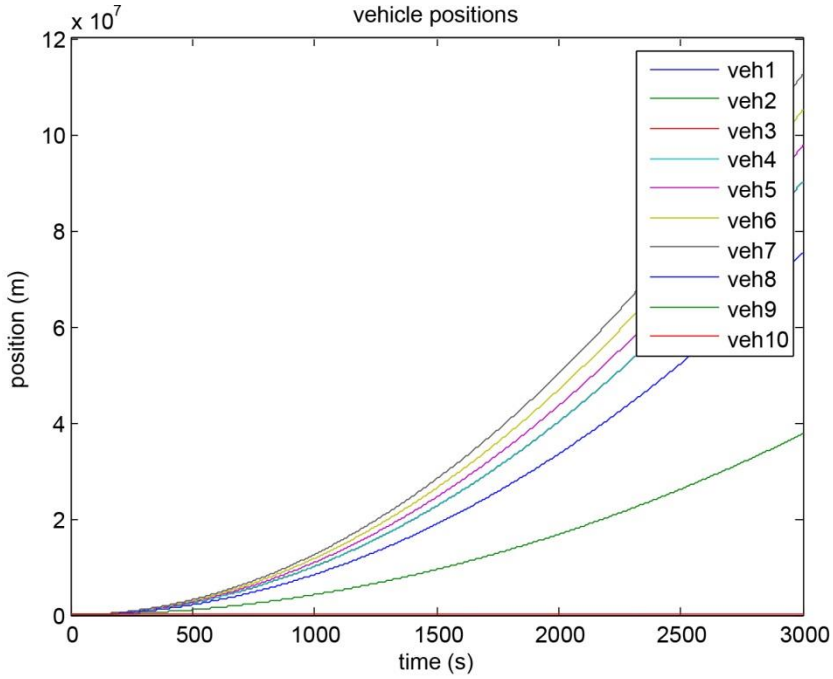

Figure 7.3 The vehicles are absolutely not string stable.

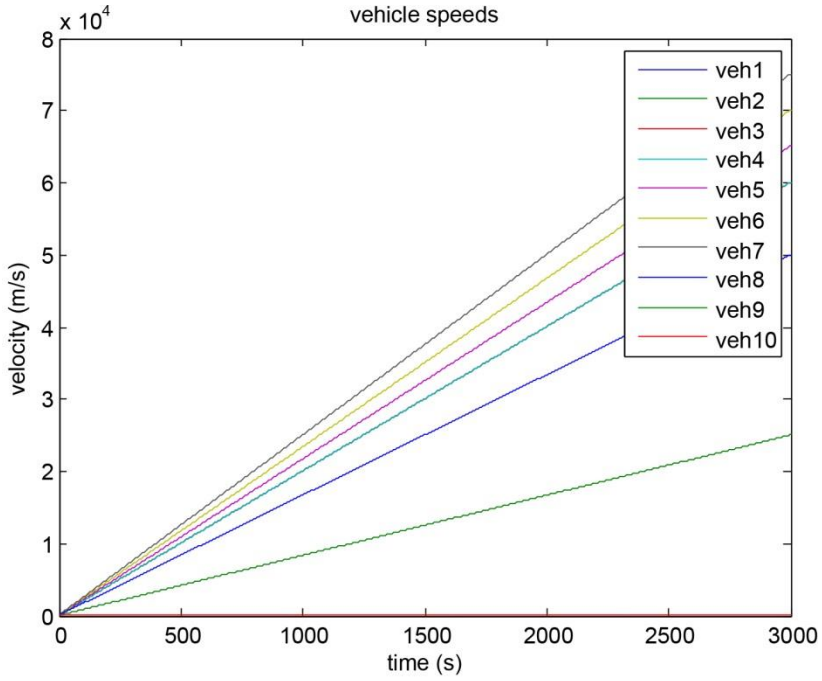

Figure 7.4 The vehicles attain varying velocities.

8. REFERENCES

[1] H. Zhou, “Two applications of intelligent transportation system,” Ph.D. dissertation, The University of Michigan, 2013.

[2] R. Vugts, “String-stable cacc design and experimental validation,” Ph.D. dissertation, Technische Universiteit Eindhoven, 2010.

[3] M. A. Khan, “Specifications and strategies for state estimation of vehicle and platoon,” master’s thesis, KTH School of Electrical Engineering, 2011.

[4] D. Yanakiev and I. Kanellakopoulos, “A simplified framework for string stability analysis in AHS,” in Proceedings of the 13th IFAC World Congress, Citeseer, pp. 177–182, 1996.

[5] S. Cheon, “An overview of automated highway systems (AHS) and the social and institutional challenges they face,” 2003.

[6] N. Congress, “The automated highway system: an idea whose time has come,” *Public Roads*, vol. 58, no. 1, 1994.

[7] D. Swaroop and J. Hedrick, “String stability of interconnected systems,” IEEE Transactions on Automatic Control, vol. 41, no. 3, pp. 349–357, 1996.

[8] S. Mammar, N. A. Oufroukh, L. Nouveliere, and D. Gruyer, “Integrated automated vehicle string longitudinal control,” in Intelligent Vehicles Symposium (IV), IEEE, pp. 803–808, 2013.

[9] M. Tai and M. Tomizuka, “Robust longitudinal velocity tracking of vehicles using traction and brake control,” in Proceedings of the 6th International Workshop on Advanced Motion Control, IEEE, pp. 305–310, 2000.

[10] K. El Majdoub, F. Giri, H. Ouadi, L. Dugard, and F. Z. Chaoui, “Vehicle longitudinal motion modeling for nonlinear control,” *Control Engineering Practice*, vol. 20, no. 1, pp. 69–81, 2012.

[11] M. El Zarki, S. Mehrotra, G. Tsudik, and N. Venkatasubramanian, “Security issues in a future vehicular network,” in *European Wireless*, vol. 2, 2002.

[12] S. Zhu, S. Setia, S. Jajodia, and P. Ning, “An interleaved hop-by-hop authentication scheme for filtering of injected false data in sensor networks,” in Proceedings of the Symposium on Security and Privacy, IEEE, pp. 259–271, 2004.

[13] A. Studer, M. Luk, and A. Perrig, “Efficient mechanisms to provide convoy member and vehicle sequence authentication in VANETs,” in Third International Conference on Security and Privacy in Communications Networks and the Workshops, SecureComm, IEEE, pp. 422–432, 2007.

[14] Z. Cao, J. Kong, U. Lee, M. Gerla, and Z. Chen, “Proof-of-relevance: Filtering false data via authentic consensus in vehicle ad-hoc networks,” in INFOCOM Workshops, IEEE, pp. 1–6, 2008.

[15] Y. Mo, E. Garone, A. Casavola, and B. Sinopoli, “False data injection attacks against state estimation in wireless sensor networks,” in 49th Conference on Decision and Control (CDC), IEEE, pp. 5967–5972, 2010.

[16] L. Xie, Y. Mo, and B. Sinopoli, “False data injection attacks in electricity markets,” in First International Conference on Smart Grid Communications (SmartGridComm), IEEE, pp. 226–231, 2010.

[17] Y. Mo and B. Sinopoli, “False data injection attacks in control systems,” in Preprints of the 1st workshop on Secure Control Systems, pp. 1–6, 2010.

[18] B. Sinopoli and Y. Mo, “Integrity attacks on cyber-physical systems,” in Proceedings of the 1st ACM International Conference on High Confidence Networked Systems, pp. 47–54, 2012.

[19] Y. Liu, P. Ning, and M. K. Reiter, "False data injection attacks against state estimation in electric power grids," *ACM Transactions on Information and System Security (TISSEC)*, vol. 14, no. 1, p. 13, 2011.

[20] W. Yu, "False data injection attacks in smart grid: Challenges and solutions," in Proceeding of NIST Cyber Security for Cyber-Physical System (CPS) Workshop, 2012.

[21] A. Aijaz, B. Bochow, F. Dötzer, A. Festag, M. Gerlach, R. Kroh, and T. Leinmüller, "Attacks on inter vehicle communication systems-an analysis," Proceedings of WIT, pp. 189–194, 2006.

[22] P. Golle, D. Greene, and J. Staddon, "Detecting and correcting malicious data in VANETs," in Proceedings of the 1st ACM international workshop on Vehicular ad hoc networks, pp. 29–37, 2004.

[23] F. Dötzer, "Privacy issues in vehicular ad hoc networks," in Privacy enhancing technologies. Springer, pp. 197–209, 2006.

[24] M. Gerlach, "Vanese-an approach to VANET security," Proceedings of V2VCOM, 2005.

[25] T. Leinmüller, E. Schoch, F. Kargl, and C. Maihöfer, "Influence of falsified position data on geographic ad-hoc routing," in *Security and Privacy in Ad-hoc and Sensor Networks*. Springer, pp. 102–112, 2005.

[26] J.-P. Hubaux, S. Capkun, and J. Luo, "The security and privacy of smart vehicles*," IEEE Security & Privacy Magazine*, vol. 2, no. LCA-ARTICLE-007, pp. 49–55, 2004.

[27] M. Raya and J.-P. Hubaux, "Securing vehicular ad hoc networks," *Journal of Computer Security*, vol. 15, no. 1, pp. 39–68, 2007.

[28] S. Brennan and A. Alleyne, "The Illinois roadway simulator: A mechatronic testbed for vehicle dynamics and control," *IEEE/ASME Transactions on Mechatronics*, vol. 5, no. 4, pp. 349–359, 2000.

[29] A. B. Will and S. H. Zak, "Modelling and control of an automated vehicle," *Vehicle System Dynamics*, vol. 27, no. 3, pp. 131–155, 1997.

[30] S. Sheikholeslam and C. A. Desoer, "Longitudinal control of a platoon of vehicles with no communication of lead vehicle information: a system level study," *IEEE Transactions on Vehicular Technology*, vol. 42, no. 4, pp. 546–554, 1993.

[31] D. Yanakiev and I. Kanellakopoulos, "Speed tracking and vehicle follower control design for heavy-duty vehicles," *Vehicle System Dynamics*, vol. 25, no. 4, pp. 251–276, 1996.

[32] K.-T. Chong, D.-H. Roh et al., "A lyapunov function approach to longitudinal control of vehicles in a platoon," *IEEE Transactions on Vehicular Technology*, vol. 50, no. 1, pp. 116–124, 2001.

[33] X. Liu, A. Goldsmith, S. Mahal, and J. K. Hedrick, "Effects of communication delay on string stability in vehicle platoons," in *Intelligent Transportation Systems Proceedings, IEEE*, pp. 625–630, 2001.

[34] A. Nalecz and A. Bindemann, "Investigation into the stability of four wheel steering vehicles," *International Journal of Vehicle Design*, vol. 9, no. 2, pp. 159–178, 1988.

[35] R. Mohajerpoor, S. Salavati Dezfuli, and B. Bahadori, "Teleoperation of an unmanned car via robust adaptive backstepping control approach," in ASME International Conference on Advanced Intelligent Mechatronics (AIM), IEEE, pp. 1540–1545, 2013.

[36] P. P. Ramanata, "Optimal vehicle path generator using optimization methods," Ph.D. dissertation, Virginia Polytechnic Institute and State University, 1998.

[37] F. Biral, D. Giovannini, D. Moser, and L. Zaccarian, “Longitudinal speed control of a prototype vehicle via engine map identification and backstepping approach,” in 39th IEEE Annual Conference of the Industrial Electronics Society, IECON, pp. 6484–6489, 2013.

[38] Y.-F. Peng, “Adaptive intelligent backstepping longitudinal control of vehicle platoons using output recurrent cerebellar model articulation controller,” *Expert Systems with Applications*, vol. 37, no. 3, pp. 2016–2027, 2010.

[39] J. W. Choi and T. H. Fang, “Optimal channel scheduling for remote control of lead vehicle in a platoon,” in IEEE Intelligent Transportation Systems Proceedings, vol. 1, pp. 31–36, 2003.

[40] Y.-F. Peng, C.-F. Hsu, C.-M. Lin, and T.-T. Lee, “Robust intelligent backstepping longitudinal control of vehicle platoons with hâL tracking performance,” in IEEE International Conference on Systems, Man and Cybernetics (SMC’06), vol. 6, pp. 4648–4653, 2006.

[41] D.-J. Kim, K.-H. Park, and Z. Bien, “Hierarchical longitudinal controller for rear-end collision avoidance,” *IEEE Transactions on Industrial Electronics*, vol. 54, no. 2, pp. 805–817, 2007.

[42] S. Huang, K. K. Tan, and T. H. Lee, “Autonomous cruise control using neural networks in platooning,” *Advanced Robotics*, vol. 19, no. 2, pp. 169–189, 2005.

[43] M. Nieuwenhuijze, “String stability analysis of bidirectional adaptive cruise control,” Master’s thesis, Eindhoven University of Technology, 2010.

[44] J. Ploeg, B. T. Scheepers, E. van Nunen, N. van de Wouw, and H. Nijmeijer, “Design and experimental evaluation of cooperative adaptive cruise control,” in 14th International IEEE Conference on Intelligent Transportation Systems (ITSC), pp. 260–265, 2011.

[45] D. Yanakiev and I. Kanellakopoulos, “Longitudinal control of automated CHVS with significant actuator delays,” in Proceedings of the 36th IEEE Conference on Decision and Control, vol. 5, pp. 4756–4763, 1997.

[46] Y. Tan, A. Robotis, and I. Kanellakopoulos, “Speed control experiments with an automated heavy vehicle,” in Proceedings of the 1999 IEEE International Conference on Control Applications, vol. 2, pp. 1353–1358, 1999.

[47] D. Yanakiev, J. Eyre, and I. Kanellakopoulos, “Longitudinal control of heavy vehicles with air brake actuation delays,” in Proceedings of the American Control Conference (American Automatic Control Council), vol. 3, pp. 1613–1617, 1997.

[48] D. Yanakiev and I. Kanellakopoulos, “Analysis, design and evaluation of AVCS for heavy-duty vehicles,” California Partners for Advanced Transit and Highways (PATH), 1996.

[49] I. Kanellakopoulos, J. Eyre, and D. Yanakiev, “Longitudinal control of heavy duty vehicles: Experimental evaluation,” California Partners for Advanced Transit and Highways (PATH), 1998.

[50] D. Yanakiev, J. Eyre, and I. Kanellakopoulos, “Analysis, design, and evaluation of AVCS for heavy-duty vehicles with actuator delays,” California Partners for Advanced Transit and Highways (PATH), 1998.

[51] B. He and Q. Lu, “Trafficability analysis at traffic crossing and parameters optimization based on particle swarm optimization method,” Mathematical Problems in Engineering, 2014.

[52] K. Junaid, W. Shuning, K. Usman, and T. Wencheng, “Intelligent longitudinal cruise control by quadratic minimization and robust synthesis,” in IEEE International Conference on Vehicular Electronics and Safety, pp. 182–187, 2005.

[53] L. Xiao, S. Darbha, and F. Gao, “Stability of string of adaptive cruise control vehicles with parasitic delays and lags,” in 11th International IEEE Conference on Intelligent Transportation Systems (ITSC), pp. 1101–1106, 2008.

[54] R. Attia, R. Orjuela, and M. Basset, “Nonlinear cascade strategy for longitudinal control in automated vehicle guidance,” Control Engineering Practice, 2014.

[55] U. Kiencke and L. Nielsen, Automotive Control Systems for Engine, Driveline, and Vehicle. Springer-Verlag, Berlin, 2000.

[56] R. Attia, R. Orjuela, and M. Basset, “Combined longitudinal and lateral control for automated vehicle guidance,” *Vehicle System Dynamics*, vol. 52, no. 2, pp. 261–279, 2014.

[57] F. Giri, K. El Majdoub, and H. Ouadi, “Accounting for tire effect in longitudinal vehicle control,” in American Control Conference (ACC), IEEE, pp. 3325–3330, 2009.

[58] M. A. Henson and D. E. Seborg, Nonlinear process control. Prentice-Hall, Inc., 1997.

[59] P. A. Cook, “Stable control of vehicle convoys for safety and comfort,” *IEEE transactions on automatic control*, vol. 52, no. 3, pp. 526–531, 2007.

[60] F. L. Lewis, H. Zhang, K. Hengster-Movric, and A. Das, Cooperative control of multi-agent systems: optimal and adaptive design approaches. Springer Publishing Company, Incorporated, 2014.

[61] J. Hedrick and A. Girard, “Control of nonlinear dynamic systems: Theory and applications,” Controllability and Observability of Nonlinear Systems, 2005.

[62] C.-T. Chen, Linear system theory and design. Oxford University Press, Inc., 1995.

[63] R. W. Brockett et al., “Asymptotic stability and feedback stabilization,” 1983.

[64] D. N. Godbole and J. Lygeros, “Longitudinal control of the lead car of a platoon,” *IEEE Transactions on Vehicular Technology*, vol. 43, no. 4, pp. 1125–1135, 1994.

[65] M. Jensen, J. Wagner, and K. Alexander, “Analysis of in-vehicle driver behaviour data for improved safety,” *International Journal of Vehicle Safety*, vol. 5, no. 3, pp. 197–212, 2011.